WESTFÄLISCHE WILHELMS-UNIVERSITÄT
MÜNSTER

PHD THESIS

Ward Identities and Baryonic States in $\mathcal{N} = 1$ Supersymmetric Yang-Mills Theory on the Lattice

Sajid Ali

supervised by
Prof. Dr. Gernot MÜNSTER

June 2019

Theoretische Physik

Ward Identities and Baryonic States in $\mathcal{N}=1$ Supersymmetric Yang-Mills Theory on the Lattice

vorgelegt von
Sajid Ali
aus Lahore (Pakistan)
- 2019 -

"This version of the thesis differs slightly from the official document submitted to the faculty. Typos are corrected while results and conclusions are unchanged."

Abstract

The $\mathcal{N} = 1$ supersymmetric Yang-Mills (SYM) theory describes the interaction between the gluon and its supersymmetric partner, the gluino. We investigate this theory on the 4D space-time lattice. The introduction of the lattice as a regulator of the theory breaks the supersymmetry explicitly. Additionally, the supersymmetry is broken softly by a non-zero gluino mass. The supersymmetric Ward identity is a key instrument for extrapolating the theory to the chiral limit where it is characterised by massless gluinos, and for probing the size of supersymmetry breaking by the lattice regulator. In this thesis we present improved methods for the analysis of the supersymmetric Ward identity of SYM theory with the gauge group SU(3) and formulate a method based on the generalised least squares fit, the so-called GLS method. This method considers the correlations among different observables present in the formula of the supersymmetric Ward identity. We obtain the subtracted gluino mass by the GLS method for each gauge ensemble and obtain the remnant gluino mass in the chiral limit. The lattice artifacts for the remnant gluino mass at finite lattice spacing are of the order a^2 and vanish in the zero lattice spacing limit. This agrees with our theoretical expectations.

In addition, this thesis discusses baryonic states composed of three gluino fields. We derive correlation functions of these states and implement them in the simulation code. Preliminary results of the effective masses of the baryonic states for SYM theory with the gauge group SU(2) are presented.

Zusammenfassung

Die $\mathcal{N} = 1$ Supersymmetrische Yang-Mills-Theorie beschreibt die Wechselwirkung zwischen dem Gluon und seinem supersymmetrischen Partnerteilchen dem Gluino. Wir untersuchen diese Theorie auf dem 4D-Raum-Zeit-Gitter. Die Einführung des Gitters als Regulator der Theorie bricht die Supersymmetrie explizit. Zusätzlich wird die Supersymmetrie durch einen Gluino-Massenterm weich gebrochen. Die supersymmetrische Ward-Identität ist ein Schlüsselinstrument, um die Theorie zum chiralen Limes zu extrapolieren, wo sie durch masselose Gluinos charakterisiert ist, und um die Größe der Supersymmetriebrechung durch den Gitterregulator zu untersuchen. In dieser Arbeit stellen wir für SYM verbesserte Methoden zur Analyse der supersymmetrischen Ward-Identität mit der Eichgruppe SU(3) vor und formulieren eine Methode, die auf der verallgemeinerten Methode der kleinsten Fehlerquadrate basiert. Diese Methode berücksichtigt die Korrelationen zwischen verschiedenen Observablen in der Formel der supersymmetrischen Ward-Identität. Die Gitterartefakte in Form einer nicht verschwindenden Gluino Masse im chiralen Limes sind von Ordnung a^2 und verschwinden im Limes des Gitterabstands Null. Dies stimmt mit unseren theoretischen Erwartungen überein.

Darüber hinaus behandelt diese Arbeit Baryonenzustände, die aus drei Gluino-Feldern bestehen. Wir leiten Korrelationsfunktionen dieser Zustände her und implementieren sie im Simulationscode. Es werden vorläufige Ergebnisse der effektiven Massen mit der Eichgruppe SU(2) vorgestellt.

Dedication

"I dedicate this thesis to my:

Wife, Samrah Fatima, who has always sacrificed every thing for me, born lot of stress to support me during my Ph.D studies: you are and always will be my perfect wife and mother to our children.

Mother, Rasheeda BiBi, there are no words that can express my feelings, I still remember those days when you always looked for me on every evening in the streets and waited for me until I got back home. Whenever I was sick you did every thing to keep me happy, there were no limits to the things you did.

Father, Niamat Ali, who alway loves me, supports me and prays for me.

Brother, Abid Ali, who takes good care of me, loves me and respects me just like his own son."

Acknowledgements

Contents

CONTENTS

Chapter 1

Introduction

The fundamental constituents, of which the whole known matter is composed of, are leptons and quarks. They interact via four fundamental forces of nature, namely strong, weak, electromagnetic and gravitational forces[1]. In particle physics, the Standard Model (SM) describes the electromagnetic, weak and strong interactions within the framework of Quantum Field Theory (QFT). Despite the fact that the Standard Model is the most successful theory valid up to the weak scale (100 GeV), some problems are still unsolved, i.e. what happens at smaller distances (higher energies), large number of free parameters, smallness of the weak scale, mismatch of three couplings at higher energies, mass hierarchy, neutrino masses, dark matter, etc [2]. Therefore, it is natural to study physics beyond the Standard Model (BSM), for example, Grand Unified Theories (GUT), technicolor theories, string theories and supersymmetric theories. These theories have been proposed and studied over the past decades. Supersymmetric extensions of the Standard Model have become very popular among theorists and experimentalists since they provide natural solutions to some non-trivial problems of the SM.

$\mathcal{N} = 1$ supersymmetric Yang-Mills (SYM) theory is a supersymmetric extension of pure gauge part of the SM [3]. In this thesis we focus on the non-perturbative dynamics of the strong interaction between the gluon and its superpartner, the gluino in $\mathcal{N} = 1$ SUSY Yang-Mills theory. Supersymmetry on the lattice at non-zero gluino mass is broken explicitly. To find the point

in parameter space where supersymmetry is restored and the theory has vanishing gluino mass as well as zero lattice spacing a, we have to fine tune the theory. For this purpose it is sufficient to tune the hopping parameter κ which is related to the gluino mass, and the inverse gauge coupling β which is related to the lattice spacing. In addition to the adjoint pion mass squared we employ supersymmetric Ward identities in order to tune $\mathcal{N} = 1$ SUSY Yang-Mills theory on the lattice [4]. In our collaboration, the major goal is to study, among other quantities, the mass spectrum of bound states in $\mathcal{N} = 1$ SUSY Yang-Mills theory on the lattice [3, 5, 6, 7, 8], to confirm the theoretical prediction based on effective actions [9, 10]. The particles of the spectrum arrange themselves in supermultiplets with same mass, this is the major motivation to investigate this model non-perturbatively. We also investigate the soft breaking of supersymmetry introduced by a non-zero gluino mass and the difference of mass between the particles belonging to the same supermultiplet. We also, for the first time, investigate an interesting particle composed of three gluinos called "baryon". This object is not a part of a chiral supermultiplet of effective actions VY [9] and and generalisation of VY [10]. The major focus of this thesis is the search for the supersymmetric point with the help of supersymmetric Ward identities. In addition, we also derive the correlation functions of the baryon and simulate them in order to find the mass of the baryon in $\mathcal{N} = 1$ supersymmetric Yang-Mills theory. In this thesis we proceed in the following way

1. In the first chapter, besides the general introduction we introduce supersymmetry and explain the importance of this symmetry. In addition, we also give a concise review of chiral and vector superfields.

2. In the second chapter we briefly explain $\mathcal{N} = 1$ SUSY Yang-Mills theory in the continuum reviewing the construction of the supersymmetric Yang-Mills action with $U_A(1)$ anomaly and the first order phase transition. We also discuss predictions based on effective actions about the mass spectrum of $\mathcal{N} = 1$ SUSY Yang-Mills theory and consequences of soft breaking of supersymmetry. In addition, we describe how the $\mathcal{N} = 1$ SUSY Yang-Mills theory can be simulated on the lattice, re-

lated challenges and techniques. Moreover, we give the details of the simulation parameters and perform the chiral and continuum extrapolations of our results to verify the mass degeneracy formation of the supermultiplet.

3. Chapter three essentially is about the data analysis techniques including effective mass, fitting correlation functions and variational analysis that we use to determine expectation values of masses and their uncertainties. These techniques rely on theoretical considerations of correlation functions and their lattice prescriptions which are also discussed in this chapter. For the measurements of the correlation functions with the help of powerful computing machines we need gauge ensembles which can be produced using a variety of algorithms. In particular, we discuss very briefly the two-step multi-boson (TSMB) algorithm for SYM theory with the gauge group SU(2) and the rational hybrid Monte Carlo (RHMC) algorithm with the gauge group SU(3).

4. The full analysis of supersymmetric Ward identities is provided in chapter four. We start from the derivation of the master formula for the Ward identities and then specify it for $\mathcal{N} = 1$ SUSY Yang-Mills theory in the continuum. To answer the question whether an anomaly appears in the supersymmetric Ward identity, we renormalise it. We also show numerical results of the correlation functions appearing in the formula of the Ward identities and do discrete symmetry tests in order to check the correctness of the numerical data from simulations. An important task is to estimate the subtracted gluino mass, which is done by three different methods that we call the Local, the Global and the GLS methods. Finally, the remnant gluino mass is obtained at vanishing adjoint pion mass squared to perform the chiral and continuum extrapolations in order to find the supersymmetric point.

5. The fifth chapter comprises the derivation of baryon correlation functions starting from the Rarita Schwinger field for SYM theory with the SU(2) and SU(3) gauge groups. We use discrete symmetries in order to

check the correctness of correlation function obtained numerically. The baryon correlation function has two contributions, the so-called sunset piece and the spectacle piece. The implementation of the sunset piece in the simulation code is simple whereas the spectacle piece is rather challenging. The signal for the spectacle piece obtained so far is noisy and the work is in progress to improve the signal-to-noise ratio.

6. The chapter six summarises the overall work and discusses possible future perspectives.

1.1 Supersymmetry (SUSY)

Since the seventies SUSY has played a vital role in the progress of theoretical physics, introduced in 2D world sheet theory in the context of string theory as a theoretical tool [11]. Soon after, it was believed that SUSY could be adopted in the elementary particle physics as a space-time symmetry in QFT: it was the birth of superstrings. Thereafter, innumerable supersymmetric theories have been formulated. These theories are invariant under global supersymmetry transformation or even under local SUSY i.e. supergravity.

Supersymmetry is a fascinating and an elegant idea that relates fermions to bosons whose spin differs by $\frac{1}{2}$ through the supercharge Q as

$$Q \left|\text{Boson}\right\rangle \sim \left|\text{Fermion}\right\rangle, \quad Q \left|\text{Fermion}\right\rangle \sim \left|\text{Boson}\right\rangle. \tag{1.1}$$

SUSY requires each particle to have its SUSY partner with equal mass, other properties could also be different but with spin difference of $\frac{1}{2}$ [12]. The bound states of fundamental particles arrange themselves into supermultiplets. SUSY transforms the members of multiplets into each other. Each supermultiplet is forced to include at least one fermion and one boson with spin difference of $\frac{1}{2}$. Many supersymmetric models are toy models. They have a high degree of symmetry, are simple to be solved, and serve as a guide towards realistic theories. As an example, the SUSY Yang-Mills theory may provide insights of the strong dynamics and quark confinement expected in Super QCD [13]. These models are dual between weak and strong coupling

and therefore are easily solvable whereas it is way more difficult to extend the same duality to non-symmetric theories. Up to now SUSY has not yet been observed in any of the experiments despite many searches at CERN laboratory. Hence SUSY is not exactly realised in nature otherwise we would have observed superpartners of the Standard Model particles, for example selectron with mass 0.51 MeV. However, there are several motivations to investigate the theories comprising supersymmetry.

To fill some of the gaps, SUSY is a potential extension of the Standard Model. Among the several reasons that particle physicists are interested in SUSY theories, the major motivation is that, in perturbation theory, the fermion and boson loops cancel each other which results in severe radiative corrections [11]. Outstanding examples consist of "the hierarchy problem" (large gap between the Higgs mass and the Planck scale), "extreme smallness of the cosmological constant", and "renormalisation of quantum gravity". Low energy limit of superstring theory is a promising candidate for unification of four fundamental forces. Supersymmetric theories unify three running couplings at large energy scale (10^{16} GeV) [14, 15]. SUSY has become a necessary ingredient so that the theories are consistent and more importantly it is being vastly used in non-abelian Yang-Mills theories which are strongly coupled theories like QCD [13]. A large number of new results on strong coupling and in non-perturbative sector of Yang-Mills theories have been obtained by supersymmetrising these theories. For the dark matter, an additional component of matter density, the "lightest supersymmetric particles (LSP)" are good candidates [16].

For the sake of completeness, we introduce briefly the SUSY-algebra and the superfields. For further reading and definitions of the quantities being used, references are given accordingly.

1.2 SUSY-algebra

SUSY-algebras are Z_2-graded Lie algebras which means that operators have "even" or "odd" labels. These operators obey the following (anti-)commutator

relations [13]

$$[even, even] = even, \tag{1.2}$$

$$[odd, even] = odd, \tag{1.3}$$

$$\{odd, odd\} = even. \tag{1.4}$$

To determine the structure of general SUSY-algebra, let's consider $[odd, even] = odd$ first

$$\left[Q_\alpha^i, B_a\right] = -(h_a)_{\alpha j}^{\beta i} Q_\beta^j. \tag{1.5}$$

where Q_α^i, $i = 1, \ldots, \mathcal{N}$ are the supercharges and B_a are the generators of the Poincaré group (Translations plus Lorentz group) with the index a as the number of generators. Further, h_a are structure constants of the graded algebra. The (Q, B_a, B_b)-Jacobi identity forces h_a matrices to show bosonic symmetry algebra

$$[h_a, h_b] = \mathrm{i} f_{abc} h_c, \tag{1.6}$$

where f_{abc} are the structure constants. Particular examples of B_a are P_μ (Translations) and $J_{\mu\nu}$ (Lorentz generators)

$$\left[Q_\alpha^i, P_\mu\right] = 0, \tag{1.7}$$

$$\left[Q_\alpha^i, J_{\mu\nu}\right] = (b_{\mu\nu})_{\alpha\beta} Q_\beta^i, \tag{1.8}$$

where $b_{\mu\nu} = \frac{1}{2}\sigma_{\mu\nu}$ is required for Q_α^i to be in the Lorentz group representation $(0, \frac{1}{2}) \oplus (\frac{1}{2}, 0)$. Similarly

$$\left[Q_\alpha^i, T^a\right] = (l^a)_{ij} Q_\alpha^j + \mathrm{i}(t^a)_{ij}(\gamma_5)_{\alpha\beta} Q_\beta^j, \tag{1.9}$$

where $l^a + \mathrm{i} t^a \gamma_5$ is an element of the Lie algebra of the internal symmetry group and T^a are the group generators.

For $\{odd, odd\} = even$, the most general relation compatible with Coleman-Mandula theorem

$$\left\{Q_\alpha^i, Q_\beta^j\right\} = -2\delta^{ij} (\gamma_\mu C)_{\alpha\beta} P_\mu + C_{\alpha\beta} U^{ij} + (\gamma_5 C)_{\alpha\beta} V^{ij}, \tag{1.10}$$

19

here U and V are "central charges" and commute with everything. The matrix C is charge conjugation matrix.

1.2.1 Irreducible representation

Some properties, independent of representation, of the SUSY algebra are given as follows [13]

SUSY Hamiltonian:

Eq. (1.10) together with the Majorana condition $\bar{Q}^i = (Q^i)^T C$, leads to

$$\left\{ Q^i_\alpha, \bar{Q}^j_\beta \right\} = 2\delta^{ij} \not{P}_{\alpha\beta} + \delta_{\alpha\beta} U^{ij} + (\gamma_5)_{\alpha\beta} V^{ij}. \tag{1.11}$$

By multiplying with γ_0 on both sides and taking the trace, we get

$$P_0 = \frac{1}{8N} \left\{ Q^i_\alpha \left(Q^i_\alpha \right)^\dagger + h.c. \right\} \geq 0. \tag{1.12}$$

This simply means that the Hamiltonian of SUSY theory is positive definite.

Same number of fermionic and bosonic degrees of freedom:

If N_F be the fermion number operator then we define a trace as

$$N_{b-f} = \text{tr} \left[(-1)^{N_F} \left\{ Q^i_\alpha, \bar{Q}^i_\beta \right\} \right]. \tag{1.13}$$

Using $(-1)^{N_F} Q^i_\alpha = -Q^i_\alpha (-1)^{N_F}$, we have

$$N_{b-f} = 2\not{P}_{\alpha\beta} \text{tr} \left[(-1)^{N_F} \right], \tag{1.14}$$

$$N_{b-f} = 0, \quad \text{for } P_0 \neq 0, \tag{1.15}$$

here $w = \text{tr} \left[(-1)^{N_F} \right] = n_{\text{boson}} - n_{\text{fermion}}$ is called Witten index, where n_{boson} is number of zero energy bosonic states and n_{fermion} is number of zero energy fermionic states. Note here that the Witten index w is zero, therefore n_{boson} and n_{fermion} degree of freedom is same. However, we can not generalise this,

for example in the adjoint representation of SUSY-algebra at $P = 0$, the n_{boson} and the n_{fermion} are different from each other.

Regarding the breaking of SUSY we have the following cases [17]:

Case I, $w \neq 0$:

If there is imbalance between n_{boson} and the n_{fermion} then SUSY is not broken spontaneously.

Case II, $w = 0$ and $n_{\text{boson}} = n_{\text{fermion}} \neq 0$:

In this case SUSY is not broken spontaneously.

Case III, $w = 0$ and $n_{\text{boson}} = n_{\text{fermion}} = 0$:

If there are not zero energy states at all then SUSY is broken spontaneously.

1.2.2 Chiral superfield

In order to obtain chiral supermultiplet we consider $S_\chi(x, \theta, \bar{\theta})$ as chiral (or left chiral) superfield and its complex conjugate field $S_\chi^*(x, \theta, \bar{\theta})$ as anti-chiral (or right chiral) superfield [18]. Where θ and $\bar{\theta}$ are anti-commuting Grassmannian coordinates whereas x is a space-time coordinate, they span a superspace. Introducing the coordinates $y^\mu = x^\mu + i\theta\sigma^\mu\bar{\theta}$, these superfields have the following constraints

$$\bar{D}_{\dot{\alpha}} S_\chi = 0, \tag{1.16}$$

$$D_\alpha S_\chi^* = 0. \tag{1.17}$$

with the chiral covariant derivatives

$$D_\alpha = \frac{\partial}{\partial\theta^\alpha} + 2i\left(\sigma^\mu\bar{\theta}\right)_\alpha \frac{\partial}{\partial y^\mu}, \tag{1.18}$$

$$\bar{D}_{\dot{\alpha}} = \frac{\partial}{\partial\bar{\theta}^{\dot{\alpha}}}, \tag{1.19}$$

where σ^μ are the Pauli matrices with σ^0 as 2×2 identity matrix [18]. From Eq. (1.19) it is obvious that $S_\chi(y, \theta, \bar{\theta})$ can be chosen as any function excluding $\bar{\theta}$ dependence. In the simplest model, for the case of a free chiral supermultiplet, one possible choice for chiral superfield can be

$$S_\chi(y, \theta) = \phi(y) + \sqrt{2}\theta\chi(y) + \theta^2 H(y). \tag{1.20}$$

The factor $\sqrt{2}$ is conventional. The fields represent

- $\phi(y)$ is a complex scalar field,

- $\chi(y)$ is a two-component fermion field,

- $H(y)$ is an auxiliary field.

Their explicit forms will be given in Sec. (2.1.4)

1.2.3 Vector superfield

To obtain a vector (or real) superfield $V(x, \theta, \bar{\theta})$, we impose the condition $V^\dagger = V$. The vector superfield in terms of its components reads [18]

$$V(x, \theta, \bar{\theta}) = \phi(x) + \sqrt{2}\theta\chi(x) + \sqrt{2}\bar{\theta}\bar{\chi}(x) + \theta^2 H(x) + \bar{\theta}^2 \bar{H}(x) \tag{1.21}$$
$$+ \theta\sigma^\mu\bar{\theta}A_\mu(x) + \bar{\theta}^2\theta\eta_\alpha(x) + \theta^2\bar{\theta}\bar{\eta}_\alpha(x) + \theta^2\bar{\theta}^2 d(x), \tag{1.22}$$

where

$$\eta_\alpha(x) = \lambda_\alpha(x) - \frac{\mathrm{i}}{\sqrt{2}}\left(\bar{\sigma}^\mu\partial_\mu\bar{\chi}\right), \tag{1.23}$$

$$d(x) = \frac{1}{2}D(x) + \frac{1}{4}\partial_\mu\partial^\mu\phi(x). \tag{1.24}$$

This vector supermultiplet consists of

- $A_\mu(x)$ is a gluon field,

- $\lambda(x)$ is a gluino field,

- $D(x)$ is a gauge auxiliary field.

22

To make full field theory representation we have to formulate an invariant action for the multiplets that will be given in the next chapter.

1.3 Motivations

$\mathcal{N} = 1$ SUSY Yang-Mills theory is the minimal supersymmetric extension of the gluonic part of the Standard Model of particle physics. It describes the strong interaction of the gluon and the gluino, the supersymmetric partner of the gluon [3]. It is a simple model with gauge invariance and supersymmetry. Moreover, it is similar to QCD [19], where we have the asymptotic freedom and the confinement of fundamental constituents. In the low energy regime, the numerical simulations are possible. In addition, we verify the mass spectrum predicted by effective actions [9, 10]. In this model, the bound states of the spectrum arrange themselves in a chiral supermultiplet, if SUSY is not broken. However, on the lattice SUSY is broken due to a non-zero gluino mass and due to the lattice regulator, which motivates us to study it on the lattice to check whether the chiral supermultiplet is still formed in the chiral and in the continuum limits.

Chapter 2

$\mathcal{N} = 1$ SUSY Yang-Mills theory

In this chapter we shall briefly introduce theoretical background of the $\mathcal{N} = 1$ SUSY Yang-Mills theory. The answer of a very interesting and important question regarding spontaneous breaking of SUSY will also be addressed here. We include predictions for the bound states of the theory from the effective actions, these bound state form mass degenerate supermultiplets at vanishing gluino mass. At non-zero gluino mass the degeneracy of the spectrum is broken, this scenario is called soft breaking of SUSY and will also be addressed. In addition, we give the lattice formalism of SYM theory and discuss related challenges. Finally, we show the mass degeneracy formation of the chiral supermultiplet by performing the chiral and the continuum extrapolations.

2.1 $\mathcal{N} = 1$ SUSY Yang-Mills theory in the continuum

$\mathcal{N} = 1$ SUSY Yang-Mills theory (SYM) is the minimal supersymmetric extension of the pure gauge part of the Standard Model of particle physics. It describes the strong interaction of gluons and gluinos, the supersymmetric partners of gluons. It is a gauge theory with fermions as degrees of freedom and similar to QCD in this respect, see Ref. [3] and Refs. therein. An important difference is, however, that the gauge invariance together with

supersymmetry requires the gluinos to be Majorana fermions transforming in the adjoint representation of $SU(N_c)$. In order to construct a model with SUSY and gauge invariance, one has to consider a vector superfield $V(x, \bar{\theta}, \theta)$, satisfying $V^\dagger = V$, and in Wess-Zumino gauge [20] it is given as

$$V_{WZ}(x, \theta, \bar{\theta}) = \theta \sigma^\mu \bar{\theta} A_\mu + \mathrm{i}(\theta\theta)\bar{\theta}\bar{\psi} - \mathrm{i}(\bar{\theta}\bar{\theta})\psi + \frac{1}{2}(\theta\theta)(\bar{\theta}\bar{\theta})D, \qquad (2.1)$$

where the gauge boson A_μ is a real vector field of gauge boson, ψ is complex Weyl-spinor field representing the superpartner of the gauge boson and D is an auxiliary field. This vector superfield transforms under the non-abelian gauge transformation according to [11]

$$e^{V'} = e^{-\mathrm{i}\Lambda^\dagger} e^V e^{\mathrm{i}\Lambda}, \qquad (2.2)$$

where Λ is a chiral superfield. To obtain an action that contains SUSY together with gauge invariance, based on "superfields" [21, 22, 23], we introduce the spinorial field strength superfield $W_\alpha \equiv W_\alpha(x, \theta_\alpha, \bar{\theta}_{\dot{\alpha}})$ that depends upon space time coordinates x_μ for $\mu = 0, 1, 2, 3$ and on the anti-commuting Weyl-spinor variables $\theta_\alpha, \bar{\theta}_{\dot{\alpha}}$ for $\alpha, \dot{\alpha} = 1, 2$, and it is given as [18]

$$W_\alpha = -\frac{1}{8}(\bar{D}\bar{D})e^{-2V}D_\alpha e^{2V}, \qquad (2.3)$$

with the superspace derivatives

$$\bar{D}_{\dot{\alpha}} = -\bar{\partial}_{\dot{\alpha}} - \mathrm{i}\theta^\beta \sigma^\mu_{\beta\dot{\alpha}}\partial_\mu, \quad D_\alpha = \partial_\alpha + \mathrm{i}\sigma^\mu_{\alpha\dot{\beta}}\bar{\theta}^{\dot{\beta}}\partial_\mu. \qquad (2.4)$$

The general form of Wess-Zumino gauge action in Minkowski space for $\mathcal{N} = 1$ SUSY Yang-Mills theory with $SU(N_c)$ gauge group in terms of W_α is written as

$$S_{SYM} = \mathrm{Re}\left\{ \int d^4x \, d^2\theta \, \mathrm{tr}_c\left[W^\alpha W_\alpha\right]\right\}, \qquad (2.5)$$

where tr_c represents the trace over colour indices. In the Wess-Zumino gauge the bosonic vector field A_μ reads

$$A_\mu = -\mathrm{i}gT^a A^a_\mu, \qquad (2.6)$$

where g is the gauge coupling and a is the colour index, where $a = 1, \ldots, N_c^2 - 1$. T^a is $N_c \times N_c$ matrix called generators of the gauge group $SU(N_c)$ with the normalisation relation $2\,\mathrm{tr}[T^a T^b] = \delta^{ab}$, its explicit form is given in Appendix (A.1). SUSY requires a fermionic superpartner of the bosonic field A_μ which is a spin-$\frac{1}{2}$ complex Weyl-spinor field, and is defined as

$$\psi_\alpha = \psi_\alpha^a T^a. \tag{2.7}$$

The invariance of the action under SUSY and gauge transformation demands the fermionic fields to be in the adjoint representation of the gauge group $SU(N_c)$. Therefore the fermion, associated to fermion field, is spin-$\frac{1}{2}$ Majorana particle satisfying the following Majorana condition

$$\bar{\psi} = \psi^T C, \tag{2.8}$$

where C is the charge conjugation matrix that relates particle and antiparticle fields, which means that particles and anti-particles in this model are same. Note that Eq. (2.8) is derived from analytical continuation of correlation functions from Minkowski to Euclidean space and holds for a Euclidean Majorana field [25, 26]. The Grassmannian integration w.r.t. θ of the action in Eq. (2.5) leaves the following result

$$S_{SYM} = \int d^4x \left\{ -\frac{1}{4} F_{\mu\nu}^a F_{\mu\nu}^a + \frac{\mathrm{i}}{2} \psi^a \sigma_\mu (D_\mu \bar{\psi})^a - \frac{\mathrm{i}}{2} (D_\mu \bar{\psi})^a \bar{\sigma}_\mu \psi^a + \frac{1}{2} D^a D^a \right\}, \tag{2.9}$$

where D^a is the auxiliary scalar field which lacks a kinetic term and can be integrated out by Gaussian integration, and $F_{\mu\nu}^a$ is the field strength tensor which is given as

$$F_{\mu\nu} = -\mathrm{i}g F_{\mu\nu}^a T^a = \partial_\mu A_\nu - \partial_\nu A_\mu + [A_\mu, A_\nu], \tag{2.10}$$

and D_μ is the covariant derivative in the adjoint representation

$$(D_\mu \bar{\psi})^a = \partial_\mu \bar{\psi}^a + g f_{abc} A_\mu^b \bar{\psi}^c. \tag{2.11}$$

Let λ be a Majorana bi-spinor in the adjoint representation of the gauge group SU(N_c). It can be represented in terms of the Weyl-spinors ψ and $\bar{\psi}$ as

$$\lambda = \begin{pmatrix} \psi_\alpha \\ \bar{\psi}_{\dot{\alpha}} \end{pmatrix}. \tag{2.12}$$

The following transformations change the Lagrangian density leading to the action of Eq. (2.9) only by a total divergence $\delta\mathcal{L} = \partial^\mu \bar{j}_\mu \epsilon = \bar{\epsilon} \partial^\mu j_\mu$ [27]

$$\delta A_\mu = -2g\bar{\lambda}\gamma_\mu\epsilon, \tag{2.13}$$

$$\delta\lambda = -\frac{i}{g}\sigma_{\mu\nu}F^{\mu\nu}\epsilon, \tag{2.14}$$

$$\delta\bar{\lambda} = +\frac{i}{g}\bar{\epsilon}\sigma_{\mu\nu}F^{\mu\nu}, \tag{2.15}$$

where ϵ is a Grassmannian spinor parameter and $j_\mu = -\frac{1}{2}S_\mu$. This leaves the supercurrent S_μ conserved, and for $\mathcal{N} = 1$ SUSY Yang-Mills theory it gets the following form

$$S_\mu = -\frac{i}{g}\sigma^{\nu\rho}F^a_{\nu\rho}\gamma_\mu\lambda_a, \tag{2.16}$$

The on-shell Lagrangian density $\mathcal{L}_{SYM}$ in Minkowski space from the action in Eq. (2.9) reads

$$\mathcal{L}_{SYM} = -\frac{1}{4}F^a_{\mu\nu}F^{\mu\nu}_a + \frac{i}{2}\bar{\lambda}^a\gamma^\mu\left(D_\mu\lambda\right)_a. \tag{2.17}$$

2.1.1 $U_A(1)$ anomaly and first order phase transition

In addition to the SUSY and the gauge transformations, the Lagrangian density is also invariant under $U_A(1)$ transformation of the field λ which coincides with R-symmetry of the SUSY supercharges. The $U_A(1)$ symmetry transformation is given as [27]

$$\lambda' = e^{i\phi\gamma_5}\lambda, \tag{2.18}$$

the corresponding axial current

$$J^5_\mu = \bar{\psi}^a \gamma_\mu \gamma_5 \psi^a, \tag{2.19}$$

has a divergence equal to

$$\partial^\mu J^5_\mu = \frac{N_c g^2}{32\pi^2} \epsilon_{\mu\nu\rho\sigma} F^a_{\mu\nu} F^a_{\rho\sigma}. \tag{2.20}$$

Therefore, $U_A(1)$ symmetry (global chiral symmetry in this case) is anomalous. However, a subgroup Z_{2N_c} of $U_A(1)$ is still unbroken for [27]

$$\phi = \phi_k \equiv \frac{k\pi}{N_c}, \quad \text{where } k = 0, 1, \ldots, 2N_c - 1. \tag{2.21}$$

Moreover, when the fermionic condensate $\langle \bar{\lambda}\lambda \rangle$

$$\langle \bar{\lambda}\lambda \rangle \propto \mu^3 e^{2\pi k/N_c}, \quad \text{where } k = 0, 1, \ldots, N_c - 1, \tag{2.22}$$

is non-zero [28, 29], the residual discrete global chiral symmetry Z_{2N_c} is expected to be broken spontaneously to Z_2, where Z_2 is change of sign i. e. $\lambda \to -\lambda$. The parameter μ is the scale parameter for the gauge group $SU(N_c)$. The breaking of this discrete global chiral symmetry results in a first order phase transition at $m_{\tilde{g}} = 0$, see Fig. (2.5). As a consequence, N_c number of degenerate vacua exist which are related by transformations of the quotient group $\frac{Z_{2N_c}}{Z_2}$.

2.1.2 Is SUSY broken spontaneously?

The answer of this essential and interesting question is given by the value of the Witten index w [30]

$$w \equiv \text{tr}\left[(-1)^{N_F}\right] = n_{\text{boson}} - n_{\text{fermion}}, \tag{2.23}$$

it is the difference of bosonic and fermionic ground states. In pure SUSY Yang-Mills theory, in the absence of additional matter supermultiplets, the Witten index w_{SYM} is equal to number of colours N_c because there are not any fermionic ground states and bosonic states are equal to N_c [31]. There-

fore, as a consequence, the SUSY is not broken spontaneously.

2.1.3   Spectrum of $\mathcal{N} = 1$ SUSY Yang-Mills theory

Just like QCD, in $\mathcal{N} = 1$ SUSY Yang-Mills theory at low energy the fundamental particles are confined into colour-neutral bound states. Some of these states consist of mesons, glueballs and the gluino-glue. If the SUSY is realised in this model then the bound states form a chiral supermultiplet with same masses. This scenario is shown in Fig. (2.1)
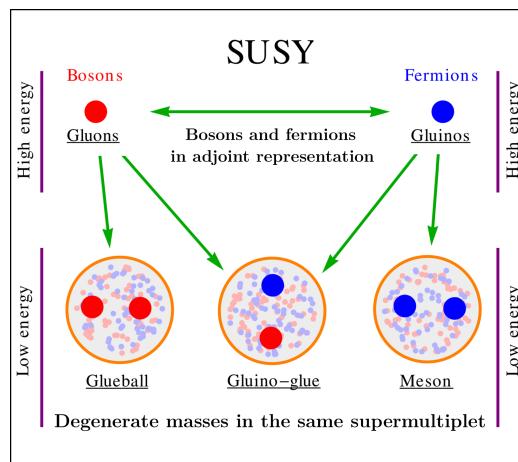
Figure 2.1: In $\mathcal{N} = 1$ SUSY Yang-Mills theory, the fundamental particles are gluon and its superpartner, the gluino. Due to asymptotic freedom they are free at high energy. At low energy, however, they show confinement and form colour-neutral bound states that result into glueballs, mesons and the gluino-glue. At zero gluino mass they have same masses belonging to the same supermultiplet. This figure is take from Ref. [17] and modified.

2.1.4   Predictions from the effective actions

The spectrum of masses is independent of the effective actions, but different effective actions provide insights into different parts of the spectrum. Here we consider the predictions from the VY effective action [9] and from the generalisation of the VY effective action [10].

The VY effective action [9]:

At the classical level, the action of $\mathcal{N} = 1$ SUSY Yang-Mills theory is symmetric under $U_A(1)$, and superconformal transformations. At the quantum level, however, these symmetries are broken by their corresponding anomalies. The chiral supermultiplet S_χ can the be expressed in terms of linear combination of operators that appear in the formulas of anomalies [32, 33]

$$S_\chi(x, \theta) = \phi(x) + \sqrt{2}\theta\chi(x) + \theta^2 H(x), \tag{2.24}$$

where $\phi(x)$ is the lowest component containing scalar and pseudoscalar composites with corresponding quantum numbers whereas $\chi(x)$ is a fermionic component describing the gluino-glue bound states. Apparently, there is no kinetic term in $H(x)$, for details see Ref. [9], and it can be integrated out from S_χ with the help of Euler-Lagrange equation. The lowest-spin scalar, pseudoscalar and fermionic operators are given as

$$\phi(x) = -\frac{\beta(g)}{2g}\lambda^\alpha\lambda_\alpha, \quad \chi(x) = \frac{\beta(g)}{2^{3/2}g}\left\{-i\lambda_\alpha D + (\sigma^{\mu\nu}\lambda)_\alpha F_{\mu\nu}\right\}. \tag{2.25}$$

Here $\beta(g)$ is defined in Ref. [34], and D is component of non-abelian vector superfield which is eliminated by means of the equations of motion. The composite operators in Eq. (2.24) are interpolating fields for $\mathcal{N} = 1$ SUSY Yang-Mills theory and have zero anomalous dimensions. Therefore, the mass of the corresponding particles can be obtained by the correlation functions (correlators) of those fields. Moreover, the VY effective action in terms of chiral superfield S_χ can be written as

$$S_{VY} = \int d^4x \frac{1}{\alpha}\left(S_\chi^+ S_\chi\right)^{1/3}\Big|_D + \gamma\left[\left(S_\chi \, log\left(\frac{S_\chi}{\mu^3}\right) - S_\chi\right)\Big|_H + h.c.\right], \tag{2.26}$$

where $(S_\chi^+ S_\chi)^{1/3}$ is the Kähler potential that obeys scale, $U_A(1)$, and superconformal symmetries. α and γ are positive constants. Based on these correlation functions, one expects the following lowest-spin supermultiplet of J^{PC} eigenstates with corresponding operators

- scalar, 0^{++}, l = 1, s = 1 $\sim \bar{\lambda}\lambda$ (a-f_0)
  gluino-gluino bound state (gluinoball);

- pscalar, 0^{-+}, l = 0, s = 0 $\sim \bar{\lambda}\gamma_5\lambda$ (a-η')
  gluino-gluino bound state (gluinoball);

- spinor, $\frac{1}{2}^{i+}$, l = 1, s = $\frac{1}{2}$ $\sim \sigma^{\mu\nu}F_{\mu\nu}\lambda$ ($g\tilde{g}$)
  gluon-gluino bound state (gluino-glueball).

Generalisation of the VY effective action [10]:

The VY effective action does not contain all possible lowest-spin composites. The bound states of gluon-gluon, after this referred as "glueballs", are absent. In order to include glueballs in the spectrum, we have to concentrate on the field $H(x)$ from Eq. (2.24) which has been ignored in VY action. By using the equations of motion for D and for λ in $H(x)$, we obtain

$$H(x) \equiv \frac{\beta(g)}{4g}\Big[F^{\mu\nu}F_{\mu\nu} + \frac{\mathrm{i}}{2}F^{\mu\nu}\epsilon_{\mu\nu\rho\sigma}F^{\rho\sigma}\Big], \qquad (2.27)$$

The first term of Eq. (2.27) represents a scalar glueball and from the second term, by means of three-form potential and real tensor superfield, one obtains a pseudo-scalar glueball and a gluino-glue, for further details see Ref. [10]. As a consequence, an additional chiral supermultiplet with corresponding quantum numbers is given as

- scalar, 0^{++}, l = 0, s = 0 $\sim F^{\mu\nu}F_{\mu\nu}$ (gb)
  gluon-gluon bound state (glueball);

- pscalar, 0^{-+}, l = 1, s = 1 $\sim F^{\mu\nu}\epsilon_{\mu\nu\rho\sigma}F^{\rho\sigma}$ (gb)
  gluon-gluon bound state (glueball);

- spinor, $\frac{1}{2}^{(-i)+}$, l = 0, s = $\frac{1}{2}$ $\sim \sigma^{\mu\nu}F_{\mu\nu}\lambda$ ($g\tilde{g}$)
  gluon-gluino bound state (gluino-glueball).

Generally, the operators of physical states have mixing when they share common transformation properties. Physical states of the above supermultiplets

are not purely gluon-gluon, gluino-gluino or the gluino-glue, but are rather mixtures of these composites. Therefore, it is natural to expect mixing among scalar and pseudo-scalar glueballs with corresponding mesons. The investigation of the model including mixing shows that the physical states are settled from two distinct mass "multiplets" [32]. The heavier set of physical states (m^+) from VY effective action has:

- A scalar meson $\xrightarrow{\text{without mixing}}$ a-f_0.

- A pseudoscalar meson $\xrightarrow{\text{without mixing}}$ a-η'.

- A gluino-glue fermion $(g\tilde{g})$.

The lighter set of physical states (m^-) obtained from the generalisation of the VY effective action contains:

- A scalar state $\xrightarrow{\text{without mixing}}$ 0^{++} glueball.

- A pseudoscalar state $\xrightarrow{\text{without mixing}}$ 0^{-+} glueball.

- A gluino-glue fermion $(g\tilde{g})$.

This scenario together with soft breaking of SUSY is shown in Fig. (2.2).

In addition to these supermultiplets, besides others an other interesting object interpolated by operators composed of three gluino fields. We call these objects "baryons" in analogy to the baryons in QCD with three quarks (anti-)quarks. This bound state is not present in the effective actions [9, 10], however, there is no any argument against the presence of this state. Therefore, we develop and construct the corresponding operator and discuss it in details in Ch. (5).

2.1.5 Ward identity in $\mathcal{N} = 1$ SUSY Yang-Mills theory

The SUSY Ward identity is the quantum version of the Noether theorem in the classical theory which gives a conserved current corresponding to the symmetric action of a physical system corresponding each continuous symmetry of the action of the system [35]. Due to quantum effects, however, an
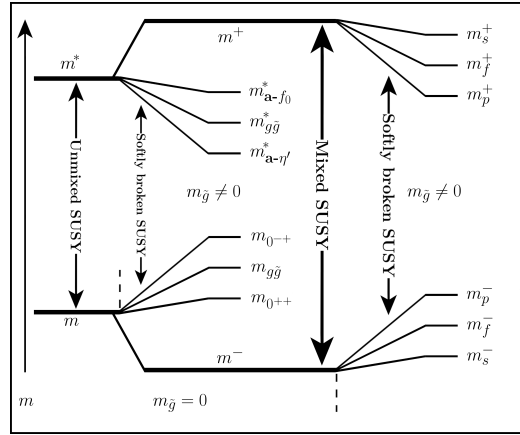
Figure 2.2: Theoretical spectrum predicted by the VY and by the generalisation of VY form two distinct supermultiplets without mixing. Physical states, however, are mixtures of particles and supermultiplets are different from the unmixed states. Furthermore, non-zero gluino mass in the action breaks the SUSY softly and the particle spectrum is shifted. The subscripts s, p and f stand for scalar, pseudoscalar and fermion. This figure is based on Ref. [32].

additional term appears which is called the contact term. If we ignore this term then the divergence of the supercurrent will be zero and one obtains a conserved supercurrent. This identity is very useful in the case where SUSY is explicitly broken. By making use of this identity one can tune the theory in order to obtain SUSY point where broken SUSY is recovered. Therefore, among the other quantities the SUSY Ward identity can also be used to tune the theory and ensures the recovery of the explicitly broken SUSY. In Ch. (4) we shall discuss its forms in the continuum and on the lattice. We also renormalise it in order to check the existence of the anomalies and treat properly the additional symmetry breaking terms [4]. SUSY Ward identity is a good candidate for a cross check of correctness of tuning of the theory in its numerical simulations.

2.1.6 Soft breaking of SUSY

In the case where the gluino has a non-zero mass ($m_{\tilde{g}} \neq 0$), an additional mass term ($-\frac{1}{2} m_{\tilde{g}} \bar{\lambda}^a \lambda_a$) will appear in the potential of Lagrangian density

which modifies it as follows [3]

$$\mathcal{L}_{SYM} = -\frac{1}{4}F^a_{\mu\nu}F^{\mu\nu}_a + \frac{\mathrm{i}}{2}\bar{\lambda}^a\gamma^\mu\left(D_\mu\lambda\right)_a - \frac{1}{2}m_{\tilde{g}}\bar{\lambda}^a\lambda_a. \qquad (2.28)$$

This Lagrangian density is not invariant under SUSY transformation anymore. Due to the non-zero mass of the gluino field, the breaking of SUSY is soft. The degeneracy of N_c vacua is broken, this means that there exist N_c non-degenerate vacuum states for $m_{\tilde{g}} \neq 0$. According to Eq. (2.22), in Dirac representation, one gets two condensates: a scalar condensate $\langle\bar{\lambda}\lambda\rangle$ and a pseudoscalar condensate $\langle\bar{\lambda}\gamma_5\lambda\rangle$. In $\mathcal{N} = 1$ SUSY Yang-Mills theory with the gauge group SU(2) we expect that the theory is characterised by 2 vacua whereas with the gauge group SU(3) it is characterised by 3 vacua. Qualitatively, it is represented in Fig. (2.3) where x-axis has $\langle\bar{\lambda}\lambda\rangle$ and on y-axis we put $\langle\bar{\lambda}\gamma_5\lambda\rangle$, for details see Ref. [31] and Refs. therein. The spectrum of particle masses predicted by means of the effective actions is modified too. According to Ref. [32], masses of the physical states in the m^+ multiplet at non-zero gluino mass gets lowered whereas this behavior is opposite in the m^- multiplet. In the scalar channel this shift is small and the pseudoscalar channel gets the largest change, whereas the fermion stays in between the scalar and pseudoscalar in both multiplets. The whole shift, due to softly broken SUSY of mixed case and of unmixed case, is demonstrated in Fig. (2.2).

2.2 $\mathcal{N} = 1$ **SUSY Yang-Mills theory on the lattice**

Discretisation of the space-time with lattice spacing a spoils most of the symmetries related to space-time and Poincaré invariance. Eq. (1.10) for SYM theory reads

$$\{Q_\alpha, Q_\beta\} = (C\gamma_\mu)_{\alpha\beta}\,P_\mu, \qquad (2.29)$$

It is apparent from Eq. (2.29) that SUSY itself is broken on the lattice. Here Q_α are the SUSY generators and P_μ are the generators of translations. The infinitesimal translations generated by P_μ are not possible any more if

(a) SU(2) (b) SU(3)
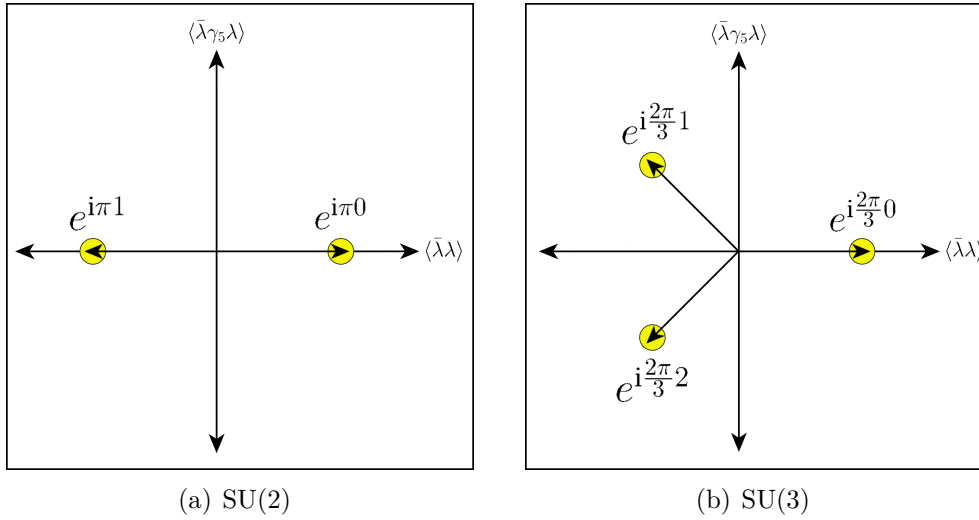
Figure 2.3: Vacua of $\mathcal{N} = 1$ SUSY Yang-Mills theory with SU(2) and SU(3) gauge groups.

the formalism is put onto the lattice, which breaks SUSY unavoidably, for details see [36]. The restoration of broken SUSY is an important test for the validity of numerical simulations for $\mathcal{N} = 1$ SUSY Yang-Mills theory where this restoration is shown in terms of degeneracies of the mass spectrum of bound states [8] and can be cross checked by SUSY Ward identities [37]. For this purpose, we have to tune some parameters, see Sec. (2.3.1).

2.2.1   Lattice formulation

To put the whole formulation of $\mathcal{N} = 1$ SUSY Yang-Mills theory on the hypercubic space-time lattice, we consider the lattice action (S_{CV}^{lat}) suggested by Curci and Veneziano [38] in the Wilsonian framework. It consists of a gauge part (S_g) and the fermionic part (S_f) as

$$S_{CV}^{lat} = S_g + S_f, \tag{2.30}$$

where

$$S_g = \beta \sum_{\mu\nu} \left(1 - \frac{1}{N_c} \mathrm{Re}\Big[\mathrm{tr}[U_{\mu\nu}]\Big]\right), \tag{2.31}$$

with the inverse gauge coupling $\beta = \frac{2N_c}{g^2}$. The trace is over the colour indices and over all lattice sites. The plaquette variable $U_{\mu\nu}(x)$, which is related to the field strength by $U_{\mu\nu}(x) = e^{-a^2 F_{\mu\nu}(x)}$, is the product of path-ordered links $U_\mu(x)$ around the boundary of "U" [24]. It is shown in Fig. (2.4) and mathematically given as
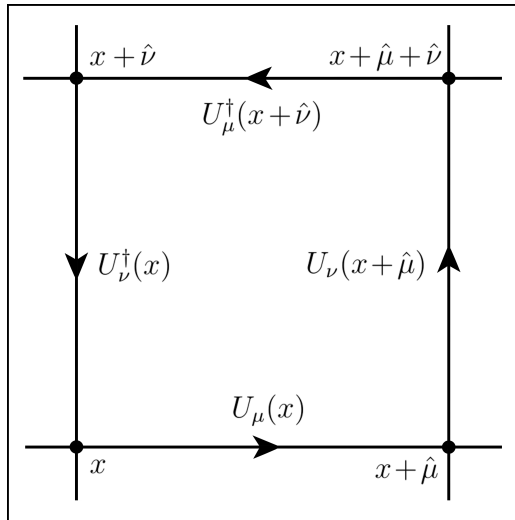
Figure 2.4: Elementary plaquette $U_{\mu\nu}(x)$ at space-time coordinate x in the $\mu\nu$-plane.

$$U_{\mu\nu}(x) = U_\mu(x)U_\nu(x + \hat{\mu})U_\mu^\dagger(x + \hat{\nu})U_\nu^\dagger(x), \tag{2.32}$$

here gauge link is connected to gauge field by the relation $U_\mu(x) = e^{-aA_\mu(x)}$. We define the anti-symmetrized clover plaquette $P_{\mu\nu}^{(cl)}(x)$ as

$$P_{\mu\nu}^{(cl)}(x) = \frac{1}{8\,\mathrm{i}g}\Big(U_{\mu\nu}^{(cl)}(x) - U_{\mu\nu}^{(cl)\dagger}(x)\Big). \tag{2.33}$$

The $P_{\mu\nu}^{(cl)}(x)$ is constructed from the clover plaquette $U_{\mu\nu}^{(cl)}(x)$ in fundamental representation that shares the same time-reversal and parity transformation as the field strength tensor $F_{\mu\nu}$ [39]. In terms of link variables the clover

plaquette is given as [51]

$$
\begin{aligned}
U_{\mu\nu}^{(cl)} &= U_\mu(x)U_\nu(x+\mu)U_\mu^\dagger(x+\nu)U_\nu^\dagger(x) \quad\quad (2.34) \\
&+ U_\nu^\dagger(x-\nu)U_\mu(x-\nu)U_\nu(x-\nu+\mu)U_\mu^\dagger(x) \\
&+ U_\mu^\dagger(x-\mu)U_\nu^\dagger(x-\mu-\nu)U_\mu(x-\mu-\nu)U_\nu(x-\nu) \\
&+ U_\nu(x)U_\mu^\dagger(x+\nu-\mu)U_\nu^\dagger(x-\mu)U_\mu(x-\mu).
\end{aligned}
$$

The fermionic part (S_f) of the full action (S_{CV}^{lat}) reads

$$
\begin{aligned}
S_f = \frac{1}{2}\sum_x \Big\{ &\bar{\lambda}_a^\alpha(x)\lambda_a^\alpha(x) - \kappa \sum_{\mu=1}^4 \Big[\bar{\lambda}_a^\alpha(x+\hat{\mu})V_{ab,\mu}(x)(\mathbf{1}+\gamma_\mu)^{\alpha\beta}\lambda_b^\beta(x) \quad (2.35) \\
&+ \bar{\lambda}_a^\alpha(x)V_{ab,\mu}^T(x)(\mathbf{1}-\gamma_\mu)^{\alpha\beta}\lambda_b^\beta(x+\hat{\mu})\Big] \Big\},
\end{aligned}
$$

where the λ and $\bar{\lambda}$ are not independent, but are related by the Majorana condition $\lambda = C\bar{\lambda}^T$. The hopping parameter κ is related to the gluino mass by the relation given in Eq. (2.49). The adjoint link variables get the form [52]

$$
V_{ab,\mu}(x) = 2\,\mathrm{tr}\Big[U_\mu^\dagger(x)T_a U_\mu(x)T_b\Big], \quad\quad (2.36)
$$

where $V_{ab,\mu}(x)$ satisfies the following properties

$$
V_{ab,\mu}(x) = V_{ab,\mu}^*(x) = \Big(V_{ab,\mu}^T(x)\Big)^{-1}. \qu\quad (2.37)
$$

The S_f can also be written like

$$
S_f = \frac{1}{2}\sum_{x,y}\bar{\lambda}_a^\alpha(x)(D_w)_{ab}^{\alpha\beta}(x,y)\lambda_b^\beta(y), \qu\quad (2.38)
$$

where the fermionic matrix (D_w) reads

$$
\begin{aligned}
(D_w)_{ab}^{\alpha\beta}(x,y) = \delta_{ab}\delta_{xy}\delta^{\alpha\beta} - \kappa \sum_{\mu=1}^4 \Big[&\delta_{y,x+\hat{\mu}}V_{ab,\mu}(x)(\mathbf{1}+\gamma_\mu)^{\alpha\beta} \quad (2.39) \\
&+ \delta_{y+\hat{\mu},x}V_{ab,\mu}^T(y)(\mathbf{1}-\gamma_\mu)^{\alpha\beta}\Big].
\end{aligned}
$$

The eigenvalues of matrix D_w are not real. We define $\tilde{D}_w = \gamma_5 D_w$ which is Hermitian due to the γ_5 hermiticity of D_w ($D_w^\dagger = \gamma_5 D_w \gamma_5$) and has doubly degenerate real eigenvalues. Furthermore, D_w satisfies the following relations

$$C\gamma_5 D_w \gamma_5 C^{-1} = D_w^*, \quad C D_w C^{-1} = D_w^T, \tag{2.40}$$

$$\det(D_w) = \det(\tilde{D}_w) = \prod_i \tilde{w}_i^2 \geq 0. \tag{2.41}$$

Where $\tilde{w}_i$ are the eigenvalues of matrix $\tilde{D}_w$. The following path integral representation in Euclidean space gives the two point correlation function for the gluino field

$$\langle T\{\lambda(x)\bar{\lambda}(y)\}\rangle = \frac{\int [dU][d\lambda]\,\lambda(x)\bar{\lambda}(y)\,e^{-S_{CV}^{lat}}}{\int [dU][d\lambda]\,e^{-S_{CV}^{lat}}}. \tag{2.42}$$

Here the integration is over $[d\bar{\lambda}]$ is ignored because λ and $\bar{\lambda}$ are not independent. Moreover, number of degrees of freedom for Majorana fermions is half than the one of Dirac fermions. For the sake of convenience we integrate out the gluino field from the above path integral. The integral

$$\int [d\lambda]\,e^{-\frac{1}{2}\bar{\lambda}D_w\lambda}, \tag{2.43}$$

is the "Pfaffian" of the anti-symmetric matrix $M = C D_w$ and it is related to the determinant as [27]

$$\mathrm{Pf}(M)^2 = \det(D_w) = \det(M), \tag{2.44}$$

it can also be written as

$$\mathrm{Pf}(M) = \sqrt{\det(D_w)} \times \mathrm{sign}\big(\mathrm{Pf}(M)\big). \tag{2.45}$$

In terms of polynomial of M the above Pfaffian reads

$$\mathrm{Pf}(M) = \frac{1}{N!2^N}\epsilon_{\alpha_1\beta_1...\alpha_N\beta_N} M_{\alpha_1\beta_1}\ldots M_{\alpha_N\beta_N}, \tag{2.46}$$

where $\alpha, \beta = 1, \ldots, 2N$. Using the definition $D_w^{-1}(x, y) = \triangle(x, y)$ the resultant gluino propagator is given as

$$\langle T\{\lambda(x)\bar{\lambda}(y)\}\rangle = \mathcal{Z}_0^{-1} \int [dU] \operatorname{Pf}(M) \triangle (x, y) e^{-S_g}, \qquad (2.47)$$

where

$$\mathcal{Z}_0 = \int [dU] \operatorname{Pf}(M) e^{-S_g}. \qquad (2.48)$$

Now the variables depend mainly on gauge link on the gauge field U which can be produced using some Monte Carlo algorithms, discussed in Sec. (3.1). Alternatively, one can also find the result (2.47) by considering some source $J(x)$ of gluino field in the path integral approach and doing shift in the gluino field where this field is easily integrated out, for details see Ref [39]. The two point function in Eq. (2.47) is the basic ingredient of different operators on the lattice and this integral can be solved numerically by means of Monte Carlo simulations.

2.2.2 Non-zero gluino mass and hopping parameter

The hopping parameter κ and bare gluino mass $m_{\tilde{g}}$ are related as follows [40]

$$\kappa = \frac{1}{2(m_{\tilde{g}} + 4)}. \qquad (2.49)$$

We calculate adjoint pion mass squared $m_{\text{a-}\pi}^2$ which is related to κ by

$$m_{\text{a-}\pi}^2 = A \left(\frac{1}{\kappa} - \frac{1}{\kappa_c} \right). \qquad (2.50)$$

The above relation is analogous to the PCAC relation. We also obtain the subtracted gluino mass from the Ward identities and calculate it numerically in simulations, full details are given in Ch. (4). As a consequence of the non-zero gluino mass, the chiral symmetry is broken. We change κ in small steps and monitor the above masses in order to approach to the critical value of the hopping parameter κ_c where $m_{\text{a-}\pi}^2$ and the subtracted gluino mass vanish. At this point, the first order phase transition occurs and we observe a jump in

gluino condensate $\langle \bar{\lambda}\lambda \rangle$, it is shown in Fig. (2.5) qualitatively. Furthermore, in the chiral and in the continuum limits the formation of the supermultiplet with degenerate masses is expected, and broken SUSY is recovered.
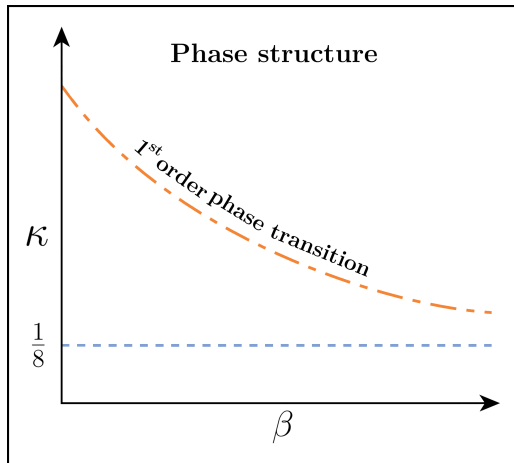
Figure 2.5: The phase structure of $\mathcal{N} = 1$ SUSY Yang-Mills theory. The dotted curve represents 1st order phase transition corresponding to $m_{\tilde{g}} = 0$. At this point N_c degenerate vacua of the theory are expected. The degeneracy of these vacua is, however, shifted when $m_{\tilde{g}}$ is switched on.

2.2.3   Sign of the Pfaffian

The Pfaffian (2.45) is gauge invariant and uniquely defined. Nevertheless, in numerical simulations especially at coarser lattices (larger lattice spacings a) and at smaller gluino masses (closer to the chiral limit) it appears to be negative for several configurations. To resolve this issue the absolute value of the Pfaffian is taken

$$|\text{Pf}(M)| = |\det(\tilde{D}_w^2)^{-\frac{1}{4}}|, \tag{2.51}$$

and it is balanced by the reweighting procedure as

$$\langle O \rangle = \frac{\left\langle O \times \text{sign}\big(\text{Pf}(M)\big) \right\rangle}{\left\langle \text{sign}\big(\text{Pf}(M)\big) \right\rangle}. \tag{2.52}$$

In the case when a considerable number of configurations have a negative sign, large cancellations in the reweighting procedure occur which leads to large statistical fluctuations. Therefore, it is important to stay away from such regions.

To compute the Pf(M), one can construct the anti-symmetric matrix M in terms of a block-diagonal matrix J and in terms of a triangular matrix P as

$$M = P^T J P, \tag{2.53}$$

for the definitions of P and J, see Ref. [41]. The Pfaffian will be given as

$$\text{Pf}(M) = \det(P). \tag{2.54}$$

This procedure, nevertheless, can only be used for small lattice due to large storage requirements, for details see Ref. [27] and Refs. therein.

2.2.4 Improved actions

There are different ways to define the action (2.30) on the lattice with the condition that they must respect all the concerned lattice symmetries. The choice is, however, made on the basis of full recovery of the continuum symmetry and a faster approach towards the continuum limit is possible if one choose a lattice formulation based on *domain wall fermions* [42]. In this case the chiral limit is achieved without fine tuning and an additional dimension is introduced where a massless fermion is supported by 4D domain wall. Another approach is to make use of *overlap fermions* [43, 44]. The advantage of these formalisms is that the chiral symmetry is improved and well protected.

Most of the work has been done by using Wilson type actions. In the previous investigations of our collaboration [3, 5], the tree-level Symanzik improved gauge action [45] has been used instead of simple Wilson action with the gauge group SU(2) along with one level of stout smearing to reduce fluctuations of the low modes of the Dirac operator. In our recent investigations [6, 7, 8], for the case of the gauge group SU(3), we have used a clover

improved fermion action. This improvement is made by adding a term

$$-\frac{c_{sw}}{4}\,\bar{\lambda}(x)\sigma_{\mu\nu}F^{\mu\nu}\lambda(x), \tag{2.55}$$

in the action (2.9). The main advantage of this improvement is that it reduces the $O(a)$ lattice artifacts significantly. The coefficient c_{sw} is called the Sheikholeslami-Wohlert coefficient and its one loop value has been used for the gauge group SU(3). Alternatively, in order to obtain the value of c_{sw} the tadpole resummation [3] has also been tested for SU(2) case that lead to a large development in obtaining the degeneracy of masses at finite lattices. Moreover, the values of c_{sw} from one loop predictions are in the same range of values obtained from the tadpole formula.

2.2.5   Smearing techniques

In order to improve the precision of the quantities measured on lattice without putting much effort on statistics and numerics, the overlap of the operators with the ground state of the particle should be enhanced. However, some operators are not well suited to achieve the overlap. In order to enhance this overlap with ground state, one can use so-called smearing techniques. In addition, the smearing removes quantum fluctuations at short distances and improves the signal-to-noise ratio. Furthermore, the smearing techniques are applied in variational analysis to construct a set of different operators used in the analysis [7]. We use APE and Jacobi smearings in $\mathcal{N} = 1$ SUSY Yang-Mills theory on the lattice for these purposes. The details of these smearing techniques are as follows [5]:

APE smearing:

In APE smearing, gauge links are smeared. Smearing of gauge links is used as a powerful tool in order to reduce UV-fluctuations of gauge configurations. In APE smearing, the individual spatial link variable $U_i(x)$, $i = 1, 2, 3$ is extended by the sum of itself and weighted staples orthogonal to the original

spatial link as

$$U_i(x) \xrightarrow{\text{APE}} U_i'(x) = U_i(x) + \epsilon_{APE} \sum_{\substack{j=\pm 1 \\ j\neq i}}^{\pm 3} U_j(x)U_i(x+\hat{j})U_j^\dagger(x+\hat{i}), \quad (2.56)$$

where the parameter ϵ_{APE} affects the strength of smearing. This procedure is shown in Fig. (2.6). The new smeared link is given by
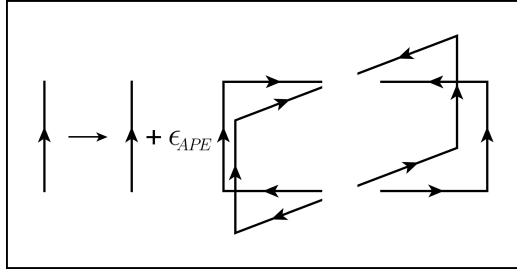
Figure 2.6: Graphical representation of APE smearing in which each link is replaced by itself plus orthogonal staples.

$$U_i^s(x) = \frac{U_i'(x)}{\sqrt{\frac{1}{2}\text{tr}U_i'^\dagger(x)U_i'(x)}}. \quad (2.57)$$

This procedure is equivalent to solving the diffusion equation with small value of ϵ_{APE}. In terms of ϵ_{APE} and N_{APE}, the smearing radius reads

$$R_s = \sqrt{N_{APE} \times \epsilon_{APE}}, \quad (2.58)$$

where N_{APE} is the APE smearing level which represents that how many times the APE smearing is applied. N_{APE} should not be much larger otherwise it would just ruin the signal. Comparison R_s to the lattice size gives an estimate about the size of the lattice volume to contain sufficiently the wave function of the particle to be simulated. The parameters ϵ_{APE} and N_{APE} have to be tuned in order to obtain best estimates of the quantities of interest. Furthermore, the choice of the parameters for different observables will be explained in Sec. (2.3.1).

Jacobi smearing:

To gain the same objective, it is important to replace also fermion operator with a smeared one. Therefore, Jacobi smearing is used for the construction of the fermion source as [46]

$$\lambda_b^\beta(\vec{x}) \xrightarrow{\text{Jacobi}} \lambda_b'^\beta(\vec{x}) = \sum_{a,\alpha,\vec{y}} F_{ba}^{\beta\alpha}(\vec{x},\vec{y})\lambda_a^\alpha(\vec{y}). \tag{2.59}$$

Where F is the Jacobi smearing operator which uses APE smeared adjoint gauge link variable $V_i(x)$ and its suitable choice is given as [7, 46]

$$F_{ba}^{\beta\alpha}(\vec{x},\vec{y}) = C_J^{N_J}\delta^{\beta\alpha}\left(\delta_{\vec{x},\vec{y}} + \sum_{i=1}^{N_J}(H^i)_{ba}(\vec{x},\vec{y})\right), \tag{2.60}$$

with

$$H_{ba}(\vec{x},\vec{y}) = \kappa_J\sum_{i=1}^3\left[\delta_{\vec{y},\vec{x}+\hat{i}}V_{i,ba}(\vec{x}) + \delta_{\vec{y},\vec{x}-\hat{i}}V_{\hat{i},ba}^\dagger(\vec{x}-\hat{i})\right]. \tag{2.61}$$

Where N_J represents Jacobi smearing level, κ_J is smearing coefficient and responsible for convergence, and C_J is a normalisation constant. The optimal choice of the set $\{N_J, \kappa_J, C_J\}$ will be explained in Sec. (2.3.1). In terms of F, 3D Klein-Gordon equation in the limit $N_J \to \infty$ is written as

$$\sum_{a',x'} K_{aa'}(\vec{x},\vec{x}')F_{a'b}(\vec{x}',\vec{y}) = \delta_{\vec{x}\vec{y}}\delta_{ab}, \tag{2.62}$$

here spin indices are omitted. The kernel K is given as

$$K_{aa'}(\vec{x},\vec{x}') = \delta_{\vec{x}\vec{x}'}\delta_{aa'} - \kappa_J\sum_{i=1}^3\left[\delta_{\vec{x}',\vec{x}+\hat{i}}V_{i,aa'}(\vec{x}) + \delta_{\vec{x}',\vec{x}-\hat{i}}V_{\hat{i},aa'}^\dagger(\vec{x}-\hat{i})\right]. \tag{2.63}$$

The Jacobi smearing radius R_J reads

$$R_J^2 = \frac{\sum\limits_{\vec{x}}|x|^2\,|F(\vec{x},0)|^2}{\sum\limits_{\vec{x}}|F(\vec{x},0)|^2}. \tag{2.64}$$

For further details on how the Jacobi smearing operator acts on different pieces of correlation functions see Ref. [7].

2.2.6 Stochastic estimator technique

In $\mathcal{N} = 1$ SUSY Yang-Mills theory, the computation of the disconnected contribution to the correlator of the adjoint meson and the spectacle contribution in baryonic states is a challenging task. It requires the computation of all-to-all propagators. The major difficulty in the determination of all-to-all propagators is to obtain the inverse of the Wilson-Dirac operator D_w. Direct inversion can only be done on small lattice volumes. However, for large volumes it is too expensive within current computational resources. Therefore, a reasonable approximation for the inverse with a reliable precision is required. The stochastic estimator technique (SET) is among the various important techniques to do this job, for details see Refs. [7, 47]. The SET is based on a set of random noise vectors $|\eta^i\rangle$ satisfying the following relation

$$\frac{1}{N_s} \sum_i^{N_s} |\eta^i\rangle \langle \eta^i| = \mathbf{1} + O(\frac{1}{\sqrt{N_s}}). \tag{2.65}$$

The noise, in our case, belongs to $\mathbb{Z}_4$ i.e. $\frac{\pm 1 \pm i}{\sqrt{2}}$. As a result the approximated inverse of preconditioned Wilson-Dirac operator will be

$$D_{pc}^{-1} = \frac{1}{N_s} \sum_i^{N_s} |s^i\rangle \langle \eta^i| + O(\frac{1}{\sqrt{N_s}}), \tag{2.66}$$

where the source vector $|s^i\rangle = D_{pc}^{-1} |\eta^i\rangle$ can be computed using conjugate gradient method. Concerning the convergence in the approximation of the inverse Wilson-Dirac matrix it has been found that the SET is considerably fast once it is combined with the truncated eigenmode approximation and even-odd preconditioning [48]. From the lowest eigenvalues λ_i and corresponding eigenvectors $|v_i\rangle$ of $\gamma_5 D_{pc}$ (the Hermitian version of D_{pc}) the approximated

inverse of preconditioned Wilson-Dirac matrix is

$$D_{pc}^{-1} \approx \sum_i^{N_e} \frac{1}{\lambda_i} |v_i\rangle \langle v_i| . \tag{2.67}$$

The Eq. (2.67) is combined with the noise vectors of SET [7] as

$$D_{pc}^{-1} \approx \sum_i^{N_e} \frac{1}{\lambda_i} |v_i\rangle\langle v_i| + \frac{1}{N_s} \sum_i^{N_s} \left|s_\perp^i\right\rangle \left\langle \eta_\perp^i\right| \doteq \sum_i^{N_e+N_s} a_i |w_i\rangle\langle u_i| , \tag{2.68}$$

where $|s_\perp^i\rangle$ and $|\eta_\perp^i\rangle$ are the source and noise vectors which are projected orthogonal to the lowest eigenvectors. The combination of above both approximations described above together with better choice of number of stochastic estimator, not only speeds up the code but also converges to the better estimation of the inverse of preconditioned Wilson-Dirac matrix.

2.3 Strategy

2.3.1 Simulation parameters

In $\mathcal{N} = 1$ SUSY Yang-Mills theory on the lattice, we need to tune two parameters. The first parameter is the inverse gauge coupling β which is related to the lattice spacing a, we tune this parameter such that the continuum limit is approached where broken SUSY due to the lattice regulator is recovered. We have generated ensembles with the gauge group SU(3) using the RHMC algorithm; the set of simulated values of β is $\{5.2, 5.3, 5.4, 5.45, 5.5, 5.6, 5.8\}$. The values 5.2 and 5.3 are excluded because there might be bulk phase traditions and algorithm does not converge. Whereas the value 5.8 is ignored as well because the corresponding lattice spacing is too small such that the topological sectors can not be sampled properly and there appear to be the large finite volume effects, the topological charge freezes and relevant quantities measured at this value are not reliable. Moreover, the value of Sheikholeslami-Wohlert coefficient c_{sw} is determined from the one-loop calculation, this value is used in the clover part of the action. The Second parameter is called the

hopping parameter κ which is related to the gluino mass by the relation given in Eq. (2.49). This parameter is tuned such that the chiral limit is obtained where theory is characterised by a massless gluino. For the case of SU(3), our choices for the inverse gauge coupling β and for the hopping parameter κ are shown in Tab. (2.1).

$\beta = 5.4$		$\beta = 5.4$		$\beta = 5.45$		$\beta = 5.5$		$\beta = 5.6$	
$c_{sw} = 1609$		$c_{sw} = 1603$		$c_{sw} = 1598$		$c_{sw} = 1587$		$c_{sw} = 1609$	
$V = 12^3 \times 24$		$V = 16^3 \times 32$		$V = 16^3 \times 32$		$V = 16^3 \times 32$		$V = 24^3 \times 48$	
κ	N_{cnfg}	κ	N_{cnfg}	κ	N_{cnfg}	κ	N_{cnfg}	κ	N_{cnfg}
0.1690	5642	0.1692	8080	0.1685	2314	0.1649	3212	0.1645	08611
0.1695	8199	0.1695	4277	0.1687	3333	0.1667	4515	0.1650	10286
0.1700	5962	0.1697	3896	0.1690	2637	0.1673	5108	0.1655	13986
0.1703	6076	0.1700	6152	0.1692	2126	0.1678	3603	0.1660	12760
0.1705	5070	0.1703	10513	0.1693	2394	0.1680	1511	-	-
-	-	0.1705	9868	-	-	0.1683	0917	-	-

Table 2.1: Gauge ensambles corresponding to the optimal values of inverse gauge coupling β for different lattice volumes. The c_{sw} values are used in clover part of the action. Here N_{cnfg} represents the total number of gauge configurations produced.

Smearing parameters for Ward identities:

For the Ward identities the best parameters are given in the Tab. (2.2). The dependence of the gluino-glue Ward identity correlation functions on these parameters is mild.

APE		Jacobi	
N_{APE}	ϵ_{APE}	N_J	κ_J
4	0.5	6	0.2

Table 2.2: The optimal values of parameters used in APE and Jacobi smearings for the Ward identities.

Smearing parameters for adjoint Mesons (a-η' and a-f_0):

The disconnected contributions of the mesons are challenging to be computed on the lattice. We apply Jacobi smearing in order to improve the signal which introduces additional noise. To cope with this, we first apply APE smearing on the gauge links and then use these links in the Jacobi smearing operator [7]. To avoid large errors, we optimise the κ_J and to keep the correlation function of the same order of magnitude, we tune C_J. The Tab. (2.3) shows the optimal choices of smearing parameters for mesons.

APE		Jacobi		
N_{APE}	ϵ_{APE}	N_J	κ_J	C_J
20	0.5	upto 80	0.2	0.87

Table 2.3: The best smearing parameters used in APE and Jacobi smearings for mesons.

Smearing parameters for the gluino-glue and glueballs:

For the gluino-glue and glueballs bound states we apply the APE smearing only and use 0.4 and 0.5 as values of ϵ_{APE} respectively with $N_{APE} = 20$.

Stochastic estimators and number of lowest eigenvalues for mesons and baryons:

In our current measurement of mesons, we choose 40 stochastic estimators along with the 20 lowest eigenvalues. For further discussions and details see Ref. [7]

Results of autocorrelation time and estimated bin size:

Tab. (2.4) shows the numerical values of integrated autocorrelation time $\tau_{\mathcal{O},\text{int}}$ calculated from Eq. (3.59) and estimated bin size L_B from Eq. (3.65).

$\beta = 5.5$				$\beta = 5.6$			
κ	N_{cnfg}	$\tau_{\mathcal{O},\text{int}}$	L_B	κ	N_{cnfg}	$\tau_{\mathcal{O},\text{int}}$	L_B
0.1649	08611	1.4997	24	0.1645	08611	1.4999	33
0.1667	10286	1.4998	27	0.1650	10286	1.4999	35
0.1673	13986	1.4998	28	0.1655	13986	1.4999	39
0.1678	12760	1.4997	25	0.1660	12760	1.4999	38
0.1680	10286	1.4993	18	-	-	-	-
0.1683	13986	1.4989	16	-	-	-	-

Table 2.4: Results for integrated autocorrelation time of the correlation functions appearing in the Ward identities and estimated bin size.

2.3.2 Finite size effects

The determination of the mass spectrum of the theory on the lattice is affected by the finite size effects. The degeneracy of the supermultiplet predicted by the effective actions [9, 10] can be lost if they are not considered and estimated properly. In principle, one should simulate the theory in infinitely large volume, but practically it is impossible. Therefore one should be very careful in choosing the size of the box. Relatively larger volumes are preferred, on the other hand the simulations are very expensive especially when fermions are in the adjoint representation. Hence, some optimal size of the box should be taken. In the lattice field theories the measurement of the physical quantities in a finite box is different from those in infinitely large box. The shifted mass due to definite size L of the box is given as

$$m(L) = m_0 + \triangle m(L), \tag{2.69}$$

where m_0 is the mass in an infinitely large box and $\triangle m(L)$ is the shift that has been investigated to all orders in PT [49]. In the lattice field theory the analogous investigations have been presented in [50] where the mass shift gets the form

$$\triangle m(L) \sim \frac{C}{L} e^{-\alpha m_0 L}. \tag{2.70}$$

This behavior is generic and does not depend on the types of interactions. In $\mathcal{N} = 1$ SUSY Yang-Mills theory the finite size L dependent mass $m(L)$ is obtained and fitted to infinite volume limit. In the fit the constants C, α and m_0 are calculated. The mass gap between the gluino-glue and a-η' is shown in Ref. [51]. It has also been argued that the functional dependence in Eq. (2.70) is valid only for sufficiently large lattice volumes. Furthermore, Fig. (2.7)
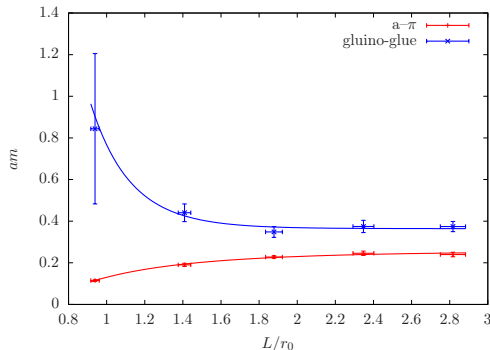
Figure 2.7: Lattice volume size dependence of the gluino-glue (blue) and a-π (red) masses. The numerical simulations are performed at $\beta = 5.6$ and $\kappa = 0.1660$. The results are obtained by fitting the data to the functional form in the Eq. (2.70).

shows the masses of the gluino-glue and a-π particles plotted against size L/r_0 at the finest lattice spacing corresponding to the inverse gauge coupling $\beta = 5.6$ and the hopping parameter $\kappa = 0.1660$ (very close to κ_c). We choose a set of different lattice volumes i.e. $\{8^3 \times 32,\ 12^3 \times 32,\ 16^3 \times 32,\ 20^3 \times 40,\ 24^3 \times 48\}$ to see the dependence of the mass on L/r_0. It seems that we are already in the safe region for volume $16^3 \times 32$ where the masses are constant and their dependence on the volume is negligible, even though we have preferred to perform simulations at the volume $24^3 \times 48$. At this lattice volume the finite size effects are irrelevant [6].

2.3.3 The sampling of topological sectors

Topological quantities have large autocorrelation time and topological charge is frozen towards the zero lattice spacing limit at the finest lattice spacing (< 0.05 fm in QCD units). The autocorrelation time increases very quickly

when the lattice spacing a is decreased, see Refs. [53, 54] for details. Monte Carlo simulations loose ergodicity if topological sectors are not treated properly. We have already very fine lattice spacing corresponding to $\beta = 5.6$, hence it is very important to sample the topological sector accordingly. The mean value of the topological charge $\langle Q \rangle$, the integrated autocorrelation time τ_Q and the susceptibility χ_Q have been measured in our recent numerical simulations. For $\beta = 5.5$ the τ_Q seems to be reasonable and it becomes more important at $\beta = 5.6$ where it is relatively large but still under control, see Fig. (2.8) which is taken from Ref. [6]. In addition, we have also performed simulations and calculated these quantities for $\beta = 5.8$ (very close to continuum), and found out that the topological charge is frozen. Hence, all related quantities at $\beta = 5.8$ are not reliable and these ensembles are excluded.
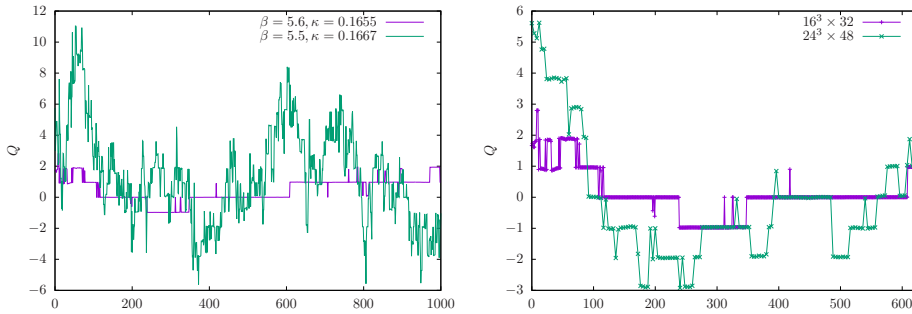
Figure 2.8: The history (β dependence) of the topological charge on a lattice volume $16^3 \times 32$ (left). The history (Volume dependence) of the topological charge at inverse gauge coupling $\beta = 5.6$ and hopping parameter $\kappa = 0.1660$ (right).

2.3.4   Scale setting

Numerical simulations give dimensionless numbers. To represent them into physical units one needs to set a scale. On the lattice, it is equivalent to put lattice spacing a to a fixed value. In principle, any dimensionful physical observable can be used for this purpose. Nevertheless, the calculation of any physical quantity from the lattice can only be as good as the determination of its scale in physical units. In addition to the physical scale, it is equally im-

portant to determine the lattice spacing at different inverse gauge couplings to perform the continuum extrapolation. To express physical quantities in terms of an accurately measured quantity it might be useful to choose a quantity which is not directly measured in experiments, but easy to be calculated with high precision and accuracy.

The Sommer parameter r_0 is one of this type which is introduced in Ref. [55]. This has been used in $\mathcal{N} = 1$ SUSY Yang-Mills theory with the gauge group SU(2) [3]. The advantage of this scale is that it makes use of the static quark anti-quark potential $V(r/a)$ from gauge fields and fits the data to extract r_0/a or string tension $a\sqrt{\sigma}$ without any expensive computation of quark propagators etc. However, its computation is non-trivial and requires asymptotic behavior of Wilson-loops. Moreover, its analysis is complicated [56] which results in large error of the scale.

Alternatively, the w_0 scale from gradient flow can be obtained with high precision. It is considered in Ref. [57] and the method how to determine w_0 scale is explained in Ref. [58]. To obtain w_0 scale, the following observable is considered

$$W(t) = t\frac{d}{dt}\left(t^2 \langle E(t) \rangle\right), \tag{2.71}$$

with the condition

$$W(t)_{t=w_0^2} = u, \tag{2.72}$$

where u is a reference scale. Different choices of u change the autocorrelation strongly. Different values have been tried in Ref. [59] and it has been found that the small value of u reduces fluctuations and spikes of w_0^u. We used $u = 0.2$ in our previous investigation [6] where topological sampling was insufficient. In our recent work [7, 8], we have used $u = 0.3$ where topological sectors are under control. $\langle E(t) \rangle$ is the expectation value of continuum-like action density E that reads

$$E = \frac{1}{4}G_{\mu\nu}^a G_{\mu\nu}^a, \tag{2.73}$$

where $G_{\mu\nu}^a$ is the chromoelectric field strength tensor. The reason why $W(t)$ is preferred over $t^2 \langle E(t) \rangle$ of Ref. [57] is that $W(t)$ is less influenced than

$t^2 \langle E(t) \rangle$ by the cutoff effects (discretisation effects). Moreover, t yields different relative scales for different values of $t^2 \langle E(t) \rangle$ whereas $W(t)$ gives very similar values of the scale.

We compute the scale w_0 for each β and for the full range of κ as a function of $m_{\text{a-}\pi}^2$. The data is fitted to a function of second order polynomial of $m_{\text{a-}\pi}^2$, the function reads

$$w_0(m_{\text{a-}\pi}^2) = w_{0,\chi} + c^{(1)} m_{\text{a-}\pi}^2 + c^{(2)} m_{\text{a-}\pi}^4, \qquad (2.74)$$

where $w_{0,\chi}$ is desired value of the scale.

2.3.5   Chiral and continuum extrapolations

In our previous investigations, we extrapolated masses to the chiral and in the continuum limits separately in a two step procedure. Contrary to that, we now perform a combined one 2D fit to obtain values of observables $O_{\chi,cont.}$ in terms of the scale w_0 by the function

$$O(m_{\text{a-}\pi}^2, w_{0,\chi}) = O_{\chi,\text{cont.}} + c^{(1)} m_{\text{a-}\pi}^2 + c^{(2)} \frac{a}{\beta^2} + c^{(3)} m_{\text{a-}\pi}^2 \frac{a}{\beta^2}. \qquad (2.75)$$

Instead of a we have used a/β^2 in Eq. (2.75) because lattice articfacts for on-shell quantities are expected to be $O(a/\beta^2)$ due to one-loop clover improved action [8].   In order to show the mass gap, we show the chiral extrapolation of the gluino-glue, the pseudoscalar a-η' and the 0^{++} glueball in Figs. (2.9,2.10) for a set of coarser and finer lattice spacings. At the coarsest lattice spacings corresponding to $\beta = 5.4$ one can see a mass gap between the gluino-glue and other observables (a-η' and 0^{++}). This gap squeezes already at $\beta = 5.45$. For $\beta = 5.5$ and $\beta = 5.6$ their is no mass gap present between the particles indicating the formation of supermultiplet in the chiral limit. Fig. (2.11) shows the continuum extrapolations of the masses using the fit function of Eq. (2.75). It is very much clear from the extrapolations that the masses are degenerate and hence form a chiral supermultiplet which indicates the restoration of broken SUSY. Moreover, a quadratic fit in the lattice spacing a has also been performed, however, the dependence of masses on the lattice

(a) $\beta = 5.4$

(b) $\beta = 5.45$
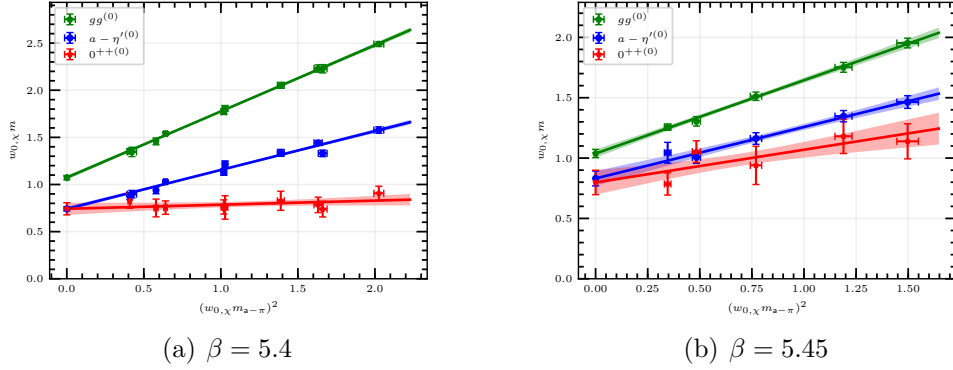
Figure 2.9: The extrapolations of the ground state masses towards the chiral point κ_c where $m_{\text{a-}\pi}^2$ vanishes at two coarser lattice spacings. These masses consist of the gluino-glue $gg^{(0)}$ which is purely fermionic state, the scalar channel $0^{++(0)}$ which is mixed state of 0^{++} glueballs and a-f_0, and the pseudoscalar channel a-$\eta'^{(0)}$ which is purely mesonic state.

(a) $\beta = 5.5$

(b) $\beta = 5.6$
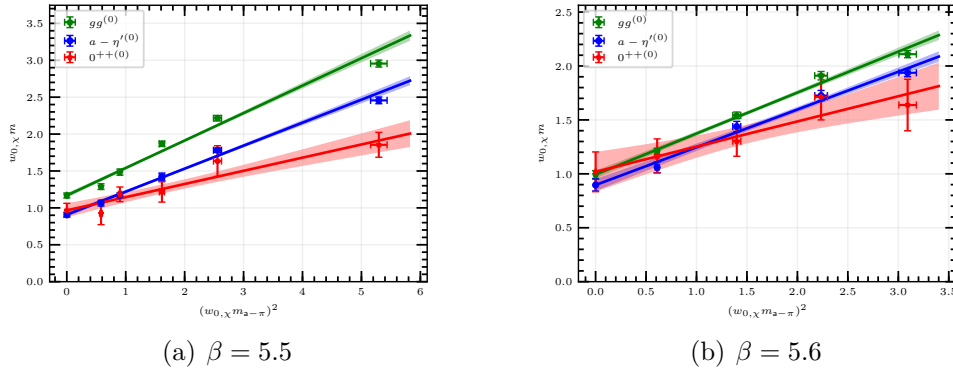
Figure 2.10: The extrapolations of the ground state masses towards the chiral point κ_c where $m_{\text{a-}\pi}^2$ vanishes at two finer lattice spacings. It is important to note here that as the lattice spacing a becomes smaller (at larger β) the lattice artifacts are significantly reduced and formation of supermultiplet is quite clear which is the hint of restoration of the broken SUSY.

spacing is mild, see Ref. [8]. Additionally, SUSY Ward identities have been employed in order to show the recovery of broken SUSY, full detail is given in Ch. (4).
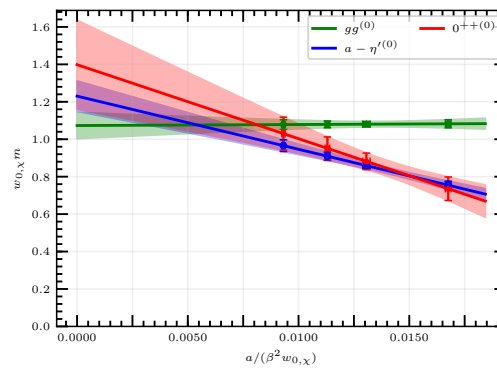
Figure 2.11: The extrapolations of the ground state masses towards the continuum limit performed at 4 different lattice spacings. These physical states are same as shown in Figs. (2.9,2.10). The masses are compatible within errors at $a = 0$, therefore they form a chiral supermultplet as predicted in Refs. [9, 10].

Chapter 3

Correlators and determination of masses

In this chapter we shall consider algorithms for the production of gauge ensembles which have been used for the determination of different observables. Moreover we discuss the correlation functions required to measure the spectrum of bound states. In addition, we review some data analysis techniques for our research work.

3.1 Production of configurations and algorithms

The gauge field configurations are the basic requirements to perform Monte Carlo simulations of $\mathcal{N} = 1$ SUSY Yang-Mills theory. The implementation of fermions on the lattice is expensive especially when they are in adjoint representation. In $\mathcal{N} = 1$ SUSY Yang-Mills theory it is more challenging to simulate the theory near the chiral and the zero lattice spacing limits. We focus mainly on algorithms which produce the gauge field configurations in order to significantly reduce computational power.

On the lattice, we compute expectation values of observables, as an example see Eq. (2.42). The exponential may suppress some regions of configuration space, therefore it is crucial to find an algorithm that produces configurations with a significant weight. This is achieved by the "importance

sampling". Moreover, we employ Markov chain process producing new configuration from the previous one, which may result into autocorrelations that can be controlled as explained in Sec. (3.3.4).

There are many algorithms to achieve the similar results. However, in our case we have used the two-step multi-boson (TSMB) and the PHMC algorithm for the gauge group SU(2) and the Rational Hybrid Monte Carlo (RHMC) algorithm for the gauge group SU(3).

3.1.1 Two-step multi-boson (TSMB) algorithm

Many pseudofermion fields are required in order to have highly precise approximations of $\left[\det(\tilde{D}_w^2)\right]^{\frac{1}{4}}$ which might result into the requirement of large storage space and long autocorrelations. To solve this issue, a two-step approximation scheme is introduced in Ref. [52] and extended to multi-step in Ref. [60]. These two steps are explained as

Step 1:

$\left[\det(\tilde{D}_w^2)\right]^{\frac{1}{4}}$ is approximated by a polynomial $\bar{P}(x)$ as

$$\left[\det(\tilde{D}_w^2)\right]^{\frac{1}{4}} \xrightarrow{\bar{\delta}} \frac{1}{\det\left(\bar{P}\left(\tilde{D}_w^2\right)\right)}. \tag{3.1}$$

With $\bar{\delta}$ as a deviation norm.

Step 2:

The polynomial $P(x)$ is factorised as

$$\left[\det(\tilde{D}_w^2)\right]^{\frac{1}{4}} \xrightarrow{\delta} \frac{1}{\det\left(\bar{P}\left(\tilde{D}_w^2\right)\right)\det\left(P\left(\tilde{D}_w^2\right)\right)}. \tag{3.2}$$

Where $\det\left(P\left(\tilde{D}_w^2\right)\right)$ is called "noisy correction" and considered in Metropolis correction step. The canonical gauge field distribution in terms of only U

is

$$w\left[U\right] = \frac{e^{-S_g[U]}}{\det\left(\bar{P}\left(\tilde{D}_w^2[U]\right)\right)\det\left(P\left(\tilde{D}_w^2[U]\right)\right)}. \tag{3.3}$$

w in terms of U and pseudofermion field $\phi(x)$ reads

$$w\left[U,\phi\right] = \frac{e^{-S_{g\bar{P}}[U,\phi]}}{\det\left(P\left(\tilde{D}_w^2[U]\right)\right)}. \tag{3.4}$$

The acceptance probability has to satisfy the condition

$$\frac{P_A\left([U'] \leftarrow [U]\right)}{P_A\left([U] \leftarrow [U']\right)} = \frac{\det\left(P\left(\tilde{D}_w^2[U]\right)\right)}{\det\left(P\left(\tilde{D}_w^2[U']\right)\right)}. \tag{3.5}$$

Where $P_A\left([U'] \leftarrow [U]\right)$ is the probability of acceptance in the correction step. To avoid prohibitively expensive simulations, we consider the simple distribution of Gaussian type

$$\frac{e^{-\eta'^{\dagger}\eta'}}{\int[d\eta']e^{-\eta'^{\dagger}\eta'}}, \tag{3.6}$$

where η can be obtained from η' as

$$\eta = P\left(\tilde{D}_w^2[U']\right)^{-\frac{1}{2}}\eta'. \tag{3.7}$$

This η will then be used in

$$P_A\left([U'] \leftarrow [U]\right) = \frac{\int_{A>1}[d\eta]e^{-\eta^{\dagger}P\left(\tilde{D}_w^2[U]\right)\eta} + \int_{A<1}[d\eta]e^{-\eta^{\dagger}P\left(\tilde{D}_w^2[U']\right)\eta}}{\int[d\eta]e^{-\eta^{\dagger}P\left(\tilde{D}_w^2[U]\right)\eta}}, \tag{3.8}$$

where

$$A\left(\eta;[U'] \leftarrow [U]\right) = e^{-\eta^{\dagger}\left\{P\left(\tilde{D}_w^2[U']\right)-P\left(\tilde{D}_w^2[U]\right)\right\}\eta}, \tag{3.9}$$

with the following step to accept the change $[U'] \leftarrow [U]$

$$\min\{1, A\left(\eta;[U'] \leftarrow [U]\right)\}. \tag{3.10}$$

The exact solution is much more difficult. However, the two-step polynomial approximation can be used for the result. The two-step multi-boson (TSMB)

algorithm is not "exact" but still good enough to have the required precision where we monitor the spectrum of the dirac operator to check whether the approximation is good enough.

3.1.2 Rational hybrid Monte Carlo (RHMC) algorithm

In our collaboration, the RHMC algorithm has been used for the production of configurations for the gauge group SU(3). This review, in order to make the whole story complete, is based on Ref. [17]. For the complex vector $\phi(x)$, the $\sqrt[4]{\det(\tilde{D}_w^2)}$ can be calculated as

$$\int d[\phi(x)]d[\phi^\dagger(x)]e^{-\phi^\dagger(x)\left([\tilde{D}_w^2]^{-\frac{1}{4}}\right)(x,y)\phi(y)} = \sqrt[4]{\det(\tilde{D}_w^2)}, \qquad (3.11)$$

where $\tilde{D}_w = \gamma_5 D_w$ and $\phi(x)$ fields represent pseudofermions. The $\phi(x)$ can be computed from $\psi(x)$ and $\tilde{D}_w^2$ as

$$\phi(x) = \left([\tilde{D}_w^2]^{\frac{1}{8}}\right)(x,y)\psi(x), \qquad (3.12)$$

here $\psi(x)$ is a complex random vector and has Gaussian distributed entries. To compute $\left([\tilde{D}_w^2]^{\frac{1}{8}}\right)(x,y)$, we introduce the rational approximation $x^{\frac{1}{8}}$

$$x^{\frac{1}{8}} = \sum_k \frac{c_k}{x + b_k}. \qquad (3.13)$$

The coefficients c_k and b_k are calculated by the Remez algorithm. The Dirac Eq.

$$(\tilde{D}_w^2 + b_k)\eta_k = \psi, \qquad (3.14)$$

is solved to compute Eq. (3.12) as

$$\phi(x) = \sum_k c_k \eta_k. \qquad (3.15)$$

If $\left([\tilde{D}_w^2]^{-\frac{1}{4}}\right)(x,y)$ is represented as a new rational approximation as in Eq. (3.13) then the force can be calculated, that leads to the Rational Hybrid Monte

Carlo (RHMC). In the rational approximation the derivative is

$$\frac{\partial}{\partial U_\mu(x)}\left\{\phi^\dagger \frac{c_k}{\tilde{D}_w^2 + b_k}\phi\right\} = c_k \eta_k^\dagger \frac{\partial\left(\tilde{D}_w^2 + b_k\right)}{\partial U_\mu(x)}. \tag{3.16}$$

The detailed steps of the algorithms are given in Ref. [17].

3.2   Measurement of correlators

To obtain the masses of bound states formed by gluons and gluinos, suitable gauge invariant operators are considered. According to the total spin of the bound states, they are divided into bosons and fermions just like the classification of particles in the Standard Model. Additionally, there is a bound state with only one valence fermion that has no analogue in QCD, the gluino-glue.

3.2.1   Bosons

Adjoint mesons:

The bound state of two Majorana gluino fields in the adjoint representation form an adjoint meson just like mesons in QCD where they are formed out of two quarks (one quark and one anti-quark). The meson with $J^{PC} = 0^{++}$ is called a-f_0 and can be interpolated by the following operator

$$\tilde{O}_{\text{a-}f_0}(x) = \bar{\lambda}(x)\lambda(x), \tag{3.17}$$

whereas the meson with quantum numbers $J^{PC} = 0^{-+}$ is called a-η' (in analogy to the η' of QCD). Its interpolating field reads

$$\tilde{O}_{\text{a-}\eta'}(x) = \bar{\lambda}(x)\gamma_5\lambda(x), \tag{3.18}$$

where the prefix "a" in both of mesons represents the adjoint representation. The corresponding lattice transcription is given as

$$C_{\tilde{g}\tilde{g}}(\Delta t) = \underbrace{\text{tr}\left[\Gamma \triangle (x,x)\right] \text{tr}\left[\Gamma \triangle (y,y)\right]}_{\text{Disconnected contribution}} - 2\underbrace{\text{tr}\left[\Gamma \triangle (x,y)\Gamma \triangle (y,x)\right]}_{\text{Connected contribution}}, \quad (3.19)$$

where tr is over color and spin indices. The factor 2 is due to the Majorana nature of the field $\lambda(x)$ and $\triangle = D_w^{-1}$. The matrix Γ is $\mathbf{1}$ for the a-f_0 whereas it is γ_5 for the a-η'. The graphical representation of the connected and the disconnected contributions is shown in Fig. (3.1).

The contribution of the connected part is rather easy to computer where we only need to compute the inversion of a δ-source for each combination of spin and gauge indices. This inversion is achieved by the Conjugate Gradient (CG) method. The disconnected piece is challenging and computationally expensive. We use the Stochastic Estimator Technique (SET) together with the truncated lowest eigenmode approximation of the operator, which is explained in Sec. (2.2.6).
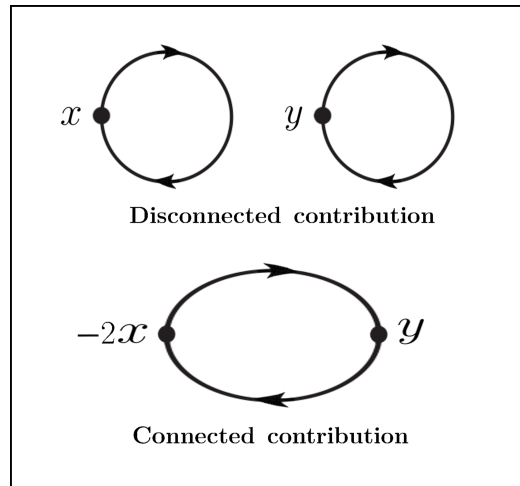
Figure 3.1: Graphical representation of "Connected" and "Disconnected" contributions of mesonic correlation functions.

Glueballs:

Glueballs are the bound states made of gluons, predicted in the generalisation of the effective action of Ref. [10]. There are scalar and pseudoscalar bosonic glueballs. The operators and their lattice versions are discussed as follows:

0^{++} **glueballs**

The operator of the $J^{PC} = 0^{++}$ (scalar) glueball reads

$$\tilde{O}_{\text{gb}^{++}} = \sum_{\mu\nu} F^{\mu\nu} F_{\mu\nu}, \tag{3.20}$$

and its lattice form in terms of space-like plaquette is given as

$$\tilde{O}_{\text{gb}^{++}}(x) = \text{tr}\left[P_{12}(x) + P_{23}(x) + P_{31}(x)\right], \tag{3.21}$$

where P_{ij} is a spacial plaquette given in Eq. (2.33). All the plaquettes which take part in the glueball operator are symmetric and connected to the same space-time lattice point x.

0^{-+} **glueballs**

The following operator corresponds to the glueball with the quantum numbers 0^{-+} (pseudo-scalar)

$$\tilde{O}_{\text{gb}^{-+}} = \sum_{\mu\nu\rho\sigma} F^{\mu\nu} \epsilon_{\mu\nu\rho\sigma} F^{\rho\sigma}. \tag{3.22}$$

There is a difficulty in using this operator to create a gluonic state with required quantum numbers because this operator has two plaquettes which are orthogonal and do not fit onto a single time-slice. Therefore the following

form of the operator is chosen

$$O_{\text{gb}^{-+}}(x) = \sum_{R \in \mathbf{O}_h} \left\{ \text{tr} \left[\mathcal{C}(x) \right] - \text{tr} \left[P\mathcal{C}(x) \right] \right\},$$
(3.23)

where $\mathcal{C}$ is the loop that is shown in Fig. (3.2), $P\mathcal{C}$ (parity conjugate) represents the mirroring of $\mathcal{C}$. $\mathbf{O}_h$ is the cubic group and the sum is over all possible rotations. From the numerical results it turns out that the signal for
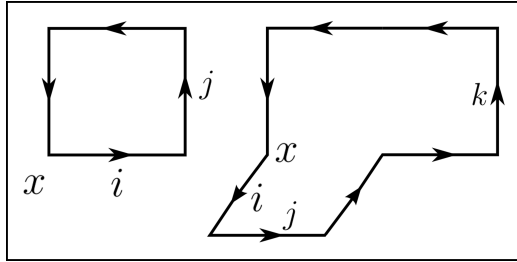
Figure 3.2: Glueballs in $\mathcal{N} = 1$ SUSY Yang-Mills theory.

glueballs is too noisy and requires some smearing techniques. APE-smearing is applied in order to improve the signal-to-noise ratio. Its details along with the choice of smearing parameters is explained in Sec. (2.2.5). For a detailed analysis see Ref. [7].

3.2.2 Fermions

Gluino-glue:

The investigations of $\mathcal{N} = 1$ SUSY Yang-Mills theory also comprises the bound state of the gluon and its fermionic superpartner, the gluino. This bound state is called the gluino-glue and predicted by effective actions [9, 10]. It is a spin-$\frac{1}{2}$ Majorana fermion, the superpartner of glueballs. Such a particle does not exist in pure QCD. However, similar bound states are present in QCD-like models with quarks in the adjoint representation of gauge group, for details see Refs. [6, 51]. The operator of such a bound state can be constructed from the gluino field and the field strength tensor as follows

$$\tilde{O}_{g\tilde{g}} = \sum_{\mu\nu} \sigma_{\mu\nu} \text{tr} \left[F^{\mu\nu} \lambda \right],$$
(3.24)

63

where $\sigma_{\mu\nu} = \frac{1}{2} [\gamma_\mu, \gamma_\nu]$. The lattice prescription of a related operator is given as

$$O_{g\tilde{g}}^\alpha = \sum_{i<j,\beta} \sigma_{ij}^{\alpha\beta} \, \text{tr} \left[P_{ij}^{(cl)} \lambda^\beta \right], \qquad (3.25)$$

where $P_{\mu\nu}^{(cl)}(x)$ is the clover-symmetrized plaquette, the lattice version of field strength tensor $F_{\mu\nu}(x)$, and defined in Eq. (2.33). The indices i and j are along space coordinates. It is graphically represented in Fig. (3.3). The
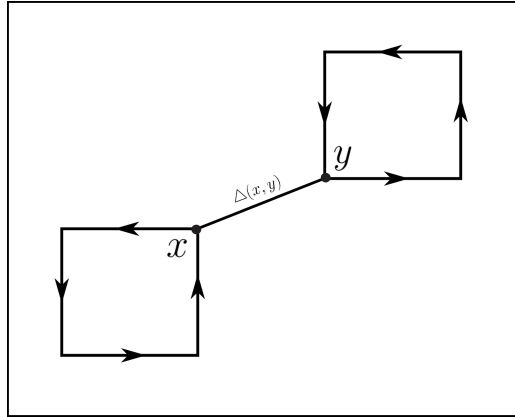
Figure 3.3: Correlation function of the gluino-glue particle in $\mathcal{N} = 1$ SUSY Yang-Mills theory.

correlation function corresponding to the identity of the Dirac basis is

$$C_{g\tilde{g}}(\Delta t) = -\frac{1}{4} \sum_{i,j,k,l} \sum_{\vec{x},\vec{y}} \sum_{\alpha,\beta,\rho} \sum_{ab} \langle \sigma_{ij}^{\alpha\beta} \text{tr} \left[P_{ij}(x) T^a \right] \left(D_w^{-1} \right)_{ab}^{\beta\rho}(x,y) \, \text{tr} \left[P_{kl}(y) T^b \right] \sigma_{kl}^{\alpha\rho} \rangle,$$
$$(3.26)$$

where $\Delta t = x_0 - y_0$ is the time slice distance. The correlation function $C_{g\tilde{g}}(\Delta t)$ can be expanded in the basis of 16 Dirac matrices, using discrete symmetries one can show that the non-vanishing contributions are only the ones proportional to the identity $\mathbf{1}$ and with γ_4, hence

$$C_{g\tilde{g}}^{\alpha\beta}(\Delta t) = C_1(\Delta t) \delta^{\alpha\beta} + C_2(\Delta t) \gamma_4^{\alpha\beta}. \qquad (3.27)$$

The time reversal gives [39]

$$C_1(\Delta t) = -C_1(N_t - \Delta t), \quad C_2(\Delta t) = C_2(N_t - \Delta t). \qquad (3.28)$$

64

Where C_1 is anti-symmetric and C_2 is symmetric. In order to verify the correctness of the correlation function of the gluino-glue the above relations can be used.

Baryons:

An interesting object that can be constructed from three gluinos is called "baryon" in analogy to the baryon of QCD. The interpolating field of such an object reads

$$\tilde{O}_{bar}(x) = t_{abc}\Gamma^A\lambda_a(x)\Big(\lambda_b^T(x)\Gamma^B\lambda_c(x)\Big), \qquad (3.29)$$

here t_{abc} is the structure constant and it is given explicitly in Appendix (B.3) whereas Γ is the spin matrix. The correlation function of baryon splits up into a "Sunset piece" and a "Spectacle piece", it is given as

$$B(x,y) = \langle B_{Sset}(x,y) + B_{Spec}(x,y)\rangle, \qquad (3.30)$$

where

$$
\begin{aligned}
B_{Sset}(x,y) = \theta\, t_{a'b'c'}t_{abc}\Gamma^{\beta\gamma}\Gamma^{\beta'\gamma'}P_\pm^{\alpha\alpha'} \times \{ & \\
+\, 2\,\triangle_{aa'}^{\alpha\alpha'}(x,y)\,\triangle_{bb'}^{\beta\beta'}(x,y)\,\triangle_{cc'}^{\gamma\gamma'}(x,y) & \\
+\, 4\,\triangle_{ab'}^{\alpha\beta'}(x,y)\,\triangle_{bc'}^{\beta\gamma'}(x,y)\,\triangle_{ca'}^{\gamma\alpha'}(x,y)\}, & \qquad (3.31)
\end{aligned}
$$

$$
\begin{aligned}
B_{Spec}(x,y) = \theta\, t_{a'b'c'}t_{abc}\Gamma^{\beta\gamma}\Gamma^{\beta'\gamma'}P_\pm^{\alpha\alpha'} \times \{ & \\
+\, 2\,\triangle_{ab}^{\alpha\beta}(x,x)\,\triangle_{ca'}^{\delta\alpha'}(x,y)\,\triangle_{c'b'}^{\delta'\beta'}(y,y)C^{\gamma\delta}C^{\gamma'\delta'} & \\
+\, 4\,\triangle_{ab}^{\alpha\beta}(x,x)\,\triangle_{b'c}^{\beta'\gamma}(y,x)\,\triangle_{c'a'}^{\gamma'\alpha'}(y,y) & \\
+\, 1\,\triangle_{aa'}^{\alpha\alpha'}(x,y)\,\triangle_{bc}^{\beta\delta}(x,x)\,\triangle_{c'b'}^{\delta'\beta'}(y,y)C^{\gamma\delta}C^{\delta'\gamma'} & \\
+\, 2\,\triangle_{ac}^{\alpha\delta'}(x,y)\,\triangle_{bc}^{\beta\delta}(x,x)\,\triangle_{b'a'}^{\beta'\alpha'}(y,y)C^{\gamma\delta}C^{\gamma'\delta'}\}, & \qquad (3.32)
\end{aligned}
$$

here $P_\pm$ are parity projectors, defined as $P_\pm = \frac{1}{2}(1\pm\gamma_4)$ and θ is defined in Tab. (5.1). The calculations, choice of spin matrices, and numerical strategies are explained in Ch. (5). The presence of the "Spectacle graph" is due to the

65

fact that we have a single flavour gluino field. The graphical representation of the two contributions above is depicted in Fig. (3.4).
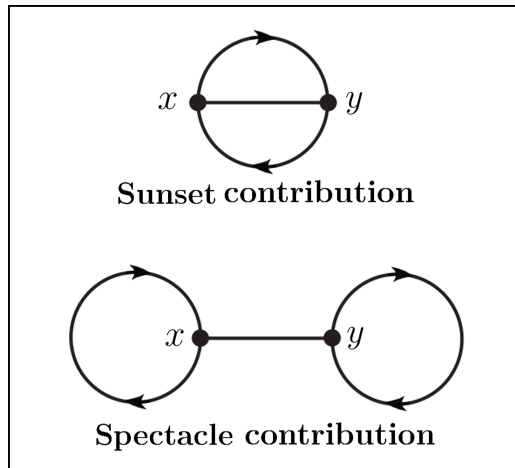
Figure 3.4: The "Spectacle" and "Sunset" contributions of baryon correlation function in $\mathcal{N} = 1$ SUSY Yang-Mills theory.

3.2.3 Mixing

The adjoint mesons and glueballs with the same quantum numbers are mixed. The physical states might not be purely gluonic or mesonic but rather be mixed. This mixing is predicted in Ref. [10] where the authors have shown that when a mixing term is included in the Lagrangian, the heavier state m^+ becomes even heavier and lighter state m^- gets even lighter. In our recent investigation [7], we have enlarged the variational basis in the variational analysis to take into account mixing between mesons and glueballs. The physical state $|n\rangle$ in terms of glueball contribution $|\phi_n^{(g)}\rangle$ and meson contribution $|\phi_n^{(m)}\rangle$ is written as

$$|n\rangle = |\phi_n^{(g)}\rangle + |\phi_n^{(m)}\rangle, \tag{3.33}$$

with,

$$|\phi_n^{(g)}\rangle = \sum_{i=1}^{n_g} v_{ni}^{(g)} |\phi_i^{(g)}\rangle, \tag{3.34}$$

$$|\phi_n^{(m)}\rangle = \sum_{i=1}^{n_m} v_{ni}^{(m)} |\phi_i^{(m)}\rangle. \tag{3.35}$$

Where $v_{ni}^{(g)}$ and $v_{ni}^{(m)}$ are the components of the generalized eigenvectors in the variational method [7]. The glueball content $c_n^{(g)}$ and the meson content $c_n^{(m)}$ are defined as

$$c_n^{(g)} = \frac{1}{N_n^{(g)} N_n} \langle \phi^{(g)}|n\rangle = \frac{1}{N_n^{(g)} N_n} \sum_i v_{ni}^{*(g)} c_{ni}^{(g)}, \tag{3.36}$$

$$c_n^{(m)} = \frac{1}{N_n^{(m)} N_n} \langle \phi^{(m)}|n\rangle = \frac{1}{N_n^{(m)} N_n} \sum_i v_{ni}^{*(m)} c_{ni}^{(m)}. \tag{3.37}$$

where N_n's are normalisation constants. It has been found that in the scalar channel the ground state is more glueball like whereas this behavior is opposite in the excited state. In the pseudoscalar channel, however, the physical state is dominated by a-η' and hence 0^{-+} glueball is ignored. The numerical results of mixing and details of the full analysis is given in Ref. [7].

3.3 Determination of masses

To determine the masses of the bound states predicted by effective actions [9, 10] in $\mathcal{N} = 1$ SUSY Yang-Mills theory we construct suitable operators with corresponding quantum numbers. These operators are gauge invariant and respect required symmetries. We exploit asymptotic behavior of Euclidean time correlators of these operators to obtain their masses. There is a large variety of the operators which keep the same quantum numbers as that of the particles. The choice, however, is made on the basis of large overlap with ground states and good signal-to-noise ratio. The choice of the operators and their lattice prescriptions is discussed in Sec. (3.2).

Numerical data of correlation functions obtained from Monte Carlo simulations on the lattice is fitted to the functional form of the operators. As a

first result, the effective mass m_{eff} of each correlation function is calculated to have a rough estimate of the mass. Let's first discuss how m_{eff} is obtained from the correlation functions.

3.3.1   Effective mass

In order to obtain the effective mass, a typical correlation function is given as

$$C(x,y) = \langle O^\dagger(x)O(y)\rangle. \tag{3.38}$$

We fix the position y at 0 and apply Fourier transformation on spatial coordinates as

$$C(t,\vec{p}) = \frac{1}{L^3}\sum_{\vec{x}} C(x,0)e^{-i\vec{p}.\vec{x}}. \tag{3.39}$$

We are interested in the mass only, therefore a zero-momentum interpolating field is considered as

$$S(t) = \frac{1}{L^{3/2}}\sum_{\vec{x}} O(t,\vec{x}), \tag{3.40}$$

and

$$C(\Delta t) = \langle S^\dagger(t + \Delta t)S(t)\rangle, \tag{3.41}$$

where $\Delta t = x_0 - y_0$. With the help of the identity $\sum_n |n\rangle\langle n| = 1$ for n possible eigenstates of the Hamiltonian. The correlation function $C(\Delta t)$ gives the spectral decomposition as [61]

$$\begin{aligned}
C(\Delta t) &= \sum_{n=0}\left(|\langle n|S(t)|0\rangle|^2 e^{-E_n \Delta t} \pm |\langle 0|S^\dagger(t)|n\rangle|^2 e^{-E_n(N_t - \Delta t)}\right), \\
&= a_0^2 + \sum_{n=1}\left(a_n^2 e^{-E_n \Delta t} \pm a_n^2 e^{-E_n(N_t - \Delta t)}\right). \tag{3.42}
\end{aligned}$$

As far as the sign $\pm$ is concerned, for the periodic boundary conditions $+$, whereas for the anti-periodic BCs $-$ is chosen. It is preferred to choose periodic BCs for spatial direction. In temporal direction the periodic BCs are used for bosons, whereas anti-periodic BCs for fermions. The correlation function of Eq. (3.42) decays exponentially and the lowest state corresponds to $n = 1$ with energy $E_1 = m_1$ as $t \to \infty$. The quantum numbers of this

lower energy state are the same as of the corresponding operator itself. The constant a_0^2 is non-zero for scalars and can be omitted by redefinition of the operator as

$$\tilde{S}(t) = S(t) - \langle S(t) \rangle_U. \tag{3.43}$$

Here U represents the gauge configuration ensemble. The numerical data of $C(\Delta t)$ is fitted to the following function to obtain the mass $m_1 = E_1 = m$ of the particle

$$C(\Delta t) = a^2 \left(e^{-m\Delta t} \pm e^{-m(N_t - \Delta t)} \right). \tag{3.44}$$

The effective mass can be obtained as follows

$$m_{\text{eff}} = \ln \left(\frac{C(\Delta t)}{C(\Delta t + 1)} \right). \tag{3.45}$$

When plotting m_{eff} against Δt one sees a plateau, that can be used to set the fitting interval. Note that the m_{eff} is just a guide towards the estimation of mass, in order to obtain more reliable results one has to adopt a proper fitting procedure.

3.3.2 Fitting correlators

In order to obtain the best estimates of masses from numerical data of the correlation function evaluated on the hypercubic lattice with the help of Monte Carlo simulations, we need to have the functional form of the these correlators. The functional form of the correlation function at large distance in case of periodic BCs is given as [40]

$$C(t) \approx c_0 + c_1 \cosh \left(m \left(t - \frac{N_t}{2} \right) \right), \tag{3.46}$$

whereas for the case of anti-periodic BCs it reads

$$C(t) \approx c_1 \sinh \left(m \left(t - \frac{N_t}{2} \right) \right), \tag{3.47}$$

where c_0 is a constant that is zero if $\langle 0 | S(t) | 0 \rangle = 0$, N_t is the time extent of the lattice and m is the mass of the particle. The mass can be obtained by

fitting the functional forms of Eqs. (3.46,3.47) to the numerical data of the correlators of Sec. (3.2). At early time slice distance t there is a contribution from excited state and at large t the noise shows up. Therefore, for a the good estimate of the mass, the fit range should be taken appropriately. To improve the signal-to-noise ratio APE and Jacobi smearings are performed depending upon the interpolating field. These smearing techniques are explained in Sec. (2.2.5).

3.3.3   Variational method

The variational method is used in order to further improve the determination of the ground state mass and to separate it from the excited state. As a result of this improvement, the variational method has a significant influence on the mass determination of excited states, too.

The main idea is to build a set of interpolating operators O_i, $i = 1, 2, \ldots, N$ with the same quantum numbers J^{PC} as that of physical state of choice. The construction and the choice of these operators influence the precision directly, therefore it is crucial to optimise these operators. Ideally, the interpolating operators should have large overlap with the physical state of interest. The cross correlation matrix in terms of time-slice correlation functions is given as

$$C_{ij}(t) = \left\langle O_i^\dagger(t) O_j(0) \right\rangle. \tag{3.48}$$

Smearing techniques play a crucial role in the construction of these operators. APE and Jacobi smearings are used in order to have a full correlation matrix of the operators. Each operator differs from the other by taking different set of smearing parameters. The spectral decomposition of the correlation function reads

$$C_{ij}(t) = \sum_n \langle 0 | O_i^\dagger | n \rangle \langle n | O_j | 0 \rangle \, e^{-m_n t}. \tag{3.49}$$

Where m_n is the mass of nth state. The corresponding solution of the $C_{ij}(t)$ by generalised eigenvalue problem (GEVP) is

$$C(t)\vec{v}^{(n)} = \lambda^{(n)}(t, t_0) C(t_0) \vec{v}^{(n)}, \tag{3.50}$$

where the $\lambda^{(n)}$, $n = 1, 2, \ldots, N$ are the eigenvalues and $\vec{v}^{(n)}$ are the corresponding eigenvectors. The eigenvalues $\lambda^{(n)}$ decay exponentially with t, it is given by the relation [62]

$$\lim_{t \to \infty} \lambda^{(n)}(t, t_0) \propto \mathrm{e}^{-m_n(t - t_0)} \left[1 + \mathcal{O}\left(\mathrm{e}^{-\Delta m_n(t - t_0)} \right) \right], \qquad (3.51)$$

here

$$\Delta m_n = \min_{l \neq n} |m_l - m_n|. \qquad (3.52)$$

The largest eigenvalue contains the mass of the ground state and second largest has the mass of the 1st excited state. There is a possibility of excited state contamination in the ground state; to get rid of that, in principle, one should consider the results at $t_0 \geq t/2$, for details see Ref. [63]. To have an idea about the mass one calculates the effective mass as a first result as

$$m_{\text{eff}}^{(n)}(t, t_0) = \ln \left[\frac{\lambda^{(n)}(t, t_0)}{\lambda^{(n)}(t + 1, t_0)} \right]. \qquad (3.53)$$

For more precise and reliable results of the mass with proper estimation of errors, it is important to fit a proper function to the data from numerical simulations. The numerical results obtained by the variational method and full details of the analysis are explained in Ref. [7].

3.3.4 Error analysis

The data obtained by Monte Carlo lattice simulations has unavoidable errors. It is important to distinguish between statistical errors and systematic errors. Let's first discuss about possible systematic errors. Systematic errors have multiple sources namely lattice discretisation and finite volume effects. Furthermore, in the evaluation of the data, systematic errors can occur in the mass determination when fitting to the correlation function. One can get rid of these errors by continuum extrapolation, performing simulations on a lattice with a larger volume and choosing the proper fit interval, etc [64].

In Monte Carlo simulations the random variables are used repeatedly causing fluctuations around the true values of the observable of interest and

give approximate results. Therefore, it is pertinent to estimate their statistical errors with the help of statistical methods. The values of primary observables x_i are obtained by averaging the values measured on the N configurations. Where $\bar{x}$ is only an estimate of the true value of x and must therefore always be given in together with its statistical error. For uncorrelated data

$$\bar{x} = \sum_{i=1}^{N} x_i, \quad \sigma_x^2 = \frac{1}{N-1} \sum_{i=1}^{N} (x_i - \bar{x})^2 \,. \tag{3.54}$$

It is shown in [65] that the mean value of measurement x_i with its statistical error is given as

$$\bar{x} \pm \sigma, \quad \text{with } \sigma = \frac{\sigma_x}{\sqrt{N}}. \tag{3.55}$$

Note that the accuracy depends strongly on the number of measurements and the statistical error decreases inversely with $\sqrt{N}$.

Integrated autocorrelation time:

In the process of generation of the configurations in a Markov chain where new configurations are generated from previous ones, configurations are correlated in Monte Carlo time. If the error for correlated data is determined by the above method, it will be underestimated. To compensate for this, we need to calculate the integrated autocorrelation time [66]. It is given as

$$\tau_{\mathcal{O},\text{int}} = \frac{1}{2} + \sum_{j=1}^{N} A(j) \left(1 - \frac{j}{N}\right), \tag{3.56}$$

with

$$A(j) = \frac{\langle \mathcal{O}_i \mathcal{O}_{i+j} \rangle - \langle \mathcal{O}_i \rangle^2}{\langle \mathcal{O}_i^2 \rangle - \langle \mathcal{O}_i \rangle^2} \tag{3.57}$$

For normalised autocorrelation function we put $A(0) = 1$. If the time separation is sufficiently large then this function decays exponential as

$$A(j) \xrightarrow{j \to \infty} a e^{-\frac{j}{\tau_{\mathcal{O},\text{exp}}}}, \tag{3.58}$$

72

where a is constant and $\tau_{\mathcal{O},\exp}$ represents the exponential autocorrelation time. The exponential behavior of $A(j)$ and for $N \gg \tau_{\mathcal{O},\exp}$ the quantity $\left(1 - \frac{j}{N}\right)$ is neglected without any problem. Thus the integrated autocorrelation time is

$$\tau_{\mathcal{O},\text{int}} = \frac{1}{2} + \sum_{j=1}^{N} A(j). \tag{3.59}$$

The error from Eq. (3.55) of the correlated data now modifies to

$$\sigma = \sqrt{\frac{2\,\tau_{\mathcal{O},\text{int}}}{N}}\,\sigma_x. \tag{3.60}$$

Data blocking method (Binning):

For large data produced in Monte Carlo simulations if it is expensive to compute autocorrelation time, the simplest way to obtain the statistically independent data is to apply binning. In this procedure the data x_i is divided into N_B sub-blocks called bins with bin size L_B. The number of new data points will be

$$N_B = \frac{N}{L_B} \tag{3.61}$$

where N is total number of data points. The mean values of sub-blocks $x_{B,i}$ will then serve as new data points. The variance of new data set is

$$\sigma_B^2 = \frac{1}{N_B\,(N_B - 1)} \sum_{i=1}^{N_B} (x_{B,i} - \bar{x})^2. \tag{3.62}$$

The variance σ_B^2 of the new data set should decrease with $\frac{1}{N_B}$. The bin size should be large enough to have statistically independent data. One way to estimate size of L_B is: increase L_B, the corresponding variance will also increase, choose L_B where the variance is stable. The autocorrelation time can also be calculated from this procedure as [66]

$$\tau_{\text{int}} = L_B \frac{\sigma_B^2}{2\sigma_x^2}. \tag{3.63}$$

where σ_x^2 is from Eq. (3.54). This estimation of the integrated autocorrelation time is not as accurate as determined by the autocorrelation function, but it can be implemented easily. The error of the variance σ_B^2 of the binned mean value $x_{B,i}$, it can be found in [68], is

$$\Delta \sigma_B^2 = \sqrt{\frac{2}{N_B - 1}} \, \sigma_B^2. \tag{3.64}$$

Estimation of bin size (L_B):

Once the integrated autocorrelation time is known, the optimal bin size can be estimated to make the data statistically independent. In this case the error calculated by Jackknife procedure will be reliable. According to Ref. [69], the optimal bin size is given as

$$L_B^{(\text{opt})} = \tau_{\mathcal{O},\exp} \left(\frac{2N}{\tau_{\mathcal{O},\exp}} \right)^{\frac{1}{3}}. \tag{3.65}$$

This formula keeps the balance between number of resultant data points N_B after binning and statistical errors. If L_B is too large then N_B will be small, resulting in large statistical errors as $\sigma_B \propto \frac{1}{\sqrt{N_B}}$.

Jackknife:

For normal observables, the expectation value together with its statistical error can be obtained using standard way of taking its mean value and variance, or fitting observable etc. However, for functions which depend non-linearly upon the expectation values of the correlation functions, the standard error propagation methods are more complicated. Therefore, we use an alternative approach called Jackknife method. It is a systematic way of getting the standard error of stochastic measurements.

Let's consider a set of N data points in a measurement and let $\hat{\theta}$ be an observable computed from this original set. N subsets can be constructed by omitting ith entry of the given set. The mean value θ_i is obtained from each

subset. The standard error of $\hat{\theta}$ reads [65]

$$\sigma_{\hat{\theta}} = \sqrt{\frac{N-1}{N} \sum_{i=1}^{N} \left(\theta_i - \hat{\theta} \right)^2}. \tag{3.66}$$

The final result would be

$$\langle \theta \rangle = \hat{\theta} \pm \sigma_{\hat{\theta}}. \tag{3.67}$$

If the $\hat{\theta}$ is biased , it is replaced by the unbiased estimator $\hat{\theta} - (N-1)(\tilde{\theta} - \hat{\theta})$, where

$$\tilde{\theta} = \frac{1}{N} \sum_{i=1}^{N} \theta_i. \tag{3.68}$$

Bootstrap:

Just like Jackknife let's consider again a data set of N entries. Suppose that the object of interest is θ. Let's call the observable obtained from the original set $\hat{\theta}$. The $\hat{\theta}$ can be obtained by taking simple mean or by fitting the data. Let's take K number of sets each of N data points. This recycling of the data actually costs nothing. Some data points may appear more than once, that would not harm. From each set θ_j is computed. The mean value of the θ_j and its error is calculated as [65]

$$\tilde{\theta} = \frac{1}{N} \sum_{j=1}^{N} \theta_j, \quad \sigma_{\tilde{\theta}} = \sqrt{\frac{1}{K} \sum_{j=1}^{K} \left(\theta_j - \tilde{\theta} \right)^2}. \tag{3.69}$$

The final result would be

$$\langle \theta \rangle = \tilde{\theta} \pm \sigma_{\tilde{\theta}}. \tag{3.70}$$

If the observables are biased, then $\tilde{\theta} \neq \hat{\theta}$. The difference gives the bias and provides an estimate of divergence from the true value $\langle \theta \rangle$.

Chapter 4

Ward identities in $\mathcal{N} = 1$ SYM theory

4.1 Introduction

In this chapter we shall discuss the full analysis of the SUSY Ward identities (WIs). We start with the derivation of a master formula for the Ward indentity followed by its supersymmetric form in the continuum and on the lattice. We renormalise it and include all relevant operators of dimensions 9/2 and lower. Furthermore, we determine numerical results of correlation functions appearing in the formula of the Ward identities. We explain three different methods, namely the Local method, the Global method and the GLS method to estimate the subtracted gluino mass which will then be used together with the adjoint pion mass squared to obtain the remnant gluino mass in the chiral limit. Finally, we perform the continuum extrapolation using the remnant gluino mass in physical units as a function of the physical lattice spacing squared to see whether SUSY is recovered.

4.1.1 Noether's theorem

The Noether's theorem provides, at the classical level, the relation between symmetries and conservation laws [35]. It is stated as "*every symmetry of the action of a physical system has corresponding conservation law*" [70].

Let's consider a field $\phi(x) = \left(\phi^k(x)\right)$ at space-time coordinates x in a field theory. An infinitesimal transformation of the field by a set of infinitesimal real valued parameters $\omega^a(x)$, with $a = 1, \ldots, N$, results

$$\phi(x) \rightarrow \phi^{'}(x) = e^{i\omega^a(x)T^a}\phi(x) = (1 + i\omega^a(x)T^a + \cdots)\phi(x), \qquad (4.1)$$

as $\omega^a(x)$ are small, the higher order terms can be ignored, therefore the variation of the field reads

$$\delta\phi(x) = \phi^{'}(x) - \phi(x) = i\omega^a(x)T^a\phi(x). \qquad (4.2)$$

Here we assume that internal symmetries hold and they do not change the coordinates x. In Eq. (4.1) $e^{i\omega^a(x)T^a}$ is an element of Lie group and the matrices T^a are the group generators satisfying

$$\left[T^a, T^b\right] = if_{abc}T^c, \qquad (4.3)$$

where f_{abc} are the structure constants, they can in general be the real or the complex numbers. Now let's consider the variation of the action in a given theory

$$\delta S = \int d^4x \left(\frac{\partial \mathcal{L}}{\partial \phi(x)}\delta\phi(x) + \frac{\partial \mathcal{L}}{\partial\left(\partial_\mu\phi(x)\right)}\delta\left(\partial_\mu\phi(x)\right)\right) \qquad (4.4)$$

$$= \int d^4x \left(\frac{\partial \mathcal{L}}{\partial \phi(x)} + \pi^\mu\partial_\mu\right)\delta\phi(x), \qquad (4.5)$$

with $\pi^\mu = \frac{\partial \mathcal{L}}{\partial(\partial_\mu\phi(x))}$. The Lagrangian density $\mathcal{L}\left(\phi(x), \partial_\mu\phi(x)\right)$ depends upon field $\phi(x)$ and its first derivative. By partial integration and assuming the boundary terms to vanish, Eq. (4.5) is reduced to

$$\delta S = \int d^4x \frac{\delta S}{\delta\phi(x)}\delta\phi(x), \qquad (4.6)$$

where $\frac{\delta S}{\delta \phi(x)} = \frac{\partial \mathcal{L}}{\partial \phi(x)} - \partial_\mu \pi^\mu$. Plugging Eq. (4.2) into Eq. (4.6) we get

$$\delta S = i \int d^4x \, \frac{\delta S}{\delta \phi(x)} \omega^a(x) T^a \phi(x). \tag{4.7}$$

Here $\frac{\delta S}{\delta \phi(x)}$ are the classical field equations and this expression vanishes

$$\frac{\delta S}{\delta \phi(x)} = 0. \tag{4.8}$$

Let's take the functional derivative of Eq. (4.7) with respect to $\omega^a(x)$. We have

$$\frac{\delta S[\phi']}{\delta \omega^a(x)} = i \frac{\delta S}{\delta \phi(x)} T^a \phi(x). \tag{4.9}$$

Suppose that, there exist some local functions $j_\mu^a(x)$ and $\Delta^a(x)$ of field $\phi(x)$ such that

$$\frac{\delta S}{\delta \omega^a(x)} = -\partial^\mu j_\mu^a(x) + \Delta^a(x). \tag{4.10}$$

If the equations of motion are satisfied then the left hand side of Eq. (4.10) will be zero. Hence we are left with $\partial^\mu j_\mu^a(x) = \Delta^a(x)$ where $\Delta^a(x)$ is symmetry breaking term. If symmerty holds then $\Delta^a(x) = 0$ and $\partial^\mu j_\mu^a(x) = 0$, which is a continuity equation where $j_\mu^a(x)$ is conserved current according to Noether's theorem. In this case the action is invariant under transformation with constant $\omega^a(x) = \omega^a$

$$\frac{\partial S}{\partial \omega^a} = \int d^4x \, \frac{\delta S}{\delta \omega^a(x)} = - \int d^4x \, \partial^\mu j_\mu^a(x) = 0. \tag{4.11}$$

To determine the $j_\mu^a(x)$ of Eq. (4.10), we consider the variation of $\mathcal{L}$ as

$$\delta \mathcal{L} = \frac{\partial \mathcal{L}}{\partial \phi(x)} \delta \phi(x) + \frac{\partial \mathcal{L}}{\partial \left(\partial^\mu \phi(x) \right)} \partial^\mu \left(\delta \phi(x) \right) \tag{4.12}$$

$$= \frac{\partial \mathcal{L}}{\partial \phi(x)} \delta \phi(x) + \pi_\mu(x) \partial^\mu \delta \left(\phi(x) \right) \tag{4.13}$$

$$= \left(\frac{\partial \mathcal{L}}{\partial \phi(x)} - \partial^\mu \pi_\mu(x) \right) \delta \phi(x) + \partial^\mu \left(\pi_\mu(x) \delta \phi(x) \right), \tag{4.14}$$

from Eq. (4.2)

$$\delta\mathcal{L} = \mathrm{i}\frac{\delta S}{\delta\phi(x)}\omega^a(x)T^a\phi(x) + \mathrm{i}\partial^\mu\left(\pi_\mu(x)\omega^a(x)T^a\phi(x)\right), \qquad (4.15)$$

from Eq. (4.9)

$$\delta\mathcal{L} = \omega^a(x)\frac{\delta S}{\delta\omega^a(x)} + \mathrm{i}\partial^\mu\Big(\pi_\mu(x)\omega^a(x)T^a\phi(x)\Big), \qquad (4.16)$$

from Eq. (4.10)

$$\delta\mathcal{L} = -\,\omega^a(x)\left(\partial^\mu j_\mu^a(x) - \Delta^a(x)\right) + \mathrm{i}\partial^\mu\left(\pi_\mu(x)\omega^a(x)T^a\phi(x)\right) \qquad (4.17)$$

$$= -\,\omega^a(x)\partial^\mu\left(j_\mu^a(x) - \mathrm{i}\pi_\mu(x)T^a\phi(x)\right) + \omega^a(x)\Delta^a(x) \qquad (4.18)$$

$$+ \mathrm{i}\pi_\mu(x)\left(\partial^\mu\omega^a(x)\right)T^a\phi(x).$$

If $\omega^a(x) \equiv \omega^a$, it is global in this case

$$\delta\mathcal{L} = -\omega^a\partial^\mu\left(j_\mu^a(x) - \mathrm{i}\pi_\mu(x)T^a\phi(x)\right) + \omega^a\Delta^a(x). \qquad (4.19)$$

As $\Delta^a(x)$ is a symmetry breaking term, if $\Delta^a(x) = 0$ then

$$\delta\mathcal{L} = -\omega^a\partial^\mu\left(j_\mu^a(x) - \mathrm{i}\pi_\mu(x)T^a\phi(x)\right). \qquad (4.20)$$

Let

$$f_\mu^a(x) = j_\mu^a(x) - \mathrm{i}\pi_\mu(x)T^a\phi(x), \qquad (4.21)$$

we have

$$\delta\mathcal{L} = -\omega^a\partial^\mu f_\mu^a(x), \qquad (4.22)$$

Let's consider a case in which $\mathcal{L}$ is invariant under the given transformation, that means $\delta\mathcal{L} = 0$ and Eq. (4.22) reduces to

$$\partial^\mu f_\mu^a(x) = 0, \qquad (4.23)$$

hence $f_\mu^a(x)$ is a constant and we choose it to be 0 without loss of generality. Consequently, Eq. (4.21) gets the form

$$j_\mu^a(x) = \mathrm{i}\pi_\mu(x)T^a\phi(x). \tag{4.24}$$

4.1.2 Ward identities

In the classical field theory, the Noether's theorem gives the conserved current $j_\mu(x)$. If field equations are satisfied then the divergence of the current vanishes i.e. $\partial^\mu j_\mu(x) = 0$. However, in quantum field theory the functional integral integrates over all field configurations and the field equations are not satisfied. In this case we use quantum version of the Noether's theorem, the so-called Ward identities.

Now lets consider the generating functional of Green's functions

$$Z[J] = \int [d\phi]e^{-S[\phi]+(J,\phi)}, \tag{4.25}$$

where

$$(J,\phi) = \int d^4x\, J(x)\phi(x), \tag{4.26}$$

and $J(x)$ is a source term. In the end we will set this source term to zero. Suppose that $[d\phi]$ is invariant under the symmetry transformation (4.1). Then

$$\begin{aligned}
Z[J] &= \int [d\phi']e^{-S[\phi']+(J,\phi')} \\
&= \int [d\phi]e^{-S[\phi']+(J,\phi')} \\
&=: Z[J,\omega].
\end{aligned} \tag{4.27}$$

Therefore

$$\begin{aligned}
0 &= \frac{\delta Z[J,\omega]}{\delta\omega^a(x)}\Big|_{\omega=0} \\
&= \int [d\phi]\left\{-\frac{\delta S[\phi]}{\delta\omega^a(x)} + \frac{\delta(J,\phi)}{\delta\omega^a(x)}\right\}e^{-S[\phi]+(J,\phi)}.
\end{aligned} \tag{4.28}$$

Also

$$\frac{\delta(J, \phi)}{\delta\omega^a(x)} = \int d^4y \, \frac{\delta\left(J(y)\phi(y)e^{i\omega^a(y)T^a}\right)}{\delta\omega^a(x)}$$
$$= iT^a J(x)\phi(x). \tag{4.29}$$

Put Eqs. (4.10,4.29) in Eq. (4.28) we get

$$\left\langle \left\{\partial^\mu j_\mu^a(x) - \Delta^a(x) + iT^a J(x)\phi(x)\right\} e^{(J,\phi)}\right\rangle = 0. \tag{4.30}$$

This is the master formula for the Ward identities. If we set $J(x) = 0$ in Eq. (4.30) naively it becomes

$$\left\langle \partial^\mu j_\mu^a(x)\right\rangle = \langle \Delta^a(x)\rangle, \tag{4.31}$$

where $\Delta^a(x)$ is symmetry breaking term. If we take the derivative of Eq. (4.30) with respect to $J(y)$ and set $J(x) = 0$ we obtain

$$\underbrace{\left\langle \partial^\mu j_\mu^a(x)\phi(y)\right\rangle}_{\text{Divergence of current}} = \underbrace{\left\langle \Delta^a(x)\phi(y)\right\rangle}_{\text{Symmetry breaking term}} + \underbrace{i\delta(x-y)\left\langle T^a\phi(y)\right\rangle}_{\text{Contact term}}. \tag{4.32}$$

In general, for fields $\phi^{k_i}(y_i)$ we get

$$\left\langle \partial^\mu j_\mu^a(x)\phi^{k_1}(y_1)\ldots\phi^{k_n}(y_n)\right\rangle = \left\langle \Delta^a(x)\phi^{k_1}(y_1)\ldots\phi^{k_n}(y_n)\right\rangle \tag{4.33}$$
$$+ i\sum_{l=1}^{n} \delta(x-y_l)\left\langle \phi^{k_1}(y_1)\ldots(T^a\phi(y_l))^{k_l}\ldots\phi^{k_n}(y_n)\right\rangle.$$

4.1.3 SUSY Ward identities in the continuum

The supersymmetric version of Ward identities of Eq. (4.32) in the continuum, for any gauge invariant operator $Q(x)$ and for the supercurrent $S_\mu(x)$, reads

$$\langle \partial^\mu S_\mu(x)Q(y)\rangle = m_{\tilde{g}}\langle \chi(x)Q(y)\rangle - \left\langle \frac{\delta Q(y)}{\delta\bar{\epsilon}(x)}\right\rangle, \tag{4.34}$$

where the symmetry-breaking term $m_{\tilde{g}}\langle \chi(x)Q(y)\rangle$ appears due to non-zero gluino mass in the action of the theory and the last term of Eq. (4.34) is a

contact term. The continuum versions of the supercurrent $S_\mu(x)$ and of $\chi(x)$ have the following forms

$$S_\mu(x) = -\frac{2\mathrm{i}}{g}\mathrm{tr}\Big[F_{\nu\rho}(x)\sigma_{\nu\rho}\gamma_\mu\lambda(x)\Big], \tag{4.35}$$

$$\chi(x) = +\frac{2\mathrm{i}}{g}\mathrm{tr}\Big[F_{\mu\nu}(x)\sigma_{\mu\nu}\lambda(x)\Big]. \tag{4.36}$$

The massless limit can be obtained by determination of the subtracted gluino mass non-perturbatively on the lattice. For this purpose, we need to have a lattice version of the Ward identity and corresponding operators.

4.1.4 SUSY Ward identities on the lattice

SUSY transformations on the lattice complying with parity ($\mathcal{P}$), charge conjugation ($\mathcal{C}$), time-reversal ($\mathcal{T}$) and gauge invariance are [71]

$$\delta U_\mu(x) = -\frac{\mathrm{i}g_0 a}{2}\Big(\bar{\epsilon}(x)\gamma_\mu U_\mu(x)\lambda(x) + \bar{\epsilon}(x+\hat{\mu})\gamma_\mu\lambda(x+\hat{\mu})U_\mu(x)\Big), \tag{4.37}$$

$$\delta U_\mu^\dagger(x) = +\frac{\mathrm{i}g_0 a}{2}\Big(\bar{\epsilon}(x)\gamma_\mu\lambda(x)U_\mu^\dagger(x) + \bar{\epsilon}(x+\hat{\mu})\gamma_\mu U_\mu^\dagger(x)\lambda(x+\hat{\mu})\Big), \tag{4.38}$$

$$\delta\lambda(x) = +\frac{1}{2}P_{\mu\nu}^{(cl)}(x)\sigma_{\mu\nu}\epsilon(x), \tag{4.39}$$

$$\delta\bar{\lambda}(x) = -\frac{1}{2}\bar{\epsilon}(x)\sigma_{\mu\nu}P_{\mu\nu}^{(cl)}(x), \tag{4.40}$$

where $\epsilon(x)$ and $\bar{\epsilon}(x)$ are fermionic parameters, and $P_{\mu\nu}^{(cl)}(x)$ is the clover-symmetrised plaquette defined in Eq. (2.33). For any local insertion operator $Q(x)$, the above transformations result in the following form of the lattice Ward identity

$$\sum_\mu \left\langle \left(\nabla_\mu S_\mu(x)\right) Q(y)\right\rangle = m_{\tilde{g}}\left\langle\chi(x)Q(y)\right\rangle + \left\langle X_S(x)Q(y)\right\rangle - \left\langle\frac{\delta Q(y)}{\delta\bar{\epsilon}(x)}\right\rangle. \tag{4.41}$$

In Eq. (4.41) the operators $\nabla_\mu S_\mu(x)$ and $\chi(x)$ serve as "sink" operators whereas the opeator $Q(x)$ is the "source" operator in numerical simulations. The operator $Q(x)$ should have at least one non-zero spin-$\frac{1}{2}$ component. It

may be chosen as

$$Q(x) = \bar{\mathcal{O}}^T(x) \equiv C^{-1}\mathcal{O}(x), \tag{4.42}$$

where $\mathcal{O}(x)$ is a Majorana bispinor and must be gauge invariant. Its optimal choice can be $\chi^{(sp)}(x)$, sp stands for "spatial plaquette", the reason behind this choice is that it gives the best signal, see Ref. [4] for detailed discussion. $\chi^{(sp)}(x)$ reads

$$\chi^{(sp)}(x) = \sum_{i<j} \sigma_{ij} \text{tr}\left[P_{ij}^{(cl)}(x)\lambda(x)\right]. \tag{4.43}$$

The contact term of Eq. (4.41) is proportional to a strongly peaked function (Dirac delta function) and has only contribution when the distance $|x - y|$ is zero. In numerical simulations, if source and sink are placed apart, then the distance $|x-y|$ is non-zero, and consequently the contact term can be ignored in the following discussions. The resultant Ward identity now becomes

$$\sum_\mu \left\langle \left(\nabla_\mu S_\mu(x)\right) Q(y) \right\rangle = m_{\tilde{g}} \left\langle \chi(x)Q(y) \right\rangle + \left\langle X_S(x)Q(y) \right\rangle. \tag{4.44}$$

The term containing $\chi(x)$ arises due to the non-zero gluino mass in the action that breaks the SUSY softly and can only be recovered in the chiral limit. The term $X_S(x)$ is introduced by the lattice regulator and gives rise to a non-trivial contribution which breaks the SUSY explicitly. The broken SUSY due to the lattice regulator can only be recovered in the zero lattice spacing limit. For the moment, the term $X_S(x)$ is irrelevant because at tree level it is of the order a and will vanish in the continuum limit.

There are many definitions of the supercurrent $S_\mu(x)$, they differ from each other up to terms which go to zero in the continuum limit [4]. One choice could be the point split (ps) [72]

$$S_\mu^{(ps)}(x) = -\frac{1}{2}\sum_{\rho\sigma} \sigma_{\rho\sigma}\gamma_\mu \text{tr}\Big[P_{\rho\sigma}^{(cl)}(x)U_\mu^\dagger(x)\lambda(x+\hat{\mu})U_\mu(x) \tag{4.45}$$
$$+P_{\rho\sigma}^{(cl)}(x+\mu)U_\mu(x)\lambda(x)U_\mu^\dagger(x)\Big],$$

together with backward derivative $\nabla_\mu^{bd} f(x) = \frac{f(x)-f(x-\hat{\mu})}{a}$. Another possible

definition of the SUSY current is the local (*loc*) one, that is

$$S_\mu^{(loc)}(x) = -\sum_{\rho\sigma} \sigma_{\rho\sigma} \gamma_\mu \text{tr} \left[P_{\rho\sigma}^{(cl)}(x)\lambda(x) \right]. \tag{4.46}$$

To fulfill the Ward identity (4.44), as required by parity and by time reversal, the symmetric lattice derivative $\nabla_\mu^{sym} f(x) = \frac{f(x+\hat{\mu})-f(x-\hat{\mu})}{2a}$ for local definition is used. Moreover, the symmetry breaking terms due to the lattice regulator for the case of local and point split agree up to $O(a)$ effects i. e. $X_S^{(loc)}(x) = X_S^{(ps)}(x) + O(a)$. Finally, the operator $\chi(x)$ which is involved in the soft breaking term has the following form

$$\chi(x) = \sum_{\rho\sigma} \sigma_{\rho\sigma} \text{tr} \left[P_{\rho\sigma}^{(cl)}(x)\lambda(x) \right]. \tag{4.47}$$

The SUSY Ward identity in Eq. (4.44) connects bare correlation functions. In numerical simulations, the gluino mass has non-zero value. For small gluino mass (large κ), the inversion of Wilson-Dirac operator D_w is prohibitively expensive and additionally there is a problem of the Pfaffian sign. This symmetry breaking term has an obvious dependence on the choice of lattice SUSY transformations. Naively the symmetry breaking term $X_S(x)$ vanishes in the continuum and SUSY WI is recovered [72].

At leading order the term $X_S(x)$ gives a finite contribution, and the recovery of the broken symmetry is a challenging task. The axial Ward identity is anomalous due to this situation. If the SUSY Ward identity is anomolous too, then SUSY itself is intrinsically broken and can not be used in supersymmetrically extended Standard Model. We have to renormalise the gluino mass and the supersymmetric current in order to make this situation clear.

4.1.5 Renormalisation of SUSY Ward identities

In the renormalisation process we have to consider all operators having dimensions $\leq 9/2$. These operators should be gauge invariant and should have

same quantum numbers as that of X_S. At tree level

$$X_S = aY_S, \tag{4.48}$$

and the definition of the subtracted $\bar{X}_S$ is [38, 73]

$$\bar{X}_S = a\bar{Y}_S = a[Y_S + \sum_i Z_i O_i], \tag{4.49}$$

where the operators O_i have dimensions $\leq 11/2$. The renormalisation coefficient $Z_{11/2}$, by power counting, is logarithmically divergent

$$Z_{11/2} \sim \ln(a\mu). \tag{4.50}$$

Since Eq. (4.49) has an overall multiplicative factor a, therefore, in the continuum its contribution vanishes.

Let's now analyse gauge invariant operators with dimensions $\leq 9/2$ with the same quantum numbers as that of $\partial^\mu S_\mu$, see analysis in [40]. To construct these operators the fields at hand are the gluino field $\lambda(x)$ and the gauge field $F_{\mu\nu}(x)$ with dimensions 3/2 and 2 respectively. Further constraints on the construction of these operators are that they must have the same behavior as $\partial_\mu S_\mu$, $\chi(x)$ and X_S under parity transformation, and they are spin-$\frac{1}{2}$ colour-neutral operators. These constraints leave us no choice other than the number of gluino fields to be one or three.

The most general construction of spin-$\frac{1}{2}$ operators with dimensions $\leq 9/2$ built from three gluino fields can be written as

$$W(x) = \epsilon_{abc} \left(\lambda_a^T(x) C\Gamma \lambda_b(x) \right) \Gamma' \lambda_c(x), \tag{4.51}$$

where C is the charge conjugation matrix, Γ and Γ' are Dirac matrices and can be any element of Dirac space (A.3). Since ϵ_{abc} is an anti-symmetric tensor, therefore the product $C\Gamma$ must be symmetric otherwise $W(x)$ will be zero identically. Explicit forms of these matrices are given in Appendix (A.2). The possible choices for Γ are γ_μ and $\sigma_{\mu\nu}$. Furthermore, the Lorentz indices of Γ and Γ' must be contracted because $W(x)$ has to be transformed as a

spin-$\frac{1}{2}$ object under the Lorentz group. The object with $\Gamma' = \gamma_5 \gamma_\mu$ behaves differently under parity transformations, therefore we are left with the following choices of Γ and Γ' only

$$\Gamma, \Gamma' = \gamma_\mu, \sigma_{\mu\nu}. \tag{4.52}$$

Using Fierz identities given in Appendix (A.4), it can be shown that $W(x) = 0$ in all cases.

Now we have to proceed further with the choice of only one gluino field. The object $W(x)$ can contain, in addition to the gluino field, the field strength tensor defined in Eq. (2.10) or from the covariant derivative defined in Eq. (2.11) or from combinations of these two i. e.

$$\mathrm{tr}\Big[D_\mu D_\nu D_\rho \tilde{\Gamma}_{\mu\nu\rho}\lambda(x)\Big], \tag{4.53}$$

$$\mathrm{tr}\Big[D_\mu F_{\nu\rho}(x)\tilde{\Gamma}_{\mu\nu\rho}\lambda(x)\Big], \tag{4.54}$$

$$\partial_\mu \mathrm{tr}\Big[F_{\nu\rho}(x)\tilde{\Gamma}_{\mu\nu\rho}\lambda(x)\Big]. \tag{4.55}$$

The trace is over colour indices. The covariant derivative defined in Eq. (2.11) for the field $w(x)$, which can either be $\lambda(x)$ or $F_{\mu\nu}(x)$, is written as

$$D_\mu w(x) = \partial_\mu w(x) + \mathrm{i}\left[A_\mu(x), w(x)\right]. \tag{4.56}$$

The trace commutator is zero and we get

$$\mathrm{tr}\left[D_{\mu_1}...D_{\mu_n}w(x)\right] = \partial_{\mu_1}...\partial_{\mu_n}\mathrm{tr}\left[w(x)\right]. \tag{4.57}$$

One can easily show that the operators of Eq. (4.53) vanish identically and the operators in Eq. (4.54) can be written in the form of operators in Eq. (4.55) [4]. Hence, we conclude that the gauge invariant operators of dimension 9/2 are only of the type which is in Eq. (4.54).

We can use the tensors $\delta_{\mu\nu}$ and $\epsilon_{\mu\nu\rho\sigma}$ together with Γ in order to construct $\tilde{\Gamma}$ for Eq. (4.54). As $\delta_{\mu\nu}$ and $\epsilon_{\mu\nu\rho\sigma}$ have an even number of indices, therefore Γ must have an odd number of indices which leaves us with $\{\gamma_\mu, \gamma_5\gamma_\mu, \sigma_{\mu\nu}\gamma_\rho, \gamma_\mu\sigma_{\nu\rho}\}$. However, not all of them are independent, see Ap-

pendix (A.3). Hence the possible choices for Γ now are γ_μ and $\gamma_5\gamma_\mu$.

1. **Case 1, $\Gamma = \gamma_\mu$:**
   In this case the structure of $\tilde{\Gamma}$ will be

   (a) $\tilde{\Gamma}_{\mu\nu\rho} = \delta_{\mu\nu}\gamma_\rho$

   (b) $\tilde{\Gamma}_{\mu\nu\rho} = \epsilon_{\mu\nu\rho\sigma}\gamma_\sigma$

   The choice (1b) is forbidden by the parity. The operator in Eq. (4.54) for the case (1a) becomes

   $$\text{tr}\left[D_\mu F_{\mu\nu}(x)\gamma_\nu\lambda(x)\right]. \tag{4.58}$$

   There are three different combinations that can be formed depending upon how D_μ acts on the fields.

   $$\text{tr}\left[D_\mu\left(F_{\mu\nu}(x)\gamma_\nu\lambda(x)\right)\right], \tag{4.59}$$
   $$\text{tr}\left[D_\mu\left(F_{\mu\nu}(x)\right)\gamma_\nu\lambda(x)\right], \tag{4.60}$$
   $$\text{tr}\left[F_{\mu\nu}(x)\gamma_\nu D_\mu\left(\lambda(x)\right)\right]. \tag{4.61}$$

   Using the equations of motion

   $$D_\mu F_{\mu\nu}^a(x) = -\mathrm{i}g\epsilon_{abc}\bar{\lambda}_b(x)\gamma_\mu\lambda_c(x), \tag{4.62}$$

   in Eq. (4.60) together with the Fierz identities of Appendix (A.4)

   $$\text{tr}\left[\left(\bar{\lambda}(x)\gamma_\nu\lambda(x)\right)\gamma_\nu\lambda(x)\right] = 0. \tag{4.63}$$

   Eq. (4.59) is just the sum of Eqs. (4.60,4.61) by Leibniz rule. Therefore, the only independent operator is

   $$\text{tr}\left[D_\mu\left(F_{\mu\nu}(x)\gamma_\nu\lambda(x)\right)\right] \equiv \partial_\mu\text{tr}\left[F_{\mu\nu}(x)\gamma_\nu\lambda(x)\right] \equiv \frac{g}{2\mathrm{i}}\partial_\mu T_\mu(x), \tag{4.64}$$

   where we call $T_\mu(x)$ the mixing current.

2. Case 2, $\Gamma = \gamma_5\gamma_\mu$:

This case can also be handled in a more or less similar way as in (1). In this case the structure of $\tilde{\Gamma}$ will be

(a) $\tilde{\Gamma}_{\mu\nu\rho} = \delta_{\mu\nu}\gamma_5\gamma_\rho$

(b) $\tilde{\Gamma}_{\mu\nu\rho} = \epsilon_{\mu\nu\rho\sigma}\gamma_5\gamma_\sigma$

Again, (2a) is excluded by parity and (2b) becomes

$$\tilde{\Gamma}_{\mu\nu\rho} = \epsilon_{\mu\nu\rho\sigma}\gamma_5\gamma_\sigma = -\sigma_{\nu\rho}\gamma_\mu + (\delta_{\mu\nu}\gamma_\rho - \delta_{\mu\rho}\gamma_\nu). \tag{4.65}$$

Only the first part of Eq. (4.65) is new, the rest has the same form as the operator in (4.58). The operator (4.54) with new part of Eq. (4.65) is given as

$$- \operatorname{tr}\left[D_\mu F_{\nu\rho}(x)\sigma_{\nu\rho}\gamma_\mu\lambda(x)\right]. \tag{4.66}$$

Again, applying Leibniz rule to reduce the number of independent operators from three to two

$$-\operatorname{tr}\left[D_\mu\left(F_{\nu\rho}(x)\sigma_{\nu\rho}\gamma_\mu\lambda(x)\right)\right], \tag{4.67}$$

$$-\operatorname{tr}\left[F_{\nu\rho}(x)\sigma_{\nu\rho}\gamma_\mu D_\mu\left(\lambda(x)\right)\right]. \tag{4.68}$$

The operator in (4.67) is proportional to the divergence of the supersymmetric current in Eq. (4.35)

$$- \operatorname{tr}\left[D_\mu\left(F_{\nu\rho}(x)\sigma_{\nu\rho}\gamma_\mu\lambda(x)\right)\right] = \frac{g}{2\mathrm{i}}\partial_\mu S_\mu(x). \tag{4.69}$$

The operator in (4.68), by using equation of motion $(\gamma_\mu D_\mu + m_{\tilde{g}})\lambda = 0$, gets the form

$$- \operatorname{tr}\left[F_{\nu\rho}(x)\sigma_{\nu\rho}\gamma_\mu D_\mu\left(\lambda(x)\right)\right] = m_{\tilde{g}}\operatorname{tr}\left[F_{\nu\rho}(x)\sigma_{\nu\rho}\left(\lambda(x)\right)\right] = \frac{g}{2\mathrm{i}}m_{\tilde{g}}\chi(x). \tag{4.70}$$

Where $\chi(x)$ is the mass term that is given in Eq. (4.36) and $m_{\tilde{g}}$ is the bare gluino mass. The operators of dimensions 9/2 which contribute

to the expression of the SUSY Ward identity are

$$S_\mu(x) = -\frac{2i}{g} \text{tr} \Big[F_{\nu\rho}(x) \sigma_{\nu\rho} \gamma_\mu \lambda(x) \Big], \tag{4.71}$$

$$T_\mu(x) = +\frac{2i}{g} \text{tr} \Big[F_{\mu\nu}(x) \gamma_\nu \lambda(x) \Big], \tag{4.72}$$

$$\chi(x) = +\frac{2i}{g} \text{tr} \Big[F_{\mu\nu}(x) \sigma_{\mu\nu} \lambda(x) \Big]. \tag{4.73}$$

The next step is to find operators with dimensions 7/2. They must contain only one gluino field together with the covariant derivative and the field strength tensor

$$\text{tr} \Big[D_\mu D_\nu \Gamma_{\mu\nu} \lambda(x) \Big], \tag{4.74}$$

$$\text{tr} \Big[F_{\mu\nu} \Gamma_{\mu\nu} \lambda(x) \Big], \tag{4.75}$$

$$\tag{4.76}$$

the operators in (4.74) vanish because of Eq. (4.57). $\Gamma_{\mu\nu}$ has to be an anti-symmetric tensor with even parity, therefore the only possibility is $\sigma_{\mu\nu}$. The corresponding operator is

$$\text{tr} \, [F_{\mu\nu} \sigma_{\mu\nu} \lambda(x)] = \frac{g}{2i} \chi(x). \tag{4.77}$$

The presence of this operator produces a mass subtraction $\bar{m}(\kappa, \beta, m_{\tilde{g}})$.

For dimension 5/2 and 3/2, the relevant operators are

$$\text{tr} \Big[D_\mu \Gamma_\mu \lambda(x) \Big], \tag{4.78}$$

$$\text{tr} \Big[\Gamma \lambda(x) \Big], \tag{4.79}$$

they vanish identically.

With this we conclude renormalisation process of the SUSY current and the gluino mass. As a result we obtain the following form of properly renormalised supersymmetric Ward identity.

$$Z_S \Big\langle \partial_\mu S_\mu(x) Q(y) \Big\rangle + Z_T \Big\langle \partial_\mu T_\mu(x) Q(y) \Big\rangle = (m_{\tilde{g}} - \bar{m}) \Big\langle \chi(x) Q(y) \Big\rangle. \tag{4.80}$$

Where Z_S and Z_T are renormalisation coefficients of currents $S_\mu(x)$ and $T_\mu(x)$. According to Ref. [40, 72] they have the forms

$$Z_S = 1 + O(g_0^2), \tag{4.81}$$

$$Z_T = O(g_0^2). \tag{4.82}$$

We define $m_S = m_{\tilde{g}} - \bar{m}$ as the subtracted gluino mass and rearrange the renormalisation coefficients to get the following Ward identity.

$$\left\langle \partial_\mu S_\mu(x) Q(y) \right\rangle + Z_T Z_S^{-1} \left\langle \partial_\mu T_\mu(x) Q(y) \right\rangle = m_S Z_S^{-1} \left\langle \chi(x) Q(y) \right\rangle. \tag{4.83}$$

By defining the renormalised SUSY current $S_\mu^{(R)}(x)$ as

$$S_\mu^{(R)}(x) = Z_S S_\mu(x) + Z_T T_\mu(x), \tag{4.84}$$

and renormalise the operator $\chi(x)$ multiplicatively, for the fully renormalised Ward identity we obtain

$$\left\langle \partial_\mu S_\mu^{(R)}(x) Q(y) \right\rangle = m_{\tilde{g}}^{(R)} \left\langle \chi^{(R)}(x) Q(y) \right\rangle. \tag{4.85}$$

Where $m_{\tilde{g}}^{(R)}$ is the renormalised gluino mass and proportional to subtracted gluino mass by

$$m_S = m_{\tilde{g}}^{(R)} Z_\chi^{-1}, \tag{4.86}$$

here Z_χ is renormalisation coefficient of the operator $\chi^{(R)}(x)$ which is expected to diverge in the continuum limit [40].

For numerical analysis we use the Eq. (4.83) because we are interested in a limit where m_S is zero, this limit is called the chiral limit. The critical value of the gluino mass (m_c) at κ_c is $m_c \propto 1/\kappa_c$, and $\bar{m}(\kappa_c, \beta, r) = m_{\tilde{g}}(\kappa_c)$, therefore m_S vanishes in this limit.

The value of $a m_S Z_S^{-1}$ can be obtained in numerical simulation at fixed β and κ. More importantly its value can be used in order to tune the theory. It has been shown in [38] that the chiral and supersymmetric limits coincide in the continuum limit.

4.1.6 Zero spatial momentum and lattice prescription of the operators

Numerically it is convenient to consider zero spatial momentum Ward identity by performing a sum over all three space coordinates of the correlation functions. As a result, one obtains a Ward identity for each time slice separation $t = x_4 - y_4$. Each term in Eq. (4.83) is a 4×4 matrix in Dirac space and can be expanded in the basis of 16 Dirac matrices (Γ_i) as

$$C(t) = \sum_{\Gamma_i} C_{\Gamma_i}(t)\, \Gamma_i, \tag{4.87}$$

where $C_{\Gamma_i}(t) = \frac{1}{4}\mathrm{tr}\,[C(t)\Gamma_i]$ and tr is over Dirac indices which are not written explicitly. The elements of Dirac space are given in Appendix (A.3). Now Eq. (4.83) becomes

$$C_{\Gamma_i,t}^{(S,\mathcal{O})} + (Z_T Z_S^{-1})C_{\Gamma_i,t}^{(T,\mathcal{O})} = (am_S Z_S^{-1})C_{\Gamma_i,t}^{(\chi,\mathcal{O})}, \tag{4.88}$$

where the expectation values of lattice operators are

$$
\begin{aligned}
C_{\Gamma_i}^{(S,\mathcal{O})}(t) &= \sum_{\vec{x}} \left\langle \nabla_4 S_4^{(loc)}(x)\Gamma_i \mathcal{O}(y) \right\rangle \tag{4.89}\\
&= -\sum_{\vec{x},\rho,\sigma,i,j} \left\langle \frac{1}{2}\sigma_{\rho\sigma}^{\alpha\gamma'}\gamma_4^{\gamma'\alpha'}\Gamma_i^{\alpha\beta} \Big\{ \mathrm{tr}\,[P_{\rho\sigma}(x+\hat{\mu}_4)T^a] \triangle_{a\alpha'}^{b\beta'}(x+\hat{\mu}_4,y) \right.\\
&\quad \left. -\,\mathrm{tr}\,[P_{\rho\sigma}(x-\hat{\mu}_4)T^a] \triangle_{a\alpha'}^{b\beta'}(x-\hat{\mu}_4,y) \Big\} \mathrm{tr}\,\Big[P_{ij}(y)T^b\Big]\sigma_{ij}^{\beta'\beta} \right\rangle,\\
C_{\Gamma_i}^{(T,\mathcal{O})}(t) &= \sum_{\vec{x}} \left\langle \nabla_4 T_4^{(loc)}(x)\Gamma_i \mathcal{O}(y) \right\rangle \tag{4.90}\\
&= \sum_{\vec{x},\nu,i,j} \left\langle \gamma_\nu^{\alpha\alpha'}\Gamma_i^{\alpha\beta}\Big\{ \mathrm{tr}\,[P_{4\nu}(x+\hat{\mu}_4)T^a] \triangle_{a\alpha'}^{b\beta'}(x+\hat{\mu}_4,y) \right.\\
&\quad \left. -\,\mathrm{tr}\,[P_{4\nu}(x-\hat{\mu}_4)T^a] \triangle_{a\alpha'}^{b\beta'}(x-\hat{\mu}_4,y) \Big\} \mathrm{tr}\,\Big[P_{ij}(y)T^b\Big]\sigma_{ij}^{\beta'\beta} \right\rangle,\\
C_{\Gamma_i}^{(\chi,\mathcal{O})}(t) &= \sum_{\vec{x}} \left\langle \chi(x)\Gamma_i\mathcal{O}(y) \right\rangle \tag{4.91}\\
&= \sum_{\vec{x},\mu,\nu,i,j} \left\langle \sigma_{\mu\nu}^{\alpha\alpha'}\Gamma_i^{\alpha\beta}\Big\{ \mathrm{tr}\,[P_{\mu\nu}(x)T^a] \triangle_{a\alpha'}^{b\beta'}(x,y) \Big\} \mathrm{tr}\,\Big[P_{ij}(y)T^b\Big]\sigma_{ij}^{\beta'\beta} \right\rangle.
\end{aligned}
$$

The space time position y is fixed at any point on the lattice, usually the origin is chosen for this purpose. With the help of discrete symmetries, it is possible to show that the contributions of correlation functions of Eq. (4.88) are non-vanishing only for $\Gamma_i = \mathbf{1}, \gamma_4$ [39]. This forms a set of two overdetermined, non-trivial and independent equations [4]

$$C_{\mathbf{1},t}^{(S,\mathcal{O})} + (Z_T Z_S^{-1}) C_{\mathbf{1},t}^{(T,\mathcal{O})} = (am_S Z_S^{-1}) C_{\mathbf{1},t}^{(\chi,\mathcal{O})}, \tag{4.92}$$

$$C_{\gamma_4,t}^{(S,\mathcal{O})} + (Z_T Z_S^{-1}) C_{\gamma_4,t}^{(T,\mathcal{O})} = (am_S Z_S^{-1}) C_{\gamma_4,t}^{(\chi,\mathcal{O})}. \tag{4.93}$$

These equations will now be solved for the ratio $Z_T Z_S^{-1}$ and for the subtracted gluino mass [1] $am_S Z_S^{-1}$ using different methods which will be explained below in details.

4.1.7 Smeared sources

From the previous experience of our collaboration, it has been seen that APE and Jacobi smearings provide great improvement in the gluino-glue signal-to-noise ratio which allowed proper determination of ground state masses. Since the structure of operators of SUSY Ward identities[2] is similar as that of the gluino-glue, therefore we apply same smearing techniques on these operators. Usually smearing is applied on both source and sink sides, however, in Ward identities case the situation is slightly different. We apply smearing only on source side i.e. on the local insertion operator of Eq. (4.47). We have tested wide range of smearing parameters for APE and Jacobi smearings and have found that the dependence of signal on the parameters is mild. Nevertheless, the optimal choice of parameters used for our analysis is given in Sec. (2.2).

---

[1]In fact, $am_S Z_S^{-1}$ is subtracted mass times the renormalisation constant in lattice units, but for the sake of convenience we shall call this quantity the "subtracted gluino mass".

[2]From now on we shall call Ward identities instead of Ward identity because of the set of two independent Eqs. (4.92,4.93).

4.1.8   Numerical results of correlation functions

The 6 correlation functions of Eqs. (4.92,4.93) at each time slice distance t^3 are calculated numerically with the help of high performance facilities. The numerical results of their expectation values with errors, estimated by Jackknife procedure, are shown in Fig. (4.1).

It is very interesting to note that the data points in the correlation functions of Fig. (4.1) at the smallest and at the largest value of the time-slice distance do not behave properly and are off from the expected pattern, actually this is the price we have to pay for ignoring the contact term of Eq. (4.41). Of course, this effect will also be seen in the estimated quantities from these correlation functions. Therefore, it is pertinent to consider some reliable starting value of t.

4.1.9   Discrete symmetry test

In order to check correctness and validity of numerical data of the correlation functions, it is easy with the help of discrete symmetries to show that these functions follow some rules. We employ parity ($\mathcal{P}$) and time reversal ($\mathcal{T}$) for that purpose. We follow similar steps as have been followed in Sec. (5.1.4), on the basis of Ref. [39], to show that the correlation functions obey

$$
\begin{aligned}
C_{\mathbf{1},t}^{(S,\mathcal{O})} &= -C_{\mathbf{1},N_t-t}^{(S,\mathcal{O})}, \quad C_{\gamma_4,t}^{(S,\mathcal{O})} = C_{\gamma_4,N_t-t}^{(S,\mathcal{O})}, \\
C_{\mathbf{1},t}^{(T,\mathcal{O})} &= -C_{\mathbf{1},N_t-t}^{(T,\mathcal{O})}, \quad C_{\gamma_4,t}^{(T,\mathcal{O})} = C_{\gamma_4,N_t-t}^{(T,\mathcal{O})}, \\
C_{\mathbf{1},t}^{(\chi,\mathcal{O})} &= -C_{\mathbf{1},N_t-t}^{(\chi,\mathcal{O})}, \quad C_{\gamma_4,t}^{(\chi,\mathcal{O})} = C_{\gamma_4,N_t-t}^{(\chi,\mathcal{O})}.
\end{aligned}
\tag{4.94}
$$

Numerical values of the correlation functions are given in Appendix (B.1) and are plotted in Fig. (4.1). They clearly depict that these symmetries are being respected by these correlation functions within errors.

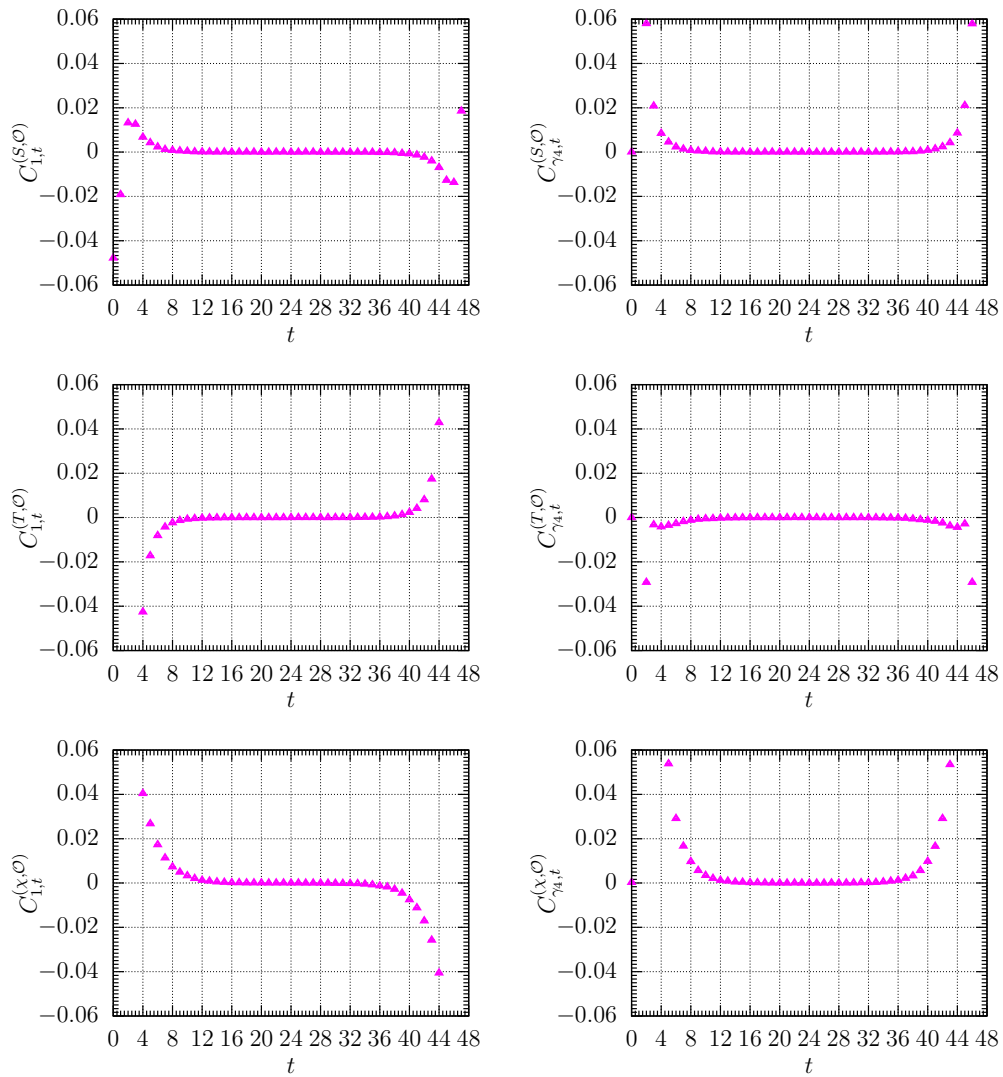[3]It is $\frac{t}{a}$, we ignore a for convenience

Figure 4.1: Average values of 6 correlation functions present in a set of two non-trivial Eqs. (4.92,4.93) for an ensemble where we have maximum statistics available i. e. $\beta = 5.6$ and $\kappa = 0.1655$.

4.1.10   Symmetrisation of correlation functions

From Eq. (4.94) it is now possible to (anti-)symmetrise the data in order to reduce statistical uncertainties. We combine the data at t and $N_t - t$, which makes the time extent of the data simply one half ($N_t/2$). In this way, we do not throw out the useful information.

4.2 Numerical analysis of SUSY Ward identities

The purpose of eployment of SUSY Ward identities is to estimate the expectation value of the subtracted gluino mass for each gauge ensemble. This will be used to tune the $\mathcal{N} = 1$ SYM theory as well as to ensure the recovery of broken SUSY on the lattice.

4.2.1 Estimation of the subtracted gluino mass $am_S Z_S^{-1}$

To obtain the best estimate for $A = Z_T Z_S^{-1}$ and $B = am_S Z_S^{-1}$ we proceed as follows. Let

$$\hat{x}_{1,t,1} = C_{\mathbf{1},t}^{(S,\mathcal{O})}, \quad \hat{x}_{1,t,2} = C_{\mathbf{1},t}^{(T,\mathcal{O})}, \quad \hat{x}_{1,t,3} = C_{\mathbf{1},t}^{(\chi,\mathcal{O})}, \tag{4.95}$$

$$\hat{x}_{2,t,1} = C_{\gamma_4,t}^{(S,\mathcal{O})}, \quad \hat{x}_{2,t,2} = C_{\gamma_4,t}^{(T,\mathcal{O})}, \quad \hat{x}_{2,t,3} = C_{\gamma_4,t}^{(\chi,\mathcal{O})}. \tag{4.96}$$

be the expectation values of the measured values $x_{b,t,\alpha}$ in Monte Carlo simulations. They are random variables with expectation values $\hat{x}_{b,t,\alpha} \equiv \langle x_{b,t,\alpha} \rangle$.

$$\hat{x}_{b,t,1} + A\hat{x}_{b,t,2} - B\hat{x}_{b,t,3} = 0, \qquad \text{where} \quad b = 1, 2, \tag{4.97}$$

The Eq. (4.97) with the notation

$$A_1 = 1, \quad A_2 = A, \quad A_3 = -B, \tag{4.98}$$

leads to

$$\sum_{\alpha} A_\alpha \, \hat{x}_{b,t,\alpha} = 0, \qquad \text{where} \quad \alpha = 1, 2, 3. \tag{4.99}$$

With double index $i = (b,t)$, running over a number of $2N_t$ values, Eq. (4.99) becomes

$$\sum_{\alpha} A_\alpha \hat{x}_{i\alpha} = 0. \tag{4.100}$$

Now the challange is to determine A_α, with A_1=1, in an overdetermined system of two non-trivial equations. Two methods for the analysis of SUSY Ward identities have already been used in our collaboration in the previous

studies of $\mathcal{N} = 1$ SYM theory with gauge group SU(2) in order to solve the Eqs. (4.100) for A and B; for details see [4] and for recent results see [3]. We call these methods "the Local method" and "the Global method". These methods do not consider proper weights in the solution of A and B, where the quantities with smaller errors have higher weights. Moreover, the statistical errors are over estimated and systematic errors, if they exist, are not considered at all. In this thesis, we shall consider proper weights for the Local and for the Global methods. In order to include correlations among the different correlators appearing in the expression of Ward identities we formulate a method based on generalised least squares fit called the GLS method.

4.2.2   The Local method

This method is based on linear fit and has been previously discussed in Ref. [4]. We improve this method by proper estimation of weighted averages. In this method, we proceed by minimising the following quantity from the Eq. (4.99)

$$F_t^{loc} = \sum_b \left(\sum_\alpha A_\alpha \, \hat{x}_{b,t,\alpha} \right)^2 , \qquad (4.101)$$

With the condition

$$\frac{\partial F_t^{loc}}{\partial A_\alpha} = 0, \qquad (4.102)$$

and the definition $\sum_b \hat{x}_{b,t,1} \hat{x}_{b,t,2} = \hat{X}_{12,t}$ results in

$$\hat{A}_t = \frac{\hat{X}_{t,13} \hat{X}_{t,23} - \hat{X}_{t,12} \hat{X}_{t,33}}{\hat{X}_{t,22} \hat{X}_{t,33} - X_{t,23}^2} \qquad (4.103)$$

$$\hat{B}_t = \frac{\hat{X}_{t,13} \hat{X}_{t,22} - \hat{X}_{t,12} \hat{X}_{t,23}}{\hat{X}_{t,22} \hat{X}_{t,33} - X_{t,23}^2} \qquad (4.104)$$

Eqs. (4.103,4.104) are valid only for averages over the whole Monte Carlo ensemble. The quantity B is of particular interest, therefore we shall only focuss on this quantity, of course the analysis techniques which are valid for B are also true for A. The estimator for the statistical variance of $\hat{B}_t$ is

obtained by standard Jackknife procedure, for further details see [65], and is given by the following formula:

$$\left(\sigma_t^{stat}\right)^2 = \frac{N-1}{N} \sum_{i=1}^{N} \left(\hat{B}_t - B_{t,i}\right)^2,$$ (4.105)

where $i = 1, ..., N$ represents a set of N Jackknife samples and $B_{t,i}$ is determined from each sample. If it turns out that the differences between the various $\hat{B}_t$ are typically larger than the statistical errors σ_t^{stat} (for a more quantitative statement see Ref. [74]), we have to suspect that there are further sources of errors σ_t^{sys}.

$$\bar{B} = \frac{\sum_t w_t B_t}{\sum_j w_j}, \qquad \text{where} \quad w_t = \frac{1}{\sigma_t^2} = \frac{1}{(\sigma_t^{stat})^2 + (\sigma^{sys})^2},$$ (4.106)

and its total error σ would be given by

$$\frac{1}{\sigma^2} = \sum_t \frac{1}{\sigma_t^2}.$$ (4.107)

In our case, however, we do not consider systematic error for this method, therefore $\sigma^{sys} = 0$.

The Local method has been deployed for all gauge ensembles. Fig. (4.2(a)) shows the numerical outcome of $B = am_S Z_S^{-1}$ for $\beta = 5.6$ (corresponds to the finest lattice spacing) and $\kappa = 0.1655$ (maximum statistics) by this method using Eq. (4.104). The x-axis represents simply the time slice distance (t), the maximum time extent in the figure is 24 instead of 48 because of symmetrisation of the data. We see a plateau as expected. To extract the value of subtracted gluino mass in lattice units by Local method we take a weighted average using Eq. (4.106). This weighted average together with its error band is also shown in the same figure.

4.2.3 The Global method

This method makes use of global fit and has also been used previously in our collaboration. We improve this method by taking proper weights into

account. In this method the following quantity from the Eq. (4.100) is minimized

$$F_t^{(glb)} = \sum_i \left(\frac{\sum_\alpha A_\alpha \hat{x}_{i\alpha}}{\sigma_t} \right)^2, \tag{4.108}$$

where the total variance $\sigma_t^2 = \sum_{b,\alpha} \sigma_{b,t,\alpha}^2$ serves as weight at each t and could be obtained from correlation functions $x_{i\alpha}$ by using Jackknife procedure.

In this method an additional sum over t is performed, where $t = t_{min}, ..., t_{max}$. The choice of t_{min}[4] depends upon the contact term present in Eq. (4.44). In principle it should influence the results only at $t = 0$, but due the presence of symmetric derivative in t direction, two more points are contaminated, therefore it is better to take $t_{min} \geq 3$. The correlation functions present in Eq. (4.95) are symmetric (anti-)symmetric, therefore they can be (anti-)symmetrised and t_{max} is then defined as $t_{max} = \frac{N_t}{2} + 1$, where N_t is the time extent of the hypercubic lattice. We apply the same condition as in Eq. (4.102) with the definition $\sum_i \hat{x}_{i,1}\hat{x}_{i,2} = \hat{X}_{12,t_{min}}$, where $i = (b,t)$, which results in the following expectation value of A and B.

$$\hat{A}_{t_{min}} = \frac{\hat{X}_{t_{min},13}\hat{X}_{t_{min},23} - \hat{X}_{t_{min},12}\hat{X}_{t_{min},33}}{\hat{X}_{t_{min},22}\hat{X}_{t_{min},33} - X_{t,23}^2} \tag{4.109}$$

$$\hat{B}_{t_{min}} = \frac{\hat{X}_{t_{min},13}\hat{X}_{t_{min},22} - \hat{X}_{t_{min},12}\hat{X}_{t_{min},23}}{\hat{X}_{t_{min},22}\hat{X}_{t_{min},33} - X_{t,23}^2} \tag{4.110}$$

Similar to the Local method, the estimation of error is done by using Jackknife procedure. This method takes full data into account at each t, therefore, there is no need to perform fit or weighted average. One has to choose values of the quatities A and B at some optimal choice of t_{min}. Using Eq. (4.110) of the Global method to estimate subtracted gluino mass we obtain Fig. (4.2(b)).

4.2.4 The GLS method

The Local and the Global methods have been used previously and discussed in the above subsections in order to find solutions for A and B numerically

---

[4]Actually it is $\frac{t_{min}}{a}$, but for simplicity we use only t_{min}
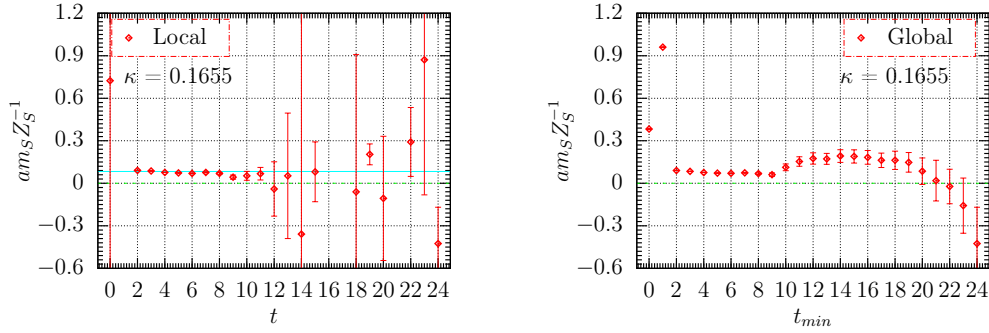
(a) Bare data of $am_S Z_S^{-1}$ at t according to Eq. (4.104) by the Local method which needs to be fitted with suitable fit range. Plateau is formed at $t = 3$ to $t = 8$.

(b) Data of $am_S Z_S^{-1}$ at t_{min} according to Eq. (4.110) by the Global method. An optimal value of t_{min} needs to be chosen.

Figure 4.2: Numerical results at $\beta = 5.6$ and $\kappa = 0.1655$ by the Local and by the Global methods for SYM theory with gauge group SU(3).

such that with the measured averages $\hat{x}_{b,t,\alpha}$ the equations are satisfied approximately in an optimal way. None of the above two methods have considered correlations among various quantities at different time slices. To consider the correlations in our present studies of $\mathcal{N} = 1$ SUSY Yang-Mills theory with gauge group SU(3) we develop a method, based on generalised least squares fit (GLS). Here we describe complete analytical calculations.

Let's assume $\bar{x}_{i\alpha}$ be the true values, and the measured values $x_{i\alpha}$ differ from the true ones by

$$y_{i\alpha} = x_{i\alpha} - \bar{x}_{i\alpha}, \tag{4.111}$$

where $y_{i\alpha}$ are stochastic variables with $\langle y_{i\alpha} \rangle = 0$ and

$$\langle y_{i\alpha} y_{j\beta} \rangle \equiv C_{i\alpha, j\beta}, \tag{4.112}$$

where $C_{i\alpha, j\beta} = \langle x_{i\alpha} x_{j\beta} \rangle - \langle x_{i\alpha} \rangle \langle x_{j\beta} \rangle$ is the covariance matrix of $x_{i\alpha}$. The probability distribution of the $y_{i\alpha}$ is given by

$$P \sim \exp \left\{ -\frac{1}{2} \sum_{i,\alpha,j,\beta} y_{i\alpha} M_{i\alpha;j\beta} y_{j\beta} \right\}, \tag{4.113}$$

where $M = C^{-1}$. The aim is to calculate A_α. We employ the method of maximum likelihood in the following way.

1. For given $x_{i\alpha}$, consider A_α to be fixed and find $\hat{x}_{i\alpha}$ such that P is maximum. The value at maximised (P_{max}) depends on the A_α.

2. Find A_α such that $P_{max}(A_\alpha)$ is maximum.

1. Let's consider

$$L = \frac{1}{2} \sum_{i,\alpha,j,\beta} (x_{i\alpha} - \hat{x}_{i\alpha}) M_{i\alpha;j\beta}(x_{j\beta} - \hat{x}_{j\beta}). \tag{4.114}$$

We want L to be minimum with constraint $\sum_\alpha A_\alpha \hat{x}_{i\alpha} = 0$ from Eq. (4.100).

$$L' = L + \sum_i \lambda_i \sum_\alpha A_\alpha \hat{x}_{i\alpha}, \tag{4.115}$$

where λ_i are Lagrange multipliers, and

$$\frac{\partial L'}{\partial \hat{x}_{i\alpha}} = 0, \quad \frac{\partial L'}{\partial \lambda_i} = 0. \tag{4.116}$$

Now

$$\frac{\partial L'}{\partial \hat{x}_{i\alpha}} = \sum_{j,\beta} M_{i\alpha;j\beta}(\hat{x}_{j\beta} - x_{j\beta}) + \lambda_i A_\alpha = 0 \tag{4.117}$$

Multiplying Eq. (4.117) by $C_{i\alpha,j\beta}$ we have

$$\hat{x}_{i\alpha} - x_{i\alpha} = -\sum_{j,\beta} C_{i\alpha,j\beta}\lambda_j A_\beta. \tag{4.118}$$

Multiplying Eq. (4.118) by $\sum_\alpha A_\alpha$ we get

$$\sum_\alpha A_\alpha x_{i\alpha} = \sum_j \lambda_j \sum_{\alpha,\beta} A_\alpha C_{i\alpha,j\beta} A_\beta. \tag{4.119}$$

We denote

$$\sum_{\alpha,\beta} A_\alpha C_{i\alpha,j\beta} A_\beta \doteq D_{ij}, \tag{4.120}$$

so that

$$\sum_{\alpha} A_{\alpha} x_{i\alpha} = \sum_j D_{ij} \lambda_j. \tag{4.121}$$

From this it follows

$$\lambda_i = \sum_j (D^{-1})_{ij} \sum_{\alpha} A_{\alpha} x_{j\alpha}. \tag{4.122}$$

Putting this result for λ_i into Eq. (4.118) gives

$$x_{i\alpha} - \hat{x}_{i\alpha} = \sum_{j,\beta} C_{i\alpha,j\beta} A_{\beta} \sum_{k\gamma} (D^{-1})_{jk} x_{k\gamma} A_{\gamma}. \tag{4.123}$$

By using Eqs. (4.120,4.123) in Eq. (4.114), we obtain

$$L_{min} = \frac{1}{2} \sum_{i,\alpha,j,\beta} (A_{\alpha} x_{i\alpha})(D^{-1})_{ij}(A_{\beta} x_{j\beta}). \tag{4.124}$$

This is the result of the first step in the maximum likelihood method. Now, for the averages $\hat{x}_{i\alpha}$ the corresponding quantity is given by

$$L_{min} = \frac{1}{2} \sum_{i,\alpha,j,\beta} (A_{\alpha} \hat{x}_{i\alpha})(D^{-1})_{ij}(A_{\beta} \hat{x}_{j\beta}), \tag{4.125}$$

where D_{ij} is estimated from the measured values by

$$D_{ij} = \sum_{\alpha,\beta} A_{\alpha} A_{\beta}(\langle x_{i\alpha} x_{j\beta} \rangle - \hat{x}_{i\alpha} \hat{x}_{j\beta}). \tag{4.126}$$

2. In the second step we have to find the minimum of L_{min} as a function of the parameters A_{α}, where we use $A_1 = 1$, so that it remains to find A_2 and A_3. The minimisation of $L_{min}(A_{\alpha})$ with respect to A_{α} must be done numerically, because D_{ij} depends on the A_{α}, it is impossible to find the solution analytically. We employ standard Jackknife method to obtain statistical errors by re-sampling the data and making subsets of the full sample by removing nth entry. We calculate A_2 and A_3 where there is global minimun of L_{min} for each subset and repeat the whole procedure for all subsets. In this way we arrive at our final result for $B = am_S Z_S^{-1}$ with error. Tab. (4.1) compares the results from these methods. The values are

compatible within errors, however, with GLS method we have more reliable measure on errors.

κ	The Local method	The Global method	The GLS method
0.1645	0.1306(18)	0.1317(17)	0.1333(20)
0.1650	0.1054(14)	0.1057(12)	0.1040(14)
0.1655	0.0712(19)	0.0706(16)	0.0701(09)
0.1660	0.0352(11)	0.0364(09)	0.0352(13)

Table 4.1: For comparison, the results of $am_S Z_S^{-1}$ from these three methods at the inverse gauge coupling $\beta = 5.6$. The subtracted gluino mass by the Global and the GLS methods is considered at $t_{min} = 5$. The weighted average of the mass by the Local method is also considered from $t = 5$ to $t = \frac{N_t+1}{2}$.

4.2.5 Adjoint pion mass ($m_{\text{a-}\pi}$)

The adjoint pion (a-π) is an unphysical particle in supersymmetric Yang-Mills theory with a fermion (the gluino) in the adjoint representation. It is related to the fermion mass by partially quenched chiral perturbation theory (χPT) and can be computed in the numerical simulation of $\mathcal{N} = 1$ SUSY Yang-Mills theory on the lattice from the connected piece of a meson whose interpolating field is $\bar{\lambda}(x)\gamma_5\lambda(x)$, for details see Ref. [75]. This meson is a colour-neutral bound state called a-η' with quantum numbers 0^{-+}. The correlation function of a-π is given by

$$C(x,y) = \langle \text{tr}_{sc} \left[\gamma_5 (\gamma^\mu D_\mu)^{-1}(x,y) \gamma_5 (\gamma^\mu D_\mu)^{-1}(y,x) \right] \rangle, \qquad (4.127)$$

where tr_{sc} is trace over spin and colour indices. The adjoint pion mass squared ($m_{\text{a-}\pi}^2$) scales linear with the gluino mass ($m_{\tilde{g}}$) near the chiral point, a point in the theory where SYM theory is characterised by a massless gluino. Mathematically

$$m_{\text{a-}\pi}^2 \propto m_{\tilde{g}} . \qquad (4.128)$$

This relation is in analogy with Gell-Mann-Oakes-Renner (GOR) relation of QCD [9]. Therefore, the adjoint pion mass can also be used for the tuning

of the chiral limit, see Ref. [76]. Fig. (4.4) shows the numerical results of the subtracted gluino mass and the adjoint pion mass squared in lattice units. Both are proportional to each other, however, there is a small discrepancy at κ_c which should be due to lattice artifacts and would go away in the zero lattice spacing limit. With recent developments, see Ref. [37], the subtracted gluino mass is also precise enough to be used for the tuning of SYM theory in the same spirit of the adjoint pion mass squared. However, the pion mass is less expensive to be computed in simulations and is used for the tuning preferably.

4.2.6 Handling of discretisation effects

In the derivation of Eq. (4.83) we have ignored the term $\langle X_S(x)Q(y)\rangle$ of Eq. (4.41). This term is introduced by the lattice discretisation and its leading order is hence $O(a)$. It has a form of a correlation function. Moreover, it is expected to depend on time slice distance t exponetially and decays with t, as this can be seen in Fig. (4.3). In principle, it vanishes in the continuum limit, however, it can be problematic in the continuum extrapolation if it is not handled with care. In $\mathcal{N} = 1$ SUSY Yang-Mills theory on the lattice we simulate the theory for different values of lattice spacing which leads to different $O(a)$ effects. This potentially influences the continuum extrapolation, see Fig. (B.1(a)) where we have used $t_{min} = 4$. Due to $O(a)$ effects the fit does not converge to zero.

To have a simplified version of the continuum extrapolations, one possibility will be to have sufficiently large t_{min} such that the contribution of the term disappears. Another way out can be to choose the fixed physical time slice distance (not the time slice distance in lattice units) so that the contribution of this term will be the same for all lattice spacings. In this way all the data points in the continuum extrapolation will be influenced equally which will lead to a constant shift (can be regarded as a systematic uncertainty). This additional shift in the data points will vanish in the zero lattice spacing limit.

4.2.7   Sufficiently large time slice distance

In principle, the subtracted gluino mass should show a plateau at earlier t/t_{min}[5], however, this is not the case due to contribution of the contact term and due to discretisation effects at first few values of t/t_{min}, and due to noise at large t/t_{min}. Therefore, the plateau can only be seen at some intermediate values of t/t_{min}. One way to get rid of these effects is to consider the data from some optimal value of t/t_{min} where the plateau is formed and other contributions vanish, one can see this in Fig. (4.3). An additional check on this choice is the χ^2/DoF calculated from Eq. (4.114). This also stabilises when discretisation effects are just absent, see Tab. (B.3). We
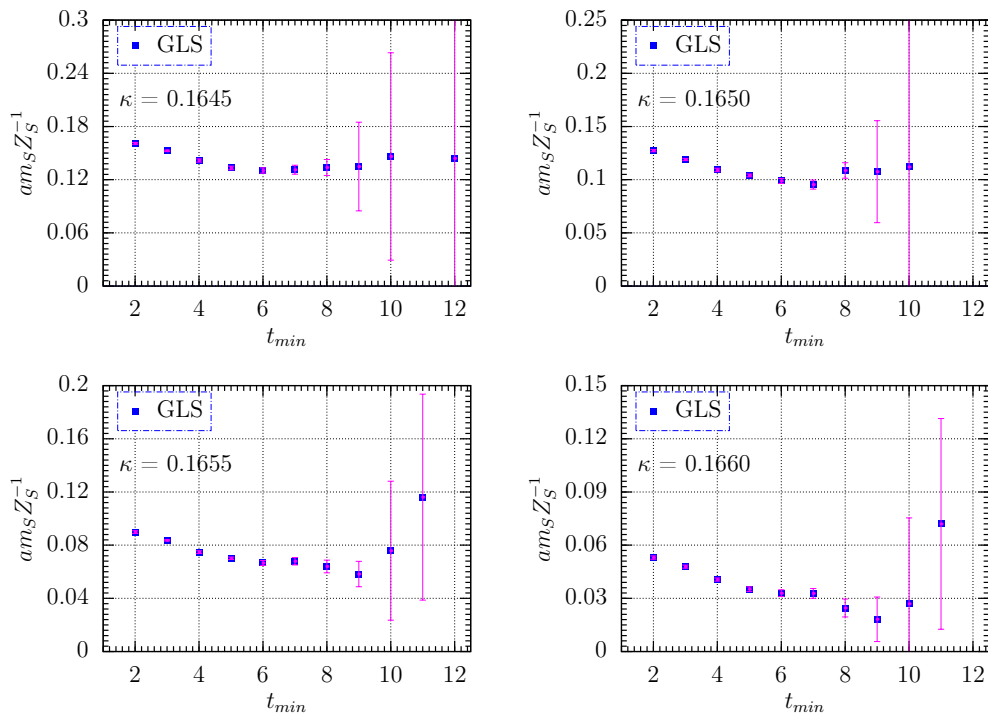
Figure 4.3: The subtracted gluino mass $am_S Z_S^{-1}$ as function of t_{min} calculated from GLS method for $\beta = 5.6$. At small values of t_{min} the signal of the mass is larger than the plateau value. This effect decays with t_{min} and can be explained by $O(a)$ discretisation effects.

repeat the same procedure for the selection of t_{min} to extract the subtracted

---

[5]The term t/t_{min} means t or t_{min}, not the ratio.

gluino mass for a full range of the inverse gauge coupling (β) and the hoping parameter (κ), the results are presented in Tab. (4.2).

$\beta = 5.4$		$\beta = 5.4$		$\beta = 5.45$		$\beta = 5.5$		$\beta = 5.6$	
$V = 12^3 \times 24$		$V = 16^3 \times 32$		$V = 16^3 \times 32$		$V = 16^3 \times 32$		$V = 24^3 \times 48$	
κ	t_{min}	κ	t_{min}	κ	t_{min}	κ	t_{min}	κ	t_{min}
0.1695	4	0.1692	4	0.1685	5	0.1667	5	0.1645	7
0.1700	4	0.1695	4	0.1687	5	0.1673	5	0.1650	7
0.1703	4	0.1697	4	0.1690	5	0.1678	5	0.1655	6
0.1705	4	0.1700	4	0.1692	5	0.1680	5	0.1660	7
-	-	0.1703	4	0.1693	4	0.1683	5	-	-
-	-	0.1705	4	-	-	-	-	-	-

Table 4.2: The choice of t_{min} for a set of all gauge ensembles corresponding to each β. This selection is made by considering sufficiently large t_{min} where plateau is formed and $O(a)$ effects go away. The shaded values have different t_{min} from the rest of gauge ensembles for each β.

4.2.8 Fixed physical time slice distance

An alternative way could be to consider the values of $am_S Z_S^{-1}$ at the same physical time slice distance for all lattice spacings. In this case, the excited state contamination would be the same for all data points and would vanish in the continuum limit. To find t_{min} corresponding the same physical time distance for each β we use the gluino-glue mass $m_{g\tilde{g}}$ and the Wilson flow parameter w_0. We select maximum possible value of t_{min} for one lattice spacing and find the t_{min} for other values of β as

$$t_{min,\beta_i} = t_{min,\beta_0} \frac{m_{g\tilde{g},\beta_0}}{m_{g\tilde{g},\beta_i}} , \qquad (4.129)$$

$$t_{min,\beta_i} = t_{min,\beta_0} \frac{w_{0,\beta_i}}{w_{0,\beta_0}} , \qquad (4.130)$$

where $i = 1, 2, 3$, $\beta_0 = 5.4$ and $\beta_i = 5.45, 5.5, 5.6$. The resultant t_{min} is a real number and rounded to nearest integer value, see Tab. (4.3). The Tab. (B.1) has chirally extrapolated values of $m_{g\tilde{g}}$ and w_0 which are used in

β	t_{min} from $m_{g\tilde{g}}$	t_{min} from w_0
5.4	4	4
5.45	5	5
5.5	5	6
5.6	7	7

Table 4.3: The choice of t_{min} at a fixed physical time slice distance from the gluino-glue mass ($m_{g\tilde{g}}$) and from the physical scale w_0 by Eqs. (4.129,4.130). The value of t_{min} at $\beta = 5.5$, obtained from $m_{g\tilde{g}}$ and from w_0, is different.

Eqs. (4.129,4.130) to produce Tab. (4.3).

4.2.9   Chiral limit

The chiral limit is a point in parametric space where the theory has massless adjoint pion and massless gluino. This limit can be achieved by plotting adjoint pion and gluino masses as a function of $1/2\kappa$, and extrapolating them to the zero masses. The value of κ at the critical point is called κ_c. The κ_c assists in order to tune further values of κ. Fig. (4.4) shows chiral extrapolations towards κ_c. The Tab. (4.4) shows all κ_c from all available ensembles.

β	κ_c from $(am_{\text{a-}\pi})^2$	κ_c from $am_S Z_S^{-1}$
5.4	0.170814(27)	0.170984(34)
5.45	0.169541(52)	0.169730(54)
5.5	0.168400(31)	0.168644(74)
5.6	0.166366(12)	0.166635(54)

Table 4.4: Values of κ_c obtained from $(am_{\text{a-}\pi})^2$ and from $am_S Z_S^{-1}$ by extrapolation towards the chiral limit for 4 optimal values of β.

4.2.10   Remnant gluino mass $\Delta(am_S Z_S^{-1})$

The remnant gluino mass is the subtracted gluino mass at vanishing adjoint pion mass squared. In principle, it should vanish at vanishing adjoint pion
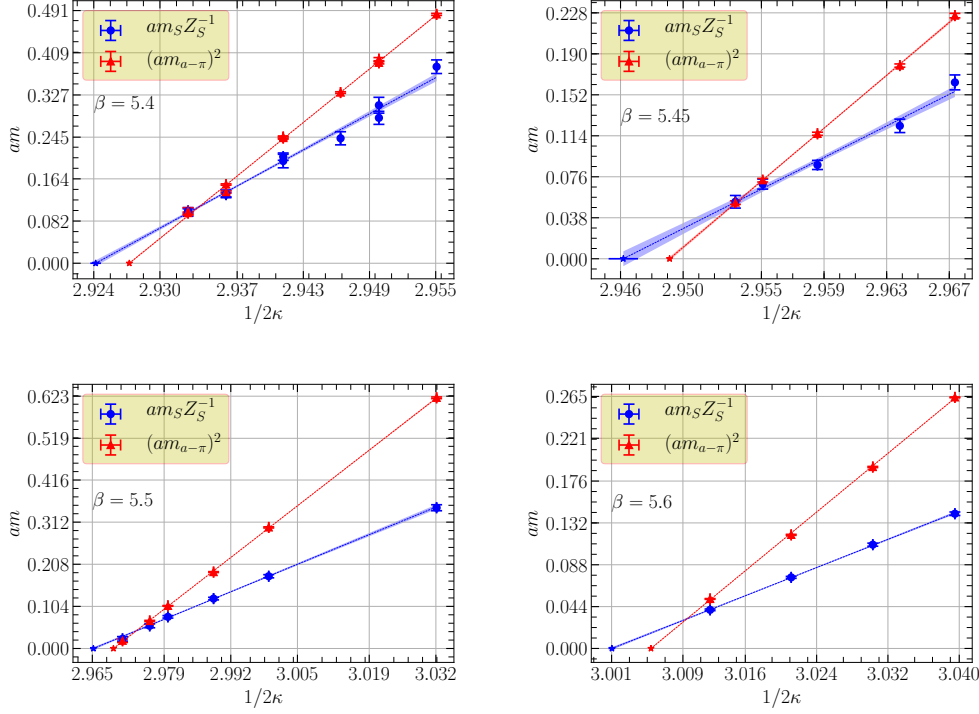
Figure 4.4: The subtracted gluino mass $am_S Z_S^{-1}$ and the adjoint pion mass squared $(am_{\text{a-}\pi})^2$ in lattice units as a function of $1/(2\kappa)$, and the corresponding extrapolations towards the chiral point (κ_c) for all available values of β.

mass squared according to the Eq. (4.128). However, due to lattice artifacts there appears a small discrepancy. It is expected to disappear in the zero lattice spacing limit. The remnant gluino masses are presented in Tab. (4.5), these values are obtained by taking an average of the values calculated using procedures explained in Secs. (4.2.7, 4.2.8).

β	5.4	5.45	5.5	5.6
$\Delta(am_S Z_S^{-1})$	0.0334(48)	0.019(12)	0.0099(88)	0.0103(33)

Table 4.5: The remnant gluino mass $\Delta(am_S Z_S^{-1})$ obtained at $m_{\text{a-}\pi}^2 = 0$ for 4 available values of β in two step procedure by taking the average of $\Delta(am_S Z_S^{-1})$ for repeated values of β from Tab. (B.4).
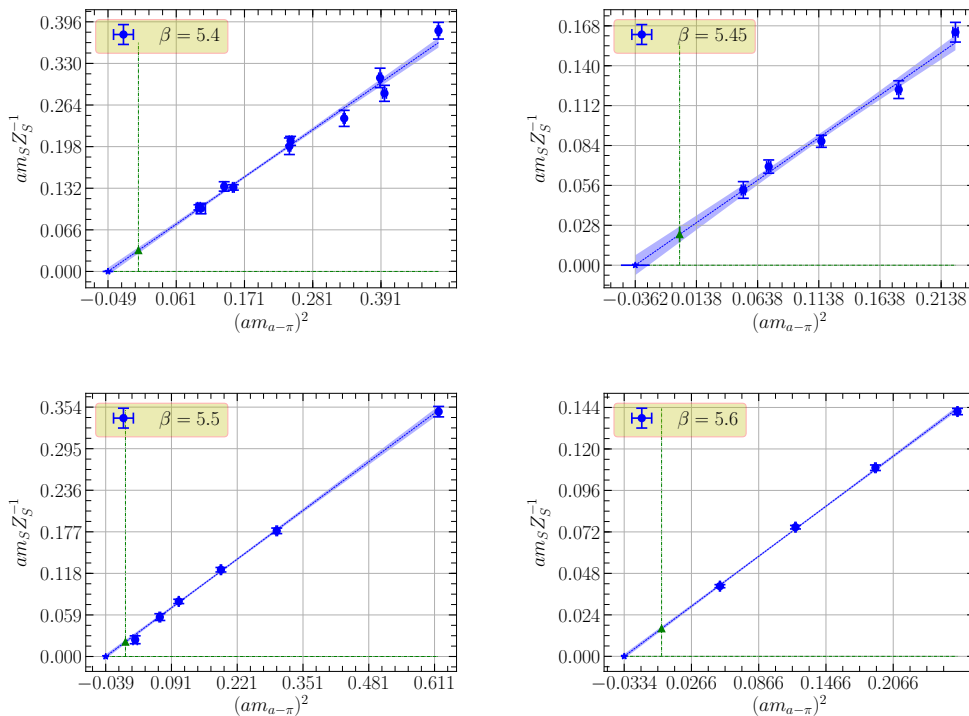
Figure 4.5: The subtracted gluino mass $am_S Z_S^{-1}$ calculated by the GLS method as function of the adjoint pion mass squared $(am_{\text{a-}\pi})^2$ for all available values of β in order to obtain the remnant gluino mass $\Delta(am_S Z_S^{-1})$. The remnant gluino mass is the value of $am_S Z_S^{-1}$ at vanishing $(am_{\text{a-}\pi})^2$.

4.2.11   Continuum limit

After careful determination of remnant gluino mass in the chiral limit, now we perform an extrapolation towards the zero lattice spacing. It is crucial to know how the remnant gluino mass should depend on the lattice spacing a. In the case of lattice QCD, the pion mass squared in leading order Wilson χPT depends linearly on the quark mass plus order a term as

$$m_{\pi,LO}^2 = 2B_0 m_q + 2W_0 a, \tag{4.131}$$

where B_0 and W_0 are low energy constants, see details in Refs. [77, 78]. On the other hand PCAC quark mass in leading order from the chiral Ward
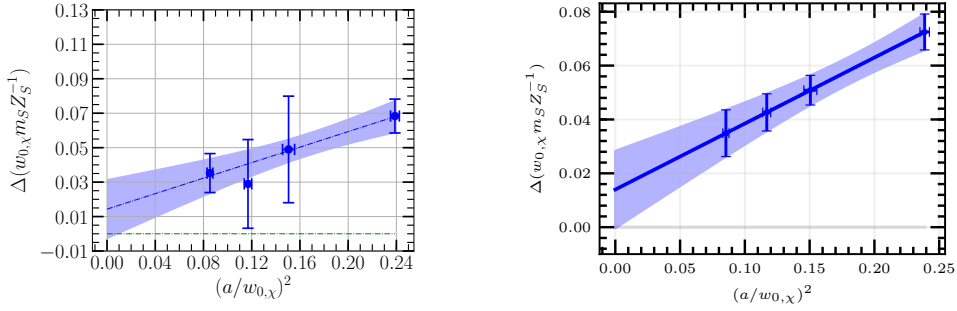
(a) Two step: The remnant gluino mass is obtained from the chiral limit where $m_{a-\pi}^2$ is zero and then extrapolated to the continuum limit.

(b) One step: Chiral and continuum extrapolation is done simultaneously, therefore data points align completely with the error band.

Figure 4.6: The remnant gluino mass $\Delta(w_0 m_S Z_S^{-1})$ in physical units (w_0) as a function of the physical lattice spacing squared, and its linear extrapolation towards the continuum limit.

identity exhibits the same shift [79],

$$2B_0 m_{PCAC,LO} = 2B_0 m_q + 2W_0 a. \tag{4.132}$$

Therefore,

$$m_{PCAC} = \frac{m_\pi^2}{2B_0} + O(a^2), \tag{4.133}$$

as a result, at zero pion mass the remnant PCAC quark mass is $O(a^2)$, and this result is true for all orders of χPT

$$m_{PCAC} = O(a^2) \quad \text{at} \quad m_\pi^2 = 0. \tag{4.134}$$

The structure of the terms in $\mathcal{N} = 1$ SUSY Yang-Mills theory is similar to QCD, therefore we believe that the remnant gluino mass in some physical units from SUSY Ward identities at vanishing adjoint pion mass squared is also of the order a^2. We express the masses in the physical scale w_0, which is defined through the gradient flow; for details see [6]. Fig. (4.6(a)) shows the remnant gluino mass of Tab. (4.5) in the physical scale as a function of a^2 in the same scale w_0. With current statistics, 4 different lattice spacings

have been used for the linear extrapolation towards the zero lattice spacing limit, and the remnant gluino mass is consistant with zero within errors, as expected. Fig. (4.6(b)) is obtained by performing 3D fit using fit function of Eq. (2.75). This fit function is implemented by Mr. Henning Gerber, the complete method is explained in his Ph.D. thesis [80]. In addition to that Fig. (B.1(b)) shows the same extrapolation, however, the remnant gluino mass is obtained by the choice of t_{min} of Tab. (4.2). Finally, the t_{min} obtained from $m_{g\tilde{g}}$ and from w_0, see Tab. (4.3), is used to obtain Figs. (B.1(c),B.1(d)).

We have presented our first complete result of the continuum extrapolation in Ref. [37] with two data points. Now we have more statistics and more data points to confirm rigorously the restoration of broken SUSY in the continuum in $\mathcal{N} = 1$ SUSY Yang-Mills theory. This result also confirms the correctness of Eq. (4.134), where the remnant gluino mass is propotional to a^2 in the continuum.

Chapter 5

Baryonic states in $\mathcal{N} = 1$ SYM theory

5.1 Rarita Schwinger object for baryons

In $\mathcal{N} = 1$ SUSY Yang-Mills theory, besides the gluon field $A_\mu(x)$, we have the gluino field $\lambda(x)$, the superpartner of the gluon. Combination of three λ's can make a colourless object provided that all the colour indices must be contracted with the indices of structure constants t_{abc} where $a, b, c = 1, \ldots, N_c^2 - 1$, which is analogous to baryons in Quantum Chromodynamics (QCD). Due to the fact that fermions are in the adjoint representation, this object can be constructed for both SU(2) and SU(3) gauge groups. We would also call this object a "baryon". A possible general construction in matrix notation of Dirac indices is given by

$$W(x) = t_{abc} \Gamma^A \lambda_a(x) \left(\lambda_b^T(x) \Gamma^B \lambda_c(x) \right), \tag{5.1}$$

which represents a Rarita Schwinger field [81]. Where Γ^A and Γ^B are the spin matrices, for the sake of convenience one can choose $\Gamma^A = \mathbf{1}$ and $\Gamma^B = \Gamma$. With all Lorentz components we consider $\Gamma = C\gamma_\mu$

$$W_\mu(x) = t_{abc} \lambda_a(x) \left(\lambda_b^T(x) C\gamma_\mu \lambda_c(x) \right). \tag{5.2}$$

If this field satisfies the following conditions, the spin-$\frac{1}{2}$ is completely projected out and this will purely be spin-$\frac{3}{2}$

$$\gamma_\mu W_\mu = 0, \tag{5.3}$$

$$\partial_\mu W_\mu = 0. \tag{5.4}$$

Using Fierz identities, the first condition is satisfied. The second condition, however, is not fulfilled, therefore we must have spin-$\frac{3}{2}$ and spin-$\frac{1}{2}$ components in the field $W(x)$. There are three possible choices, all giving rise to quantum numbers $J^P = \frac{1}{2}^+$, namely $\Gamma = C\gamma_4, C\gamma_5, \mathrm{i}\gamma_4 C\gamma_5$. Baryons with $J^P = \frac{3}{2}$, are obtained from $\Gamma = C\gamma_i$, $i = 1, 2, 3$, where γ_i are spatial gamma matrices. Two gluino fields give rise to di-gluino state with $J = 1$ and together with the left over gluino field it gives $J = \frac{3}{2}$ contributions, but also an admixture of $J = \frac{1}{2}$ [65].

5.1.1 Baryons with gauge group SU(2)

For SU(2) t_{abc} is simply replaced by an anti-symmetric tensor ε_{abc}, its values are given in Appendix (B.3.1). We choose $\Gamma = C\gamma_4$, the reason for this choice is that the spin matrix Γ must be symmetric if t_{abc} is chosen to be anti-symmetric, to prove this the analytical calculations are given in Appendix (B.4). As a result of this replacement Rarita Schwinger field reads

$$W(x) = \varepsilon_{abc}\lambda_a(x) \left(\lambda_b^T(x) C\gamma_4 \lambda_c(x) \right). \tag{5.5}$$

In addition to colour indices, the gluino field $\lambda(x)$ has Dirac index which is omitted for convenience.

5.1.2 Baryons with gauge group SU(3)

For SU(3) there are two possibilities for t_{abc}, either it is d_{abc} which is completely symmetric or f_{abc} which is anti-symmetric, for their numerical values see Appendix (B.3.2). One possible choice of Γ for SU(3) is $C\gamma_5$ which is

symmetric, therefore we have to use f_{abc}. The conjugate field is

$$W(x) = f_{abc}\lambda_a(x)\left(\lambda_b^T(x)C\gamma_5\lambda_c(x)\right).\tag{5.6}$$

Now we need to construct the correlation function which will be computed on the lattice with the help of high performance facilities.

5.1.3   Baryon correlation function

For the computation of the baryon mass the basic building block is the correlation function. A suitable function is fitted to the numerical data obtained from each gauge ensemble. To achieve this we consider here the following correlation function obtained from the interpolating field $W(x)$ and from its conjugate field $\overline{W}(x)$

$$B(x,y) = \langle W(x)\overline{W}(y)\rangle\,,\tag{5.7}$$

where conjugate field $\overline{W}(x)$ for $\Gamma = C\gamma_5$ is given as

$$\overline{W}(x) = -\left(CW(x)\right)^T.\tag{5.8}$$

For its derivation, see Appendix (B.2). Now we write correlation function $B(x,y)$ with its Dirac indices explicitly

$$\begin{aligned}
B^{\alpha\delta}(x,y) &= \langle W^\alpha(x)\overline{W}^\delta(y)\rangle \\
&= -\langle W^\alpha(x)C^{\delta\alpha'}W^{\alpha'}(y)\rangle \\
&= -\langle f_{abc}f_{a'b'c'}(C\gamma_5)^{\beta\gamma}(C\gamma_5)^{\beta'\gamma'}C^{\delta\alpha'}\times \\
&\quad \lambda_a^\alpha(x)\lambda_b^\beta(x)\lambda_c^\gamma(x)\lambda_{a'}^{\alpha'}(y)\lambda_{b'}^{\beta'}(y)\lambda_{c'}^{\gamma'}(y)\rangle.
\end{aligned}\tag{5.9}$$

The easiest way to evaluate this further, combining terms by using symmetries, is to represent the correlation function in terms of six λ, and not to write it in terms of λ and $\overline{\lambda}$. With all possible contractions

$$\lambda_a^\alpha(x)\lambda_b^\beta(y) = K_{ab}^{\alpha\beta}(x,y) = -(\triangle(x,y)C)_{ab}^{\alpha\beta}\,,\tag{5.10}$$

where the fermion propagator is simply the inverse of the Wilson-Dirac matrix i. e. $\triangle(x, y) = D_w^{-1}(x, y)$. By taking into account the fermionic signs, we get the following 15 terms

$$\lambda_a^\alpha(x)\lambda_b^\beta(x)\lambda_c^\gamma(x)\lambda_{a'}^{\alpha'}(y)\lambda_{b'}^{\beta'}(y)\lambda_{c'}^{\gamma'}(y) =$$

$$+ K_{ab}^{\alpha\beta}(x, x)K_{ca'}^{\gamma\alpha'}(x, y)K_{b'c'}^{\beta'\gamma'}(y, y) \tag{5.11}$$

$$- K_{ab}^{\alpha\beta}(x, x)K_{cb'}^{\gamma\beta'}(x, y)K_{a'c'}^{\alpha'\gamma'}(y, y) \tag{5.12}$$

$$+ K_{ab}^{\alpha\beta}(x, x)K_{cc'}^{\gamma\gamma'}(x, y)K_{a'b'}^{\alpha'\beta'}(y, y) \tag{5.13}$$

$$- K_{ac}^{\alpha\gamma}(x, x)K_{ba'}^{\beta\alpha'}(x, y)K_{b'c'}^{\beta'\gamma'}(y, y) \tag{5.14}$$

$$+ K_{ac}^{\alpha\gamma}(x, x)K_{bb'}^{\beta\beta'}(x, y)K_{a'c'}^{\alpha'\gamma'}(y, y) \tag{5.15}$$

$$- K_{ac}^{\alpha\gamma}(x, x)K_{bc'}^{\beta\gamma'}(x, y)K_{a'b'}^{\alpha'\beta'}(y, y) \tag{5.16}$$

$$+ K_{aa'}^{\alpha\alpha'}(x, y)K_{bc}^{\beta\gamma}(x, x)K_{b'c'}^{\beta'\gamma'}(y, y) \tag{5.17}$$

$$- K_{aa'}^{\alpha\alpha'}(x, y)K_{bb'}^{\beta\beta'}(x, y)K_{cc'}^{\gamma\gamma'}(x, y) \tag{5.18}$$

$$+ K_{aa'}^{\alpha\alpha'}(x, y)K_{bc'}^{\beta\gamma'}(x, y)K_{cb'}^{\gamma\beta'}(x, y) \tag{5.19}$$

$$- K_{ab'}^{\alpha\beta'}(x, y)K_{bc}^{\beta\gamma}(x, x)K_{a'c'}^{\alpha'\gamma'}(y, y) \tag{5.20}$$

$$+ K_{ab'}^{\alpha\beta'}(x, y)K_{ba'}^{\beta\alpha'}(x, y)K_{cc'}^{\gamma\gamma'}(x, y) \tag{5.21}$$

$$- K_{ab'}^{\alpha\beta'}(x, y)K_{bc'}^{\beta\gamma'}(x, y)K_{c'a'}^{\gamma'\alpha'}(y, y) \tag{5.22}$$

$$+ K_{ac'}^{\alpha\gamma'}(x, y)K_{bc}^{\beta\gamma}(x, x)K_{a'b'}^{\alpha'\beta'}(y, y) \tag{5.23}$$

$$- K_{ac'}^{\alpha\gamma'}(x, y)K_{ba'}^{\beta\alpha'}(x, y)K_{cb'}^{\gamma\beta'}(x, y) \tag{5.24}$$

$$+ K_{ac'}^{\alpha\gamma'}(x, y)K_{bb'}^{\beta\beta'}(x, y)K_{ca'}^{\gamma\alpha'}(x, y) \tag{5.25}$$

The term (5.11) can be combined with (5.14) and term the (5.12) with (5.13),(5.15) and (5.16). Terms (5.20) and (5.23) can be united to one. Terms (5.18) and (5.19) can be joined. Similarly terms (5.21), (5.22), (5.24) and (5.25) can also be merged to one. After combining most of the terms we are

left with only 6 terms and substituting back into the Eq. (5.9) we get

$$
\begin{aligned}
B^{\alpha\delta}(x,y) = -\ \langle f_{abc} f_{a'b'c'} (C\gamma_5)^{\beta\gamma} (C\gamma_5)^{\beta'\gamma'} C^{\delta\alpha'} \{ & \quad\quad (5.26) \\
- 2 K_{aa'}^{\alpha\alpha'}(x,y) K_{bb'}^{\beta\beta'}(x,y) K_{cc'}^{\gamma\gamma'}(x,y) & \\
- 4 K_{ab'}^{\alpha\beta'}(x,y) K_{bc'}^{\beta\gamma'}(x,y) K_{ca'}^{\gamma\alpha'}(x,y) & \\
- 2 K_{ab}^{\alpha\beta}(x,x) K_{ca'}^{\gamma\alpha'}(x,y) K_{c'b'}^{\gamma'\beta'}(y,y) & \\
- 4 K_{ab}^{\alpha\beta}(x,x) K_{bc'}^{\beta'\gamma}(y,x) K_{c'a'}^{\gamma'\alpha'}(y,y) & \\
- 1 K_{aa'}^{\alpha\alpha'}(x,y) K_{bc}^{\beta\gamma}(x,x) K_{c'b'}^{\gamma'\beta'}(y,y) & \\
- 2 K_{ab'}^{\alpha\beta'}(x,y) K_{bc}^{\beta\gamma}(x,x) K_{c'a'}^{\gamma'\alpha'}(y,y) \}\rangle. &
\end{aligned}
$$

Explicit calculations of each term in Eq. (5.26) are then able to represent K in terms of propagator $\triangle$, see Appendix (B.5) for the derivations. Further, we have tried different choices of Γ, all of them give rise to the same result leaving different signs. These signs are accumodatd in variable θ, see Tab. (5.1). The resulting correlation function gets the form

$$
\begin{aligned}
B^{\alpha\alpha'}(x,y) = \langle \theta\, t_{a'b'c'} t_{abc} \Gamma^{\beta\gamma} \Gamma^{\beta'\gamma'} \times \{ & \quad\quad (5.27) \\
+ 2 \triangle_{aa'}^{\alpha\alpha'}(x,y) \triangle_{bb'}^{\beta\beta'}(x,y) \triangle_{cc'}^{\gamma\gamma'}(x,y) & \\
+ 4 \triangle_{ab'}^{\alpha\beta'}(x,y) \triangle_{bc'}^{\beta\gamma'}(x,y) \triangle_{ca'}^{\gamma\alpha'}(x,y) & \\
+ 2 \triangle_{ab}^{\alpha\beta}(x,x) \triangle_{ca'}^{\delta\alpha'}(x,y) \triangle_{c'b'}^{\delta'\beta'}(y,y) C^{\gamma\delta} C^{\gamma'\delta'} & \\
+ 4 \triangle_{ab}^{\alpha\beta}(x,x) \triangle_{b'c}^{\beta'\gamma}(y,x) \triangle_{c'a'}^{\gamma'\alpha'}(y,y) & \\
+ 1 \triangle_{aa'}^{\alpha\alpha'}(x,y) \triangle_{bc}^{\beta\delta}(x,x) \triangle_{c'b'}^{\delta'\beta'}(y,y) C^{\gamma\delta} C^{\delta'\gamma'} & \\
+ 2 \triangle_{ac}^{\alpha\delta'}(x,y) \triangle_{bc}^{\beta\delta}(x,x) \triangle_{b'a'}^{\beta'\alpha'}(y,y) C^{\gamma\delta} C^{\gamma'\delta'} \}\rangle. &
\end{aligned}
$$

This correlation function can be categorised into two parts, the sunset piece $B_{Sset}(x,y)$ and the spectacle piece $B_{Spec}(x,y)$. The graphical representation of these pieces is given in Fig. (3.4). Projection to the parity states and the

θ	
+1	-1
$\Gamma = C,\ C\gamma_{1,3,4}$	$\Gamma = C\gamma_{2,5},\ \mathrm{i}\gamma_4 C\gamma_5$

t_{abc}	
f_{abc}	d_{abc}
$\Gamma = C,\ C\gamma_{1,3,4}$	$\Gamma = C\gamma_{2,5},\ \mathrm{i}\gamma_4 C\gamma_5$

Table 5.1: The values of θ and choice of t_{abc} for corresponding spin matrices.

trace over Dirac indices leave

$$
\begin{aligned}
B_{Sset}(x,y) = \theta\, t_{a'b'c'} t_{abc} \Gamma^{\beta\gamma} \Gamma^{\beta'\gamma'} P_{\pm}^{\alpha\alpha'} \times \{ & \\
+ 2 \triangle_{aa'}^{\alpha\alpha'}(x,y) \triangle_{bb'}^{\beta\beta'}(x,y) \triangle_{cc'}^{\gamma\gamma'}(x,y) & \\
+ 4 \triangle_{ab'}^{\alpha\beta'}(x,y) \triangle_{bc'}^{\beta\gamma'}(x,y) \triangle_{ca'}^{\gamma\alpha'}(x,y) \}, &
\end{aligned} \tag{5.28}
$$

and

$$
\begin{aligned}
B_{Spec}(x,y) = \theta\, t_{a'b'c'} t_{abc} \Gamma^{\beta\gamma} \Gamma^{\beta'\gamma'} P_{\pm}^{\alpha\alpha'} \times \{ & \\
+ 2 \triangle_{ab}^{\alpha\beta}(x,x) \triangle_{ca'}^{\delta\alpha'}(x,y) \triangle_{c'b'}^{\delta'\beta'}(y,y) C^{\gamma\delta} C^{\gamma'\delta'} & \\
+ 4 \triangle_{ab}^{\alpha\beta}(x,x) \triangle_{b'c}^{\beta'\gamma}(y,x) \triangle_{c'a'}^{\gamma'\alpha'}(y,y) & \\
+ 1 \triangle_{aa'}^{\alpha\alpha'}(x,y) \triangle_{bc}^{\beta\delta}(x,x) \triangle_{c'b'}^{\delta'\beta'}(y,y) C^{\gamma\delta} C^{\delta'\gamma'} & \\
+ 2 \triangle_{ac}^{\alpha\delta'}(x,y) \triangle_{bc}^{\beta\delta}(x,x) \triangle_{b'a'}^{\beta'\alpha'}(y,y) C^{\gamma\delta} C^{\gamma'\delta'} \}, &
\end{aligned} \tag{5.29}
$$

where $P_{\pm}$ are parity projectors and for zero momentum they are defined as $P_{\pm} = \frac{1}{2}(1\pm\gamma_4)$. It is important to note here that the total correlation function in terms of these two pieces can be written as

$$
B(x,y) = \langle B_{Sset}(x,y) + B_{Spec}(x,y) \rangle. \tag{5.30}
$$

We compute them separately then add the data configuration by configuration and then take the average.

5.1.4 Discrete symmetry test of correlation function

In order to cross check whether the correlation function of Eq. (5.27) is correct, we use some symmetries. The fermionic interpolating field $W(x)$ transform in the same way as spinors under time reversal ($\mathcal{T}$) and parity ($\mathcal{P}$) transformations [82, 39]

$$
\begin{align}
W(x) \quad &\rightarrow \quad W^{\mathcal{P}}(x^{\mathcal{P}}) = \gamma_4 W(x^{\mathcal{P}}), \tag{5.31}\\
\overline{W}(x) \quad &\rightarrow \quad \overline{W}^{\mathcal{P}}(x^{\mathcal{P}}) = \overline{W}(x^{\mathcal{P}})\gamma_4, \tag{5.32}\\
W(x) \quad &\rightarrow \quad W^{\mathcal{T}}(x^{\mathcal{T}}) = \gamma_4\gamma_5 W(x^{\mathcal{T}}), \tag{5.33}\\
\overline{W}(x) \quad &\rightarrow \quad \overline{W}^{\mathcal{T}}(x^{\mathcal{T}}) = \overline{W}(x^{\mathcal{T}})\gamma_5\gamma_4. \tag{5.34}
\end{align}
$$

For convenience we drop out the Dirac indices. The correlation function transforms as

$$
\begin{align}
B(x,y) \quad &\rightarrow \quad B^{\mathcal{P}}(x^{\mathcal{P}},y^{\mathcal{P}}) = \langle W^{\mathcal{P}}(x^{\mathcal{P}})\overline{W}^{\mathcal{P}}(y^{\mathcal{P}})\rangle = \gamma_4 B(x^{\mathcal{P}},y^{\mathcal{P}})\gamma_4, \tag{5.35}\\
B(x,y) \quad &\rightarrow \quad B^{\mathcal{T}}(x^{\mathcal{T}},y^{\mathcal{T}}) = \langle W^{\mathcal{T}}(x^{\mathcal{T}})\overline{W}^{\mathcal{T}}(y^{\mathcal{T}})\rangle = \gamma_4\gamma_5 B(x^{\mathcal{T}},y^{\mathcal{T}})\gamma_5\gamma_4. \tag{5.36}
\end{align}
$$

Taking zero spatial momentum correlation function

$$
B(t) = \sum_{\substack{\vec{x},\vec{y} \\ t = x_0 - y_0}} B(x,y), \tag{5.37}
$$

Eq. (5.35) implies that

$$
B(t) \quad = \quad \gamma_4 B(t)\gamma_4. \tag{5.38}
$$

Eq. (5.36) together with anti-periodicity gives

$$
B(t) \quad = \quad -\gamma_4\gamma_5 B(N_t - t)\gamma_5\gamma_4. \tag{5.39}
$$

γ_5 Hermiticity ($t = x_0$-y_0, with transpose of $B(t)$ it becomes $-t$) and anti-periodicity gives

$$
B(t) \quad = \quad -\gamma_5 B^{\dagger}(N_t - t)\gamma_5. \tag{5.40}
$$

Property of inverse Dirac matrix together with anti-periodicity

$$B(t) \;\; = \;\; -C^{-1}B^T(N_t - t)C. \tag{5.41}$$

Combining Eq. (5.39) with Eq. (5.40), we obtain

$$B(t) \;\; = \;\; \gamma_4 B^\dagger(t)\gamma_4. \tag{5.42}$$

Combining Eq. (5.40) with Eq. (5.41), we get

$$B(t) \;\; = \;\; C^{-1}\gamma_5 B^*(t)\gamma_5 C. \tag{5.43}$$

From Eqs. (5.38,5.42) we conclude that $B(t)$ is 4×4 Hermitian matrix in Dirac indices and can be expanded in the basis of 16 Dirac matrices (Γ_i) as

$$B(t) = \sum_{\Gamma_i} B_{\Gamma_i}(t)\,\Gamma_i, \tag{5.44}$$

these Γ_i are given in Appendix (A.3). By using the Eqs. (5.38,5.42,5.43), the above expression is reduced to

$$B(t) = B_{\mathbf{1}}(t)\mathbf{1} + B_{\gamma_4}(t)\gamma_4. \tag{5.45}$$

where $B_{\mathbf{1}}(t) = \frac{1}{4}\mathrm{tr}\,[B(t)]$ and $B_{\gamma_4}(t) = \frac{1}{4}\mathrm{tr}\,[B(t)\gamma_4]$. Moreover, from Eq. (5.39) we derive that

$$B_{\mathbf{1}}(t) \;\; = \;\; -B_{\mathbf{1}}(N_t - t), \tag{5.46}$$
$$B_{\gamma_4}(t) \;\; = \;\; B_{\gamma_4}(N_t - t), \tag{5.47}$$

Furthermore, $B_{\mathbf{1}}(t)$ and $B_{\gamma_4}(t)$ are also real.

In principle each term of Eq. (5.27) should obey symmetricity and anti-symmetricity of Eqs. (5.46,5.47). The Fig. (5.1) shows the numerical results of the sunset piece of the correlation functions $B_{\mathbf{1}}(t)$ and $B_{\gamma_4}(t)$. It is clear from the figure that the correlation functions satisfy the Eqs. (5.46,5.47). The spectacle piece is obtained using stochastic estimator technique for the

inverse Wilson-Dirac operator D_w^{-1}, however, it is noisy and requires some additional techniques as well as efforts to get reasonable results.
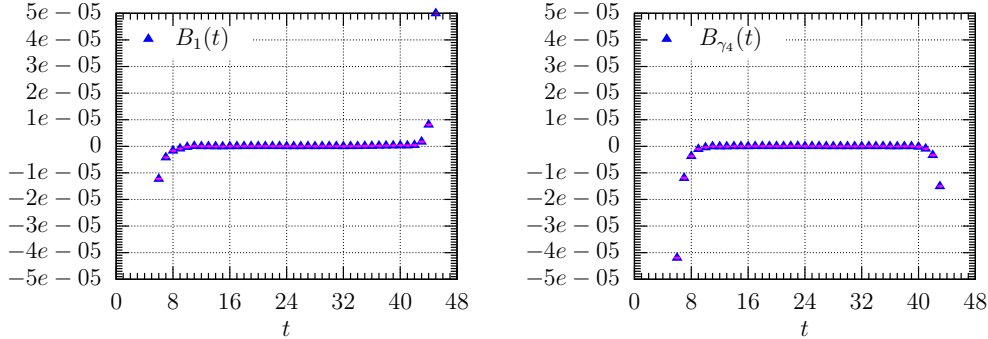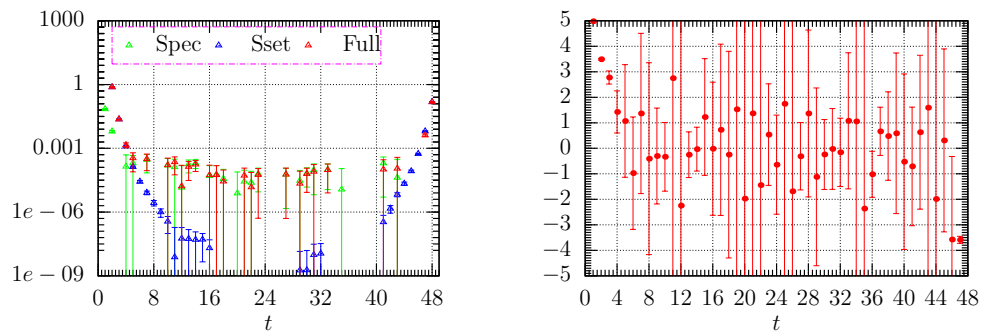

Figure 5.1: Numerical results of the sunset piece of baryon correlation functions $B_\mathbf{1}(t)$ and $B_{\gamma_4}(t)$ to varify associated symmetries at β=1.75 and $\kappa = 0.14925$ with gauge group SU(2).

5.1.5 Numerical results

For $\mathcal{N} = 1$ SYM theory, the major task to compute a correlation function is to compute the inverse of the Wilson-Dirac operator. The inverse of the Wilson-Dirac operator for the sunset piece is computed easily, where we only need to compute the inversion of a δ-source for each combination of spin and gauge indices. This inversion is achieved by the Conjugate Gradient (CG) method. However, for the spectacle piece it is calculated using stochastic estimator technique together with the truncated eigenmode approximation as explained in Sec. (2.2.6). Fig. (5.2) shows the full correlation function (including the sunset piece and the spectacle piece) and its effective mass. The results are not satisfactory at the moment and we need to test which part of the correlation function is noisy. In Fig. (B.2) we have shown the effective mass of both pieces separately and it is clear that the spectacle piece is noisy. In order to further investigate the source of noise, we have estimated the gauge noise and the stochastic noise of the spectacle piece, and the reuslts are given in Tab. (B.5). It turned out the stochastic noise is larger as compared to the gauge noise. Therefore, we need to focus on how to

improve this signal-to-noise ratio. One way could be to increase the number of stochastic estimators and to repeat the measurement for several positions of the wall-source t_{source}.

(a) Spectacle, sunset and full baryon correlation function.

(b) Effective mass of full baryon correlation function.

Figure 5.2: Numerical results of the baryon correlation function and the effective mass at $\beta = 1.75$ and $\kappa = 0.14925$. In spectacle part, 40 stochastic estimators have been used for the computation of D_w^{-1} with no smearing.

Chapter 6

Conclusion and outlook

The $\mathcal{N} = 1$ SUSY Yang-Mills theory is the supersymmetric extension of the pure gluonic part of the Standard Model of particle physics. It describes the strong interaction of the gluon and its SUSY partner, the gluino. The gluino is a Majorana fermion and it transforms according to the adjoint representation under gauge group SU(N_c). At low energy these fundamental particles exhibit confinement. According to the predictions on the basis of effective actions [9, 10] these bound states, among others, consist of mesons, glueballs and a spin-$\frac{1}{2}$ gluino-glue which form, if SUSY is realised, a chiral supermultiplet. In our collaboration we have calculated the masses of these states of $\mathcal{N} = 1$ SUSY Yang-Mills theory non-perturbatively. To do this we employed the framework of lattice QFT. The introduction of the space-time lattice as a regulator breaks SUSY explicitly. Additionally, the supersymmetry is broken softly by a non-zero gluino mass. Similar to the previous studies [3, 6, 4], we have employed SUSY Ward identities in order to obtain a limit where $\mathcal{N} = 1$ SYM theory is characterised by the massless gluino, the so-called chiral limit. In order to test whether the SUSY Ward identity is anomalous or not it has been renormalised and all relevant operators of dimensions $\leq 9/2$ have been included [4]. The resulting equations contain a ratio of renormalisation coefficients and subtracted gluino mass.

In this thesis we have explained how the subtracted gluino mass is obtained from correlation functions which are computed numerically on the lat-

tice with the help of the simulation code and supercomputers. For the data analysis we have improved the methods, namely the Local method and the Global method which have been used previously in our collaboration [3, 31]. Despite being improved these methods do not take into account the correlations present among the relevant observables. To consider these correlations we have formulated a method called the GLS method and have obtained the subtracted gluino mass for each gauge ensemble. We have extrapolated the subtracted gluino mass as a function of the adjoint pion mass squared ($m^2_{\text{a-}\pi}$) to the chiral limit. In principle, the subtracted gluino mass should have vanished at $m^2_{\text{a-}\pi} = 0$ according to Eq. (4.128), however, due to lattice artifacts there has been a small discrepancy. This remaining mass has been called remnant gluino mass. We have computed it for each lattice spacing and have discussed in Sec. (4.2.11) that it is of the order a^2. The w_0 scale based on Wilson flow has been used to represent the remnant gluino mass and lattice spacing in physical units. We have properly handled additional lattice artifacts and have extrapolated the remnant gluino mass to the zero lattice spacing limit where the remnant gluino mass is consistent with zero within error. This is exactly in accordance with the theoretical predictions.

In addition, we have investigated a bound state composed of three gluino fields, the so-called baryons in $\mathcal{N} = 1$ SUSY Yang-Mills theory. We have derived correlation functions of the baryons and implemented them in the simulation code to determine their masses non-perturbatively. The baryon correlation function consists of two parts, namely the sunset piece and the spectacle piece. Furthermore, we have used discrete symmetries to check the correctness of the numerical data of the correlation function obtained from lattice simulations. The numerical results of the sunset piece are quite encouraging whereas the spectacle piece is still noisy. Finally, we have presented numerical results of the baryon correlation functions and of the effective mass.

For the future, to improve the signal-to-noise ratio, one possibility could be to use large number of stochastic estimators and to use the full time extent of the lattice for the sources.

We have successfully determined masses of particles in $\mathcal{N} = 1$ SUSY Yang-Mills theory and have shown that they form a chiral supermultiplet [8].

This means that SUSY is realised on the lattice. This project could possibly be extended to super QCD or to extended SUSY (particularly $\mathcal{N} = 2$ SYM theory). Moreover, we have started to study the spectrum of baryons in $\mathcal{N} = 1$ SUSY Yang-Mills theory. There might be more states which can be investigated in the future.

Appendix A

Group generators and matrices

A.1 Group generators of $SU(N_c)$

The group generators, in matrix representation, are $N_c \times N_c$ matrices and are $N_c^2 - 1$ in number. We shall restrict ourself only to the generators for SU(2) and SU(3) because we have investigated the $\mathcal{N} = 1$ SUSY Yang-Mills theory only for these two gauge groups.

A.1.1 Group generators of $SU(2)$

For the case of SU(2) we have following three generators

$$T^a = \frac{\sigma^a}{2}, \quad \text{with } a = 1, 2, 3. \tag{A.1}$$

Where σ^a are Pauli matrices given in Sec. (A.2).

A.1.2 Group generators of $SU(3)$

In this case they are 8 in number and acquire the following forms

$$T^a = \frac{\lambda^a}{2}, \quad \text{with } a = 1, 2, \ldots, 8. \tag{A.2}$$

Where λ^a are Gell-Mann matrices and their conventional representation is

$$\lambda_1 = \begin{pmatrix} 0 & 1 & 0 \\ 1 & 0 & 0 \\ 0 & 0 & 0 \end{pmatrix}, \lambda_2 = \begin{pmatrix} 0 & -i & 0 \\ i & 0 & 0 \\ 0 & 0 & 0 \end{pmatrix}, \lambda_3 = \begin{pmatrix} 1 & 0 & 0 \\ 0 & -1 & 0 \\ 0 & 0 & 0 \end{pmatrix}, \tag{A.3}$$

$$\lambda_4 = \begin{pmatrix} 0 & 0 & 1 \\ 0 & 0 & 0 \\ 1 & 0 & 0 \end{pmatrix}, \lambda_5 = \begin{pmatrix} 0 & 0 & -i \\ 0 & 0 & 0 \\ i & 0 & 0 \end{pmatrix}, \lambda_6 = \begin{pmatrix} 0 & 0 & 0 \\ 0 & 0 & 1 \\ 0 & 1 & 0 \end{pmatrix}, \tag{A.4}$$

$$\lambda_7 = \begin{pmatrix} 0 & 0 & 0 \\ 0 & 0 & -i \\ 0 & i & 0 \end{pmatrix}, \lambda_8 = \begin{pmatrix} \frac{1}{\sqrt{3}} & 0 & 0 \\ 0 & \frac{1}{\sqrt{3}} & 0 \\ 0 & 0 & -\frac{2}{\sqrt{3}} \end{pmatrix}. \tag{A.5}$$

A.2 Gamma matrices

Explicit representation of Euclidean Dirac matrices (γ matrices) in a $2 \otimes 2$ block notations

$$\gamma_{1,2,3} = \begin{pmatrix} 0 & -i\sigma_{1,2,3} \\ i\sigma_{1,2,3} & 0 \end{pmatrix}, \tag{A.6}$$

Where Pauli matrices are

$$\sigma_1 = \begin{pmatrix} 0 & 1 \\ 1 & 0 \end{pmatrix}, \sigma_2 = \begin{pmatrix} 0 & -i \\ i & 0 \end{pmatrix}, \sigma_3 = \begin{pmatrix} 1 & 0 \\ 0 & -1 \end{pmatrix}. \tag{A.7}$$

Chiral representation of γ_4 and γ_5 is

$$\gamma_4 = \begin{pmatrix} \mathbf{0} & \mathbf{1} \\ \mathbf{1} & \mathbf{0} \end{pmatrix}, \gamma_5 = \begin{pmatrix} \mathbf{1} & \mathbf{0} \\ \mathbf{0} & -\mathbf{1} \end{pmatrix}. \tag{A.8}$$

These matrices obey

$$\{\gamma_\mu, \gamma_\mu\} = \delta_{\mu\nu}. \tag{A.9}$$

125

The *charge conjugation* Dirac matrix

$$C \equiv \gamma_4 \gamma_2 = -\gamma_1 \gamma_3 \gamma_5 \begin{pmatrix} 0 & 1 & 0 & 0 \\ -1 & 0 & 0 & 0 \\ 0 & 0 & 0 & -1 \\ 0 & 0 & 1 & 0 \end{pmatrix}, \tag{A.10}$$

satisfies

$$C^2 = -\mathbf{1}, \quad C^\dagger = C^T = C^{-1} = -C, \tag{A.11}$$

$$C\gamma_{1,3,5} = \gamma_{1,3,5}C, \quad C\gamma_{2,4} = -\gamma_{2,4}C, \tag{A.12}$$

$$(C\gamma_{\mu,5})^T = C\gamma_{\mu,5}, \quad C\gamma_\mu C^{-1} = -\gamma_\mu^T. \tag{A.13}$$

A.3   Dirac space

Dirac space consists of a set of following matrices

$$\Gamma_i = \{\mathbf{1}, \gamma_5, \gamma_\mu, \gamma_\mu \gamma_5, \mathrm{i}\sigma_{\mu\nu}\}, \tag{A.14}$$

where γ and σ satisfy the following relations

$$[\gamma_\mu, \sigma_{\nu\rho}] = 2\left(\delta_{\mu\nu}\gamma_\rho - \delta_{\mu\rho}\gamma_\nu\right), \tag{A.15}$$

$$\{\gamma_\mu, \sigma_{\nu\rho}\} = -2\epsilon_{\mu\nu\rho\eta}\gamma_\eta\gamma_5. \tag{A.16}$$

A.4   Fierz identities

Fierz identities are defined as [40]

$$O_V(x) = -O_A(x) = O_S(x) - O_P(x), \tag{A.17}$$

$$O_T(x) = -\left(O_S(x) + O_P(x)\right). \tag{A.18}$$

where

$$O_S(x) = \text{tr}\Big[\big(\bar{\psi}(x)\psi(x)\big)\psi(x)\Big], \tag{A.19}$$

$$O_P(x) = \text{tr}\Big[\big(\bar{\psi}(x)\gamma_5\psi(x)\big)\gamma_5\psi(x)\Big], \tag{A.20}$$

$$O_V(x) = \text{tr}\Big[\big(\bar{\psi}(x)\gamma_\mu\psi(x)\big)\gamma_\mu\psi(x)\Big], \tag{A.21}$$

$$O_A(x) = \text{tr}\Big[\big(\bar{\psi}(x)\gamma_5\gamma_\mu\psi(x)\big)\gamma_5\gamma_\mu\psi(x)\Big], \tag{A.22}$$

$$O_T(x) = \text{tr}\Big[\big(\bar{\psi}(x)\sigma_{\mu\nu}\psi(x)\big)\sigma_{\mu\nu}\psi(x)\Big]. \tag{A.23}$$

Here $\psi(x)$ is 4-component Dirac spinor. For the case of Majorana spinor the follwing results hold

$$O_S(x) = O_P(x) = O_A(x) = 0. \tag{A.24}$$

Appendix B

Derivations and results

β	$m_{g\tilde{g}}$	w_0
5.4	0.5272(86)	2.046(16)
5.45	0.4040(81)	2.577(43)
5.5	0.4292(79)	2.925(38)
5.6	0.2997(71)	3.422(48)

Table B.1: Chirally extrapolated values of the gluino-glue mass ($m_{g\tilde{g}}$) and of the scale w_0 which are used to obtain t_{min} of Tab. (4.3).

B.1   Ward identity correlation functions

| t	$C_{1,t}^{(S,\mathcal{O})}$	$C_{\gamma_4,t}^{(S,\mathcal{O})}$	$C_{1,t}^{(T,\mathcal{O})}$	$C_{\gamma_4,t}^{(T,\mathcal{O})}$	$C_{1,t}^{(x,\mathcal{O})}$	$C_{\gamma_4,t}^{(x,\mathcal{O})}$
1	-0.01918(27)	2.92598(67)	0.14820(25)	-0.14203(17)	0.29334(74)	2.10741(60)
2	0.01321(22)	0.05801(17)	-0.46084(19)	-0.02921(16)	0.09500(47)	0.63145(40)
3	0.01255(17)	0.02083(13)	-0.12500(14)	-0.00324(11)	0.06046(33)	0.23762(31)
4	0.00676(12)	0.00848(10)	-0.04257(10)	-0.00418(09)	0.04039(24)	0.10637(25)
5	0.00424(09)	0.00457(08)	-0.01719(08)	-0.00349(07)	0.02678(19)	0.05381(19)
6	0.00233(07)	0.00234(07)	-0.00812(06)	-0.00269(06)	0.01730(15)	0.02912(13)
7	0.00120(06)	0.00137(05)	-0.00425(05)	-0.00181(05)	0.01135(12)	0.01666(12)
8	0.00079(05)	0.00079(05)	-0.00236(04)	-0.00121(04)	0.00730(10)	0.00971(10)
...	...	...	...	...	...	...
40	-0.00075(05)	0.00083(05)	0.00235(04)	-0.00123(04)	-0.00752(11)	0.00980(11)
41	-0.00130(06)	0.00149(06)	0.00418(06)	-0.00164(05)	-0.01114(12)	0.01658(12)
42	-0.00232(07)	0.00245(07)	0.00806(06)	-0.00243(06)	-0.01707(16)	0.02912(14)
43	-0.00399(09)	0.00424(09)	0.01740(09)	-0.00376(07)	-0.02575(18)	0.05346(18)
44	-0.00692(12)	0.00861(10)	0.04285(10)	-0.00441(10)	-0.04057(22)	0.10671(27)
45	-0.01271(18)	0.02103(12)	0.12536(13)	-0.00284(11)	-0.06060(33)	0.23868(32)
46	-0.01366(22)	0.05793(18)	0.46036(19)	-0.02923(15)	-0.09399(45)	0.63359(40)
47	0.01852(26)	2.92603(67)	-0.14921(24)	-0.14227(18)	-0.29337(71)	2.10744(59)

Table B.2: Numerical values of correlation functions appearing in Eqs. (4.92,4.93) at $\beta = 5.6$ and $\kappa = 0.1655$. Each color at t and at $N_t - t$ is same to test symmetricity and anti-symmetricity from Eq. (4.94) within errors.

t_{min}	$\beta = 5.4\ \kappa = 0.1703$		$\beta = 5.45,\ \kappa = 0.1692$		$\beta = 5.5,\ \kappa = 0.1683$		$\beta = 5.6,\ \kappa = 0.1655$	
	$am_s Z_S^{-1}$	χ^2/DoF	$am_s Z_S^{-1}$	χ^2/DoF	$am_s Z_S^{-1}$	χ^2/DoF	$am_s Z_S^{-1}$	χ^2/DoF
2	0.1361(014)	0.0576	0.0717(029)	0.1746	0.0340(048)	0.2261	0.0899(010)	0.5489
3	0.1391(016)	0.0042	0.0742(023)	0.0210	0.0295(056)	0.0628	0.0836(005)	0.0841
4	0.1333(043)	0.0037	0.0692(046)	0.0150	0.0238(056)	0.0302	0.0747(010)	0.0170
5	0.1254(109)	0.0037	0.0597(096)	0.0142	0.0217(098)	0.0251	0.0701(009)	0.0078
6	0.1122(240)	0.0037	0.0804(146)	0.0111	0.0224(139)	0.0275	0.0666(018)	0.0071
7	0.1243(1042)	0.0036	0.0832(234)	0.0123	0.0201(167)	0.0258	0.0679(028)	0.0072
8	-	-	0.0779(790)	0.0140	0.0306(302)	0.0270	0.0640(048)	0.0076
9	-	-	-	-	-	0.0079	0.0583(095)	0.0079
10	-	-	-	-	-	0.0080	0.0758(523)	0.0080
11	-	-	-	-	-	0.0063	0.1161(774)	0.0063

Table B.3: Subtracted gluino mass $am_s Z_S^{-1}$ and χ^2/DoF obtained from GLS method for different gauge ensembles. Highlighted data points are values where plateau is formed and χ^2/DoF also shows a constant behavior. These data points are finally selected for chiral and continuum extrapolations.

β	5.4	5.45		5.5		5.6	
t_{min}	4	5	$5_{exception}$	5	6	7	$7_{exception}$
$\Delta(am_S Z_S^{-1})$	0.0334(48)	0.016(15)	0.0227(83)	0.0168(67)	0.003(11)	0.0102(34)	0.0104(32)

Table B.4: Remnant gluino mass ($\Delta(am_S Z^{-1})$) obtained at $m_{a\text{-}\pi} = 0$ for 4 available values of β in two step procedure. $5_{exception}$ and $7_{exception}$ refer to the Tab. (4.2).
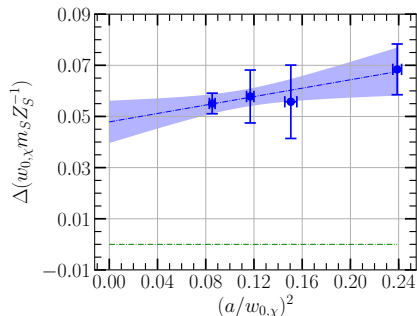
(a) $t_{min} = 4$ is used for all gauge ensembles. Incompatibility with zero is due to discretisation effects.
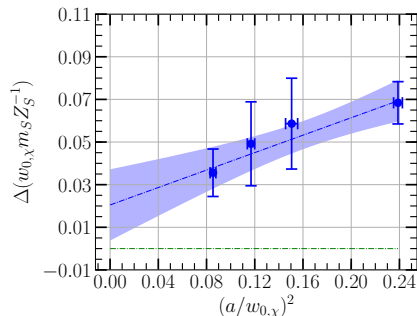
(b) $t_{min} = 4, 5, 5, 7$ for $\beta = 5.4, 5.45, 5.5, 5.6$ respectively with some exceptions, see Tab. (4.2).
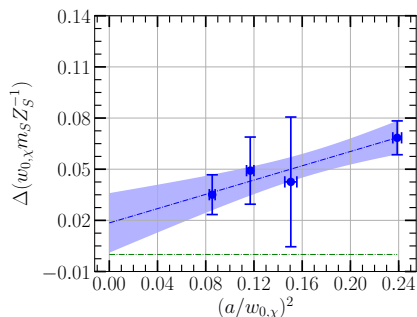
(c) $t_{min} = 4, 5, 5, 7$ for $\beta = 5.4, 5.45, 5.5, 5.6$ respectively using t_{min} from $m_{g\tilde{g}}$ of Tab. (4.3).
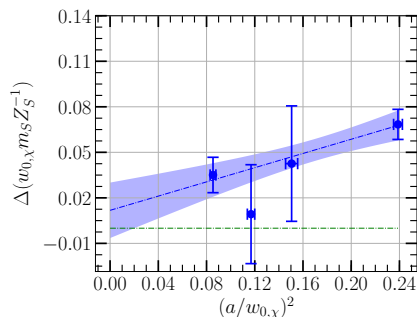
(d) $t_{min} = 4, 5, 6, 7$ for $\beta = 5.4, 5.45, 5.5, 5.6$ respectively using t_{min} from w_0 of Tab. (4.3).

Figure B.1: The remnant gluino mass $\Delta(w_0 m_S Z_S^{-1})$ in physical units (w_0) as a function of physical lattice spacing squared, and its linear extrapolation towards the continuum limit by two step procedure where we perform chiral extrapolation followed by the continuum extrapolation.

B.2 Rarita Schwinger field

The Rarita Schwinger field for $\Gamma = C\gamma_5$ is

$$W = f_{abc}\lambda_a \left(\lambda_b^T C\gamma_5 \lambda_c\right), \tag{B.1}$$

we omit dependence of fields on space-time points for the sake of simplicity. As $C\gamma_5$ is symmetric, therefore we choose anti-symmetric structure constant f_{abc}. Using properties of Eqs. (B.11,B.13) one obtains

$$W = f_{abc}\lambda_a \left(\bar{\lambda}_b\gamma_5\lambda_c\right). \tag{B.2}$$

The conjugate field $\overline{W} = W^\dagger\gamma_4$ reads

$$\overline{W} = f_{abc}\left[\lambda_a\left(\bar{\lambda}_b\gamma_5\lambda_c\right)\right]^\dagger \gamma_4, \tag{B.3}$$

$$= f_{abc}\left(-\lambda_c^\dagger\gamma_5^\dagger\bar{\lambda}_b^\dagger\right)\bar{\lambda}_a, \tag{B.4}$$

$$= f_{abc}\left(\bar{\lambda}_c\gamma_5^\dagger\lambda_b\right)\lambda_a^T C, \tag{B.5}$$

$$= f_{abc}\left[\lambda_a\left(\bar{\lambda}_b\gamma_5\lambda_c\right)\right]^T C, \tag{B.6}$$

$$= -\left(CW\right)^T. \tag{B.7}$$

Note that

$$\overline{W} = -\left(CW\right)^T, \quad \text{for } \Gamma = C\gamma_{4,5}. \tag{B.8}$$

$$\overline{W} = +\left(CW\right)^T, \quad \text{for } \Gamma = C\gamma_i, \ i = 1, 2, 3. \tag{B.9}$$

$$\tag{B.10}$$

In the derivation of above conjugate field, the following properties have been employed

$$\bar{\lambda} = \lambda^T C, \text{ Majoran condition}, \tag{B.11}$$

$$\bar{\lambda} = \lambda^\dagger\gamma_4, \tag{B.12}$$

$$C^2 = -\mathbf{1}, \ C^{-1} = C^T = -C, \tag{B.13}$$

$$\lambda_a\lambda_b = -\lambda_b\lambda_a, \text{ Grassmannian nature}, \tag{B.14}$$

$$C\gamma_{1,3,5} = \gamma_{1,3,5}C, \ C\gamma_{2,4} = -\gamma_{2,4}C, \tag{B.15}$$

$$\gamma_4\gamma_{i,5} = -\gamma_{i,5}\gamma_4, \ \gamma_{\mu,5}^\dagger = \gamma_{\mu,5}, \tag{B.16}$$

$$\gamma_{2,4,5}^T = \gamma_{2,4,5}, \ \gamma_{1,3}^T = -\gamma_{1,3}, \ \left(C\gamma_{\mu,5}\right)^T = \left(C\gamma_{\mu,5}\right). \tag{B.17}$$

B.3 Structure constants

Depending upon the choice of the gauge group and spin matrices one can use (anti-)symmetric structure constant which will be given below

B.3.1 Structure constants ε_{abc}

The anti-symmetric ε_{abc} reads

$$\varepsilon_{123} = \varepsilon_{231} = \varepsilon_{312} = +1, \tag{B.18}$$

$$\varepsilon_{321} = \varepsilon_{213} = \varepsilon_{132} = -1. \tag{B.19}$$

All other values of ε_{abc} are zero.

B.3.2 Structure constants d_{abc} and f_{abc}

These structure constrants take the following values

$$d_{118} = d_{228} = d_{338} = -d_{888} = \frac{1}{\sqrt{3}}, \tag{B.20}$$

$$d_{448} = d_{558} = d_{668} = d_{778} = -\frac{1}{2\sqrt{3}}, \tag{B.21}$$

$$d_{146} = d_{157} = -d_{247} = d_{256} = d_{344} = d_{355} = -d_{366} = -d_{377} = \frac{1}{2}, \tag{B.22}$$

$$f_{123} = +1, \tag{B.23}$$

$$f_{147} = -f_{156} = f_{246} = f_{257} = f_{345} = -f_{367} = \frac{1}{2}, \tag{B.24}$$

$$f_{458} = f_{678} = \frac{\sqrt{3}}{2}. \tag{B.25}$$

All other d_{abc} and f_{abc} not related to these by permutation are zero.

134

B.4 Choice of structure constants and spin matrices

For $\Gamma = C$ and $t_{abc} = d_{abc}$, the Eq (5.1), in Dirac indices, is given by

$$W^\sigma = d_{abc} C^{\beta\gamma} \lambda_a^\alpha \lambda_b^\beta \lambda_c^\gamma, \tag{B.26}$$

using numerical values of C from Eq. (A.10), the Eq (B.26) reduces to

$$W^\sigma = d_{abc} \lambda_a^\alpha \left\{ \lambda_b^1 \lambda_c^2 - \lambda_b^2 \lambda_c^1 - \lambda_b^3 \lambda_c^4 + \lambda_b^4 \lambda_c^3 \right\}, \tag{B.27}$$

here

$$\lambda_b^2 \lambda_c^1 = -\lambda_c^1 \lambda_b^2 = -\lambda_b^1 \lambda_c^2. \tag{B.28}$$

As λ's are Grassmannian objects, interchange of the two λ's gives an additional minus sign. It does not matter if we interchange color indices b and c because d_{abc} is symmetric in a, b and c

$$W^\sigma = 2 \, d_{abc} \lambda_a^\alpha \left\{ \lambda_b^1 \lambda_c^2 + \lambda_b^4 \lambda_c^3 \right\}, \tag{B.29}$$

this implies that

$$W^\sigma = d_{abc} C^{\beta\gamma} \lambda_a^\alpha \lambda_b^\beta \lambda_c^\gamma \neq 0. \tag{B.30}$$

Note that the charge conjugation matrix C is anti-symmetric whereas the structure constant d_{abc} is symmetric. We can show that, by performing similar steps of calculations, $W \neq 0$ for all Γ's which are anti-symmetric. It is also possible to use same analogy to show that $W = 0$ for all Γ's which are symmetric. We conclude that the field W will be non-vanishing: if t_{abc} is symmetric and Γ is anti-symmetric, and vice versa.

B.5 Derivation of different terms of baryon correlation function

In order to simplify each term of Eq. (5.26), let's consider the 1$^{\text{st}}$

$$D_1^{\alpha\delta}(x,y) = -f_{abc}f_{a'b'c'}(C\gamma_5)^{\beta\gamma}(C\gamma_5)^{\beta'\gamma'}C^{\delta\alpha'} \times \tag{B.31}$$
$$\left\{ -2K_{aa'}^{\alpha\alpha'}(x,y)K_{bb'}^{\beta\beta'}(x,y)K_{cc'}^{\gamma\gamma'}(x,y)\right\}.$$

Consider

$$C^{\delta\alpha'}K_{aa'}^{\alpha\alpha'}(x,y) = -(-\triangle(x,y)C)_{aa'}^{\alpha\alpha'}C^{\alpha'\delta} \tag{B.32}$$
$$= (\triangle(x,y)C^2)_{aa'}^{\alpha\delta} = -\triangle_{aa'}^{\alpha\delta}(x,y).$$

$$D_1^{\alpha\delta}(x,y) = -f_{abc}f_{a'b'c'}(C\gamma_5)^{\beta\gamma}(C\gamma_5)^{\beta'\gamma'} \times \tag{B.33}$$
$$\left\{ +2\triangle_{aa'}^{\alpha\delta}(x,y)\triangle_{bb'}^{\beta\sigma'}(x,y)C^{\sigma'\beta'}\triangle_{cc'}^{\gamma\rho'}(x,y)C^{\rho'\gamma'}\right\},$$

$$C^{\sigma'\beta'}(C\gamma_5)^{\beta'\gamma'}C^{\sigma\rho'} = -(C^2\gamma_5 C)^{\sigma'\rho'} = (C\gamma_5)^{\sigma'\rho'}. \tag{B.34}$$

By interchanging the idices, $\delta \leftrightarrow \alpha'$, $\sigma' \leftrightarrow \beta'$, $\rho' \leftrightarrow \gamma'$, we get

$$D_1^{\alpha\alpha'}(x,y) = -f_{abc}f_{a'b'c'}(C\gamma_5)^{\beta\gamma}(C\gamma_5)^{\beta'\gamma'} \times \tag{B.35}$$
$$\left\{ +2\triangle_{aa'}^{\alpha\alpha'}(x,y)\triangle_{bb'}^{\beta\beta'}(x,y)\triangle_{cc'}^{\gamma\gamma'}(x,y)\right\}.$$

Similarly

$$D_2^{\alpha\alpha'}(x,y) = -f_{abc}f_{a'b'c'}(C\gamma_5)^{\beta\gamma}(C\gamma_5)^{\beta'\gamma'} \times \tag{B.36}$$
$$\left\{ +4\triangle_{ab'}^{\alpha\beta'}(x,y)\triangle_{bc'}^{\beta\gamma'}(x,y)\triangle_{ca'}^{\gamma\alpha'}(x,y)\right\},$$

now

$$D_3^{\alpha\delta}(x,y) = -f_{abc}f_{a'b'c'}(C\gamma_5)^{\beta\gamma}(C\gamma_5)^{\beta'\gamma'}C^{\delta\alpha'} \times \tag{B.37}$$
$$\left\{ -2K_{ab}^{\alpha\beta}(x,x)K_{ca'}^{\gamma\alpha'}(x,y)K_{c'b'}^{\gamma'\beta'}(y,y)\right\},$$

$$C^{\delta\alpha'}K_{ca'}^{\gamma\alpha'}(x,y) = -(-\triangle(x,y)C)_{ca'}^{\gamma\alpha'}C^{\alpha'\delta}$$

$$= (\triangle(x,y)C^2)_{ca'}^{\gamma\delta} = -\triangle_{ca'}^{\gamma\delta}(x,y). \qquad \text{(B.38)}$$

Interchanging $\delta \leftrightarrow \alpha'$,

$$D_3^{\alpha\alpha'}(x,y) = -f_{abc}f_{a'b'c'}(C\gamma_5)^{\beta\gamma}(C\gamma_5)^{\beta'\gamma'} \times \qquad \text{(B.39)}$$
$$\left\{ + 2\triangle_{ab}^{\alpha\sigma}(x,x)C^{\sigma\beta}\triangle_{ca'}^{\gamma\alpha'}(x,y)\triangle_{c'b'}^{\gamma'\sigma'}(y,y)C^{\sigma'\beta'} \right\},$$

now

$$C^{\sigma\beta}(C\gamma_5)^{\beta\gamma} = -\gamma_5^{\sigma\gamma} = (\gamma_5 C^2)^{\sigma\gamma} = (C\gamma_5)^{\sigma\delta}C^{\sigma\delta}, \qquad \text{(B.40)}$$

and

$$C^{\sigma'\beta'}(C\gamma_5)^{\beta'\gamma'} = -\gamma_5^{\sigma'\gamma'} = (\gamma_5 C^2)^{\sigma'\gamma'} = (C\gamma_5)^{\sigma'\delta'}C^{\sigma'\delta'}. \qquad \text{(B.41)}$$

By interchanging the indices, $\sigma \leftrightarrow \beta$, $\sigma' \leftrightarrow \beta'$, $\delta \leftrightarrow \gamma$, $\delta' \leftrightarrow \gamma'$, we obtain

$$D_3^{\alpha\alpha'}(x,y) = -f_{abc}f_{a'b'c'}(C\gamma_5)^{\beta\gamma}(C\gamma_5)^{\beta'\gamma'} \times \qquad \text{(B.42)}$$
$$\left\{ + 2\triangle_{ab}^{\alpha\beta}(x,x)\triangle_{ca'}^{\delta\alpha'}(x,y)\triangle_{c'b'}^{\delta'\beta'}(y,y)C^{\gamma\delta}C^{\gamma'\delta'} \right\}.$$

Using the similar calculations on gets the other terms as follows

$$D_4^{\alpha\alpha'}(x,y) = -f_{abc}f_{a'b'c'}(C\gamma_5)^{\beta\gamma}(C\gamma_5)^{\beta'\gamma'} \times \qquad \text{(B.43)}$$
$$\left\{ + 4\triangle_{ab}^{\alpha\beta}(x,x)\triangle_{b'c}^{\beta'\gamma}(y,x)\triangle_{c'a'}^{\gamma'\alpha'}(y,y) \right\},$$

$$D_5^{\alpha\alpha'}(x,y) = -f_{abc}f_{a'b'c'}(C\gamma_5)^{\beta\gamma}(C\gamma_5)^{\beta'\gamma'} \times \qquad \text{(B.44)}$$
$$\left\{ + 1\triangle_{aa'}^{\alpha\alpha'}(x,y)\triangle_{bc}^{\beta\delta}(x,x)\triangle_{c'b'}^{\delta'\beta'}(y,y)C^{\gamma\delta}C^{\delta'\gamma'} \right\},$$

and

$$D_6^{\alpha\alpha'}(x,y) = -f_{abc}f_{a'b'c'}(C\gamma_5)^{\beta\gamma}(C\gamma_5)^{\beta'\gamma'} \times \qquad \text{(B.45)}$$
$$\left\{ + 2\triangle_{ac}^{\alpha\delta'}(x,y)\triangle_{bc}^{\beta\delta}(x,x)\triangle_{b'a'}^{\beta'\alpha'}(y,y)C^{\gamma\delta}C^{\gamma'\delta'} \right\}.$$

B.6   Implementation of spectacle piece

In order to implement the spectacle piece we need to have each term of the correlation function of the following form

$$B = \sum M \bigtriangleup S. \tag{B.46}$$

The 1st term of the Eq. (5.29) can be written as

$$B^{(1)}_{Spec}(t) = 2\,\theta \sum_{\substack{\vec{x},\vec{y} \\ x_0=y_0+t}} \sum_{\substack{\alpha,\alpha' \\ c,a'}} P_{\pm}^{\alpha\alpha'} M_c^{\alpha\delta}(x,x) \bigtriangleup_{ca'}^{\delta\alpha'}(x,y) S_{a'}(y,y), \tag{B.47}$$

where

$$M_c^{\alpha\delta}(x,x) = \sum_{\substack{\beta,\gamma \\ a,b}} t_{abc} \bigtriangleup_{ab}^{\alpha\beta}(x,x)\Gamma^{\beta\gamma}C^{\gamma\delta},$$

$$S_{a'}(y,y) = \sum_{\substack{\beta',\gamma',\delta' \\ b',c'}} t_{a'b'c'} \bigtriangleup_{c'b'}^{\delta'\beta'}(y,y)\Gamma^{\beta'\gamma'}C^{\gamma'\delta'}. \tag{B.48}$$

For $\Gamma = C\gamma_4$

$$M_c^{\alpha\delta}(x,x) = \sum_{a,b} t_{abc}(\bigtriangleup\gamma_4)_{ab}^{\alpha\delta}(x,x),$$

$$S_{a'}(y,y) = \sum_{\delta',b',c'} t_{a'b'c'}(\bigtriangleup\gamma_4)_{c'b'}^{\delta'\delta'}(y,y). \tag{B.49}$$

For $\Gamma = C\gamma_5$

$$M_c^{\alpha\delta}(x,x) = -\sum_{a,b} t_{abc}(\bigtriangleup\gamma_5)_{ab}^{\alpha\delta}(x,x),$$

$$S_{a'}(y,y) = -\sum_{\delta',b',c'} t_{a'b'c'}(\bigtriangleup\gamma_5)_{c'b'}^{\delta'\delta'}(y,y). \tag{B.50}$$

The 2nd term of the Eq. (5.29) can be written as

$$B_{Spec}^{(2)}(t) = -4\,\theta \sum_{\substack{\vec{x},\vec{y} \\ x_0=y_0+t}} \sum_{\substack{\alpha,\alpha',\delta,\delta' \\ c,b'}} P_{\pm}^{\alpha\alpha'} M_c^{\alpha\delta}(x,x) \triangle_{cb'}^{\delta\delta'}(x,y) S_{b'}^{\delta'\alpha'}(y,y), \quad \text{(B.51)}$$

where

$$M_c^{\alpha\delta}(x,x) = \sum_{\substack{\beta,\gamma \\ a,b}} t_{abc} \triangle_{ab}^{\alpha\beta}(x,x)\Gamma^{\beta\gamma}C^{\gamma\delta},$$

$$S_{b'}^{\delta'\alpha'}(y,y) = \sum_{\substack{\beta',\gamma' \\ a',c'}} t_{a'b'c'}C^{\delta'\beta'}\Gamma^{\beta'\gamma'} \triangle_{c'a'}^{\gamma'\alpha'}(y,y). \quad \text{(B.52)}$$

For $\Gamma = C\gamma_4$

$$M_c^{\alpha\delta}(x,x) = \sum_{a,b} t_{abc}(\triangle\gamma_4)_{ab}^{\alpha\delta}(x,x),$$

$$S_{b'}^{\delta'\alpha'}(y,y) = - \sum_{a',c'} t_{a'b'c'}(\gamma_4\triangle)_{c'a'}^{\delta'\alpha'}(y,y). \quad \text{(B.53)}$$

For $\Gamma = C\gamma_5$

$$M_c^{\alpha\delta}(x,x) = - \sum_{a,b} t_{abc}(\triangle\gamma_5)_{ab}^{\alpha\delta}(x,x),$$

$$S_{b'}^{\delta'\alpha'}(y,y) = - \sum_{a',c'} t_{a'b'c'}(\gamma_5\triangle)_{c'a'}^{\delta'\alpha'}(y,y). \quad \text{(B.54)}$$

The 3rd term of the Eq. (5.29) can be written as

$$B_{Spec}^{(3)}(t) = \pm\,\theta \sum_{\substack{\vec{x},\vec{y} \\ x_0=y_0+t}} \sum_{\substack{\alpha,\alpha' \\ a,a'}} P_{\pm}^{\alpha\alpha'} M_a(x,x) \triangle_{aa'}^{\alpha\alpha'}(x,y) S_{a'}(y,y), \quad \text{(B.55)}$$

where "+" is for the symmetric Γ and "−" in the case when it is anti-symmetric.

$$M_a(x,x) = \sum_{\substack{\beta,\gamma,\delta \\ b,c}} t_{abc} C^{\delta\gamma} \Gamma^{\gamma\beta} \triangle^{\beta\delta}_{bc}(x,x),$$

$$S_{a'}(y,y) = \sum_{\substack{\beta',\gamma',\delta' \\ b',c'}} t_{a'b'c'} \triangle^{\delta'\beta'}_{c'b'}(y,y) \Gamma^{\beta'\gamma'} C^{\gamma'\delta'}. \tag{B.56}$$

For $\Gamma = C\gamma_4$

$$M_a(x,x) = -\sum_{\delta,b,c} t_{abc} (\gamma_4 \triangle)^{\delta\delta}_{bc}(x,x),$$

$$S_{a'}(y,y) = \sum_{\delta',b',c'} t_{a'b'c'} (\triangle\gamma_4)^{\delta'\delta'}_{c'b'}(y,y). \tag{B.57}$$

For $\Gamma = C\gamma_5$

$$M_a(x,x) = -\sum_{\delta,b,c} t_{abc} (\gamma_5 \triangle)^{\delta\delta}_{bc}(x,x),$$

$$S_{a'}(y,y) = -\sum_{\delta',b',c'} t_{a'b'c'} (\triangle\gamma_5)^{\delta'\delta'}_{c'b'}(y,y). \tag{B.58}$$

The 4th term of the Eq. (5.29) can be written as

$$B^{(4)}_{Spec}(t) = 2\,\theta \sum_{\substack{\vec{x},\vec{y} \\ x_0=y_0+t}} \sum_{\substack{\alpha,\alpha' \\ a,c'}} P^{\alpha\alpha'}_{\pm} M_a(x,x) \triangle^{\alpha\delta'}_{ac'}(x,y) S^{\delta'\alpha'}_{c'}(y,y), \tag{B.59}$$

where

$$M_a(x,x) = \sum_{\substack{\beta,\gamma,\delta \\ b,c}} t_{abc} C^{\delta\gamma} \Gamma^{\gamma\beta} \triangle^{\beta\delta}_{bc}(x,x),$$

$$S^{\delta'\alpha'}_{c'}(y,y) = \sum_{\substack{\beta',\gamma' \\ a',b'}} t_{a'b'c'} C^{\delta'\gamma'} \Gamma^{\gamma'\beta'} \triangle^{\beta'\alpha'}_{b'a'}(y,y). \tag{B.60}$$

140

For $\Gamma = C\gamma_4$

$$M_a(x,x) = -\sum_{\delta,b,c} t_{abc}(\gamma_4\triangle)_{bc}^{\delta\delta}(x,x),$$

$$S_{c'}^{\delta'\alpha'}(y,y) = -\sum_{a',b'} t_{a'b'c'}(\gamma_4\triangle)_{b'a'}^{\delta'\alpha'}(y,y). \tag{B.61}$$

For $\Gamma = C\gamma_5$

$$M_a(x,x) = -\sum_{\delta,b,c} t_{abc}(\gamma_5\triangle)_{bc}^{\delta\delta}(x,x),$$

$$S_{c'}^{\delta'\alpha'}(y,y) = -\sum_{a',b'} t_{a'b'c'}(\gamma_5\triangle)_{b'a'}^{\delta'\alpha'}(y,y). \tag{B.62}$$

B.7 Effective mass of sunset and spectacle pieces

(a) Sunset.
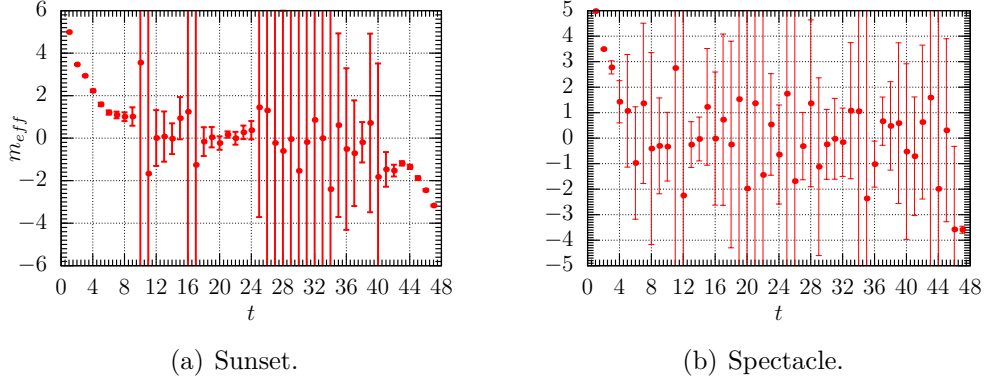
(b) Spectacle.

Figure B.2: Effective masses of sunset and spectacle pieces of correlation function with error bars at β=2.75 and $\kappa = 0.14925$ for for SYM theory with gauge group SU(2).

B.8   Comparison of stochastic noise with gauge noise

t	$B_{Spec}(t)$	$B_{\text{stoch}}(t)$
1	-0.071877(1386)	-0.070431(1955)
2	-0.006160(580)	-0.006384(947)
3	0.000134(353)	0.000659(522)
4	-0.000147(277)	0.000136(318)
5	-0.000275(224)	-0.000116(344)
6	0.000419(203)	-0.000656(309)
7	-0.000504(184)	0.000218(230)
8	0.000029(165)	-0.000005(240)
9	0.000063(139)	0.000206(161)
10	-0.000136(145)	-0.000047(157)
11	-0.000060(149)	0.000335(202)
12	-0.000068(115)	-0.000098(154)

Table B.5: $B_{Spec}(t)$ is baryon spectacle piece (40 stochastic estimators and 20 lowest eigenvalues with no smearing) with full statistics whereas $B_{\text{stoch}}(t)$ is the spectacle piece of the correlation function measured 50 times on one configuration by keeping the source fixed in order to estimate the stochastic noise at β=2.75 and $\kappa = 0.14925$ for gauge group SU(2). The overall noise of the correlation function is due to stochastic noise. For convenience we have shown only first 12 values of time slice distance and corresponding correlation functions.

Bibliography

[1] D. Griffiths, *Introduction to elementary particles* (Wiley & Sons, New York, 1987).

[2] J. D. Lykken, *Beyond the Standard Model*, [arXiv: `1005.1676` [`hep-ph`]].

[3] G. Bergner, P. Giudice, G. Münster, I. Montvay and S. Piemonte, *The light bound states of supersymmetric SU(2) Yang-Mills theory*, JHEP **1603** (2016) 080, [arXiv: `1512.07014` [`hep-lat`]].

[4] F. Farchioni, A. Feo, T. Galla, C. Gebert, R. Kirchner, I. Montvay, G. Münster and A. Vladikas, *The Supersymmetric Ward identities on the lattice*, Eur. Phys. J. C **23** (2002) 719, [arXiv: `hep-lat/0111008`].

[5] S. Ali, G. Bergner, H. Gerber, P. Giudice, S. Kuberski, I. Montvay, G. Münster and S. Piemonte, *Supermultiplets in $\mathcal{N} = 1$ SUSY SU(2) Yang-Mills theory*, EPJ Web Conf. **175** (2018) 08016, [arXiv: `1710.07464` [`hep-lat`]].

[6] S. Ali, G. Bergner, H. Gerber, P. Giudice, I. Montvay, G. Münster, S. Piemonte and P. Scior, *The light bound states of $\mathcal{N} = 1$ supersymmetric SU(3) Yang-Mills theory on the lattice*, JHEP **1803** (2018) 113, [arXiv: `1801.08062` [`hep-lat`]].

[7] S. Ali, G. Bergner, H. Gerber, S. Kuberski, I. Montvay, G. Münster, S. Piemonte, P. Scior, *Variational analysis of low-lying states in supersymmetric Yang-Mills theory*, JHEP **04** (2019) 150, [arXiv: `1901.02416` [`hep-lat`]].

[8] S. Ali, G. Bergner, H. Gerber, I. Montvay, G. Münster, S. Piemonte and P. Scior, *Numerical Results for the Lightest Bound States in $\mathcal{N} = 1$ Supersymmetric SU(3) Yang-Mills Theory*, Phys. Rev. Lett. **122**, 2216011 (2019), [arXiv: `1902.11127` [`hep-lat`]].

[9] G. Veneziano and S. Yankielowicz, *An effective Lagrangian for the pure $\mathcal{N} = 1$ supersymmetric Yang-Mills theory*, Phys. Lett. **B 113** (1982) 231.

[10] G. R. Farrar, G. Gabadadze, and M. Schwetz, *Effective action of $\mathcal{N} = 1$ supersymmetric Yang-Mills theory*, Phys. Rev. **D 58** (1998) 015009, [arXiv: `hep-th/9711166`].

[11] A. Bilal, *Introduction to Supersymmetry*, [arXiv: `hep-th/0101055`].

[12] M. P. Hokmabadi, N. S. Nye, R. El-Ganainy, D. N. Christodoulides, M. Khajavikhan, *Supersymmetric laser arrays*, **Science** (2019) 363 623, [arXiv: `1812.10690` [`hep-lat`]].

[13] I. Sachs, *Lectures on Supersymmetry*, Communications of the Dublin Institute for Advanced Studies, Series A, No. 29.

[14] A. G. Dias, V. Pleitez, *Grand Unification and Proton Stability Near the Peccei-Quinn Scale*, Phys. Rev. **D 70** (2004) 055009, [arXiv: `hep-ph/0407074`].

[15] W. M. Yao *et al*, *Review of particle physics*, J. Phys. G33 (2006) 1.

[16] G. Jungman, M. Kamionkowski, K. Griest, *Supersymmetric Dark Matter*, Phys. Rep. **267**, (1996) 195, [arXiv: `hep-ph/9506380`].

[17] S. Piemonte, *$\mathcal{N} = 1$ supersymmetric Yang-Mills theory on the lattice*, PhD thesis, University of Münster, April, 2015.

[18] S. P. Martin, *A Supersymmetry Primer*, [arXiv: `hep-ph/9709356`].

[19] D. Amati, K. Konishi, Y. Meurice, G. C. Rossi and G. Veneziano, *Nonperturbative aspects in supersymmetric gauge theories*, Phys. Rept. **162** (1988) 169.

144

[20] A. Wipf, *Introduction to Supersymmetry*, University Lecture (2001), Friedrich-Schiller-Universität Jena.

[21] J. Bagger, J. Wess, *Supersymmetry and Supergravity, Princeton University Press, 1983.*

[22] P. Fayet, S. Ferrara, *Supersymmetry*, Phys. Rep. **32**, 249 (1977).

[23] M.F. Sohnius, *Introducing supersymmetry*, Phys. Rep. **128**, 39 (1985).

[24] H. J. Rothe, *Lattice Gauge Theories*, Singapore (1998): World Scientific.

[25] H. Nicolai, *A possible constructive approach to (super-ϕ^3)$_4$ (I). Euclidean formulation of the model*, Nucl. Phys. **B 140**, 294 (1978).

[26] P. van Nieuwenhuizen, A. Waldron, *On Euclidean spinors and Wick rotations*, Phys. Lett. **B 389**, 29 (1996), [arXiv: `hep-th/9608174`].

[27] I. Montvay, *Supersymmetric Yang-Mills theory on the lattice*, Int. J. Mod. Phys. **A 17** (2002) 2377, [arXiv: `hep-lat/0112007`].

[28] V. A. Novikov, M. A. Shifman, A. I. Vainshtein, and V. I. Zakharov, *Supersymmetric instanton calculus: Gauge theories with matter*, Nucl. Phys. **B 260**, 157 (1985).

[29] M. A. Shifman and A. I. Vainshtein, *On gluino condensation in supersymmetric gauge theories with SU(N) and O(N) groups*, Nucl. Phys. **B 296**, 445 (1988).

[30] E. Witten, *Constraints on supersymmetry breaking**, Nucl. Phys. **B 202**, 253 (1982).

[31] S. Ali, G. Bergner, H. Gerber, P. Giudice, I. Montvay, G. Münster and S. Piemonte, *Simulations of $\mathcal{N} = 1$ supersymmetric Yang-Mills theory with three colours*, PoS (LATTICE2016) 222, [arXiv: `1610.10097` [`hep-lat`]].

[32] G. R. Farrar, G. Gabadadze, and M. Schwetz, *The spectrum of softly broken $\mathcal{N} = 1$ supersymmetric Yang- Mills theory*, Phys. Rev. **D 60** (1999) 035002, [arXiv: `hep-th/9806204`].

[33] S. Ferrara and B. Zumino, *Transformation properties of the supercurrent*, Nucl. Phys. **B 87**, 207 (1975).

[34] V. A. Novikov, M. A. Shifman, A. I. Vainshtein, and V. I. Zakharov, *Exact Gell-Mann-Low function of supersymmetric Yang-Mills theories from instanton calculus*, Nucl. Phys. **B 229**, 381 (1983).

[35] M. Maggiore, *A Modern Introduction to Quantum Field Theory*, Oxford Master Series in Physics (2005).

[36] G. Bergner, *Complete supersymmetry on the lattice and a No-Go theorem*, JHEP **1001** (2010) 024, [arXiv: `0909.4791` [`hep-lat`]].

[37] S. Ali, G. Bergner, H. Gerber, I. Montvay, G. Münster, S. Piemonte and P. Scior, *Analysis of Ward identities in supersymmetric Yang–Mills theory*, Eur. Phys. J. **C 78** (2018) 404, [arXiv: `1802.07067` [`hep-lat`]].

[38] G. Curci, G. Veneziano, *Supersymmetry and the lattice: A reconciliation?*, Nucl. Phys. **B 292** (1987) 555.

[39] A. Donini, M. Guagnelli, P. Hernandez und A. Vladikas, *Towards $\mathcal{N} = 1$ Super-Yang-Mills on the Lattice*, Nucl. Phys. **B 523** (1998) 529-552, [arXiv: `hep-lat/9710065`].

[40] R. Kirchner, *Ward Identities and Mass Spectrum of $\mathcal{N} = 1$ Super Yang-Mills Theory on the Lattice*, PhD thesis, DESY Hamburg, September, 2000.

[41] I. Campos, A. Feo, R. Kirchner, S. Luckmann, I. Montvay, G. Münster, K. Spanderen, J. Westphalen, *Monte Carlo simulation of SU(2) Yang-Mills theory with light gluinos*, Eur. Phys. J. **C 11**, 507 (1999), [arXiv: `hep-lat/9903014`].

146

[42] D. B. Kaplan, M. Schmaltz, *Supersymmetric Yang-Mills Theories from Domain Wall Fermions*, Chin. J. Phys. **38**, 543 (2000), [arXiv: `hep-lat/0002030`].

[43] H. Neuberger, *Vectorlike gauge theories with almost massless fermions on the lattice*, Phys. Rev. **D 57**, 5417 (1998).

[44] T. Hotta, T. Izubuchi, J. Nishimura, *Single massless Majorana fermion in the domain-wall formalism*, Mod. Phys. Lett. **A 13**, 1667 (1998), [arXiv: `hep-lat/9712009`].

[45] M. Lüscher, P. Weisz, *On-shell improved lattice gauge theories*, Commun. Math. Phys. 97 (1985) 59.

[46] S. Güsken, U. Löw, K. H. Mütter, R. Sommer, A. Patel and K. Schilling, *Non-singlet axial vector couplings of the baryon octet in lattice QCD*, Phys. Lett. **B 227** (1989) 266.

[47] S. J. Dong and K. F. Liu, *Stochastic estimation with Z(2) noise*, Phys. Lett. B **328** (1994) 130, [arXiv: `hep-lat/9308015`].

[48] G. Bergner, I. Montvay, G. Münster, U. D. Özugurel and D. Sandbrink, *Supersymmetric Yang-Mills theory: A step towards the continuum*, PoS(Lattice 2011) 055, [arXiv: `1111.3012` [`hep-lat`]].

[49] M. Lüscher, *Volume dependence of the energy spectrum in massive quantum field theories*, Commun. Math. Phys. 104 (1986) 177.

[50] G. Münster, *The size of finite size effects in lattice gauge theories*, Nucl. Phys. **B 249** (1985) 659.

[51] G. Bergner, T. Berheide, I. Montvay, G. Münster, U. D. Özugurel and D. Sandbrink, *The gluino-glue particle and finite size effects in supersymmetric Yang-Mills theory*, JHEP **1209** (2012) 108, [arXiv: `1206.2341` [`hep-lat`]].

[52] I. Montvay, *An Algorithm for Gluinos on the Lattice*, Nucl. Phys. **B 466** (1996) 259-284, [arXiv: `hep-lat/9510042`].

147

[53] L. Del Debbio, H. Panagopoulos, E. Vicari, *θ-dependence of SU(N) gauge theories*, JHEP **0208** (2002) 044, [arXiv: `hep-th/0204125`].

[54] S. Schaefer, R. Sommer, F. Virotta, *Investigating the critical slowing down of QCD simulations*, PoS (LAT2009) 032.

[55] R. Sommer, *A New way to set the energy scale in lattice gauge theories and its applications to the static force and alpha-s in SU(2) Yang-Mills theory*, Nucl. Phys. **B 411** (1994) 839-854, [arXiv: `hep-lat/9310022`].

[56] M. Donnellan, F. Knechtli, B. Leder, and R. Sommer, *Determination of the Static Potential with Dynamical Fermions*, Nucl. Phys. B849 (2011) 45-63, [arXiv: `1012.3037` [`hep-lat`]].

[57] M. Lüscher, *Properties and uses of the Wilson flow in lattice QCD*, JHEP **1008** (2010) 071, JHEP **1403** (2014) 092, [arXiv: `1006.4518` [`hep-lat`]].

[58] S. Borsanyi, S. Durr, Z. Fodor, C. Hoelbling, S. D. Katz, S. Krieg, T. Kurth, L. Lellouch, T. Lippert, C. McNeile, K. K. Szabo, *High-precision scale setting in lattice QCD*, JHEP **1209** (2012) 010, [arXiv: `1203.4469` [`hep-lat`]].

[59] G. Bergner, P. Giudice, I. Montvay, G. Münster and S. Piemonte, *Influence of topology on the scale setting*, Eur. Phys. J. Plus **130** (2015) 229, [arXiv: `1411.6995` [`hep-lat`]].

[60] I. Montvay and E. Scholz, *Updating algorithms with multi-step stochastic correction*, Phys. Lett. **B 623** (2005) 73, [arXiv: `hep-lat/0506006`].

[61] K. Demmouche, $\mathcal{N} = 1$ *SU(2) Supersymmetric Yang-Mills theory on the lattice with light dynamical Wilson gluinos*, PhD thesis, University of Münster, 2009.

[62] M. Lüscher, U. Wolff, *How to calculate the elastic scattering matrix in two-dimensional quantum field theories by numerical simulation*, Nucl. Phys. **B 339** (1990) 222-252.

[63] B. Blossier, M. Della Morte, G. von Hippel, T. Mendes and R. Sommer, *On the generalized eigenvalue method for energies and matrix elements in lattice field theory*, JHEP **0904** (2009) 094, [arXiv:`0902.1265` [`hep-lat`]].

[64] S. Kuberski, *Determination of masses in supersymmetric Yang-Mills theory using the variational method*, Master's thesis, University of Münster, March, 2017.

[65] C. Gattringer, C. B. Lang, *Quantum Chromodynamics on the Lattice: An Introductory Presentation*, Lect. Notes Phys. 788 (Springer, Berlin Heidelberg 2010).

[66] W. Janke, *Statistical Analysis of Simulations: Data Correlations and Error Estimation*, in: NIC Series 10, 423-445, John von Neumann Institute for Computing, Jülich 2002.

[67] J. Grotendorst, D. Marx, A. Muramatsu, *Quantum Simulations of Complex Many-Body Systems: From Theory to Algorithms*, NIC Series 10, John von Neumann Institute for Computing, Jülich 2002.

[68] H. Flyvbjerg, H. G. Petersen, *Error estimates on averages of correlated data*, J. Chem. Phys. **91** (1989) 461-466.

[69] U. Wolff, [ALPHA Collaboration], *Monte Carlo errors with less errors*, Comput. Phys. Commun. **156** (2004) 143-153, [arXiv:`hep-lat/0306017`], [Erratum:Comput. Phys. Commun. **176** (2007) 383].

[70] J. Hanc, S. Tuleja, M. Hancova, *Symmetries and conservation laws: Consequences of Noether's theorem*, American Journal of Physics. **72** (2004) 428-35.

[71] T. Galla, *Supersymmetrische und Chirale Ward-Identitäten in einer diskretisierten $\mathcal{N} = 1$-SUSY-Yang-Mills-Theorie*, Diploma Thesis, University of Münster, December, 1999.

149

[72] Y. Taniguchi, *One loop calculation of the SUSY Ward-Takahashi identity on the lattice with a Wilson fermion*, Phys. Rev. **D 63** (2001) 014502, [arXiv: `hep-lat/9906026`].

[73] A. Vladikas, The SUSY WIs on the lattie. A Memorandum on Strategies., (2000) unpublished.

[74] J. R. Taylor, *An Introduction to Error Analysis*, 2nd edition, University Science Books,1996.

[75] G. Münster and H. Stüwe, *The mass of the adjoint pion in $\mathcal{N} = 1$ supersymmetric Yang-Mills theory*, JHEP **1405** (2014) 034, [arXiv: `1402.6616` [`hep-th`]].

[76] K. Demmouche, F. Farchioni, A. Ferling, I. Montvay, G. Münster, E. E. Scholz and J. Wuilloud, *Simulation of 4d $\mathcal{N} = 1$ supersymmetric Yang-Mills theory with Symanzik improved gauge action and stout smearing*, Eur. Phys. J. C **69** (2010) 147, [arXiv: `1003.2073` [`hep-lat`]].

[77] S. Sharpe and R. Singleton Jr, *Spontaneous flavor and parity breaking with Wilson fermions*, Phys. Rev. **D 58** (1998) 074501, [arXiv: `hep-lat/9804028`].

[78] G. Rupak and N. Shoresh, *Chiral perturbation theory for the Wilson lattice action*, Phys. Rev. **D 66** (2002) 054503, [arXiv: `hep-lat/0201019`].

[79] S. R. Sharpe and J. M. S. Wu, *Twisted mass chiral perturbation theory at next-to-leading order*, Phys. Rev. D **71** (2005) 074501, [arXiv: `hep-lat/0411021`].

[80] H. Gerber, *Non-perturbative investigations of light bound states of $\mathcal{N} = 1$ supersymmetric Yang-Mills theory*, PhD thesis, University of Münster, May, 2019.

[81] W. Rarita and J. Schwinger, *On a Theory of Particles with Half-Integral Spin*, Phys. Rev. **60** (1941) 61.

150

[82] D. B. Leinweber, W. Melnitchouk, D. G. Richards, A. G. Williams, J. M. Zanotti, *Baryon Spectroscopy in Lattice QCD*, in: Lattice Hadron Physics, Lecture Notes in Physics 663, Springer, 2005, 71-112, [arXiv:`nucl-th/0406032`].

Curriculum Vitae

Personal information

- Name: Sajid Ali

- Sex: Male

- Date of Birth: 16.10.1987

- Place of Birth: Skeikhupura, Pakistan

- Nationality: Pakistani

- Language(s): Pujabi (Mother toungue), Urdu (National language), English (Fluent), German (B1)

- Marital Status: Married

- Contact: sajid.ali@uni-muenster.de, sajid.ali@gcu.edu.pk

Education

- Ph.D. (Lattice Field Theory): Institute for Theoretical Physics, University of Münster, Germany (2015-19)

- M.Phil. (High Energy Physics): Centre for High Energy Physics, University of the Punjab Lahore, Pakistan (2009-12)

- M.Sc. (Computational Physics): Centre for High Energy Physics, University of the Punjab Lahore, Pakistan (2007-09)

- B.Sc. (Physics and Mathematics): Government Islamia College Civil Lines Lahore, Pakistan (2005-07)

- F.Sc. (Pre-Engineering): Government Inter College, Sharaqpur Sharif, Pakistan (2003-05)

- Matric (Science): Government Pilot Secondary School Sharaqpur Sharif, Pakistan (2001-03)

Publications

1. S. Ali, G. Bergner, H. Gerber, I. Montvay, G. Münster, S. Piemonte and P. Scior, *Numerical Results for the Lightest Bound States in $\mathcal{N} = 1$ Supersymmetric SU(3) Yang-Mills Theory*, Phys. Rev. Lett. **122**, 2216011 (2019), [arXiv: `1902.11127` [`hep-lat`]].

2. S. Ali, G. Bergner, H. Gerber, S. Kuberski, I. Montvay, G. Münster, S. Piemonte and P. Scior, *Variational analysis of low-lying states in supersymmetric Yang-Mills theory*, JHEP **04** (2019) 150, [arXiv: `1901.02416` [`hep-lat`]].

3. S. Ali, G. Bergner, H. Gerber, C. Lopez, I. Montvay, G. Münster, S. Piemonte and P. Scior, *Baryonic states in supersymmetric Yang-Mills theory*, [arXiv: `1811.02297` [`hep-lat`]].

4. S. Ali, G. Bergner, H. Gerber, P. Giudice, I. Montvay, G. Münster, S. Piemonte and P. Scior, *The light bound states of $\mathcal{N} = 1$ supersymmetric SU(3) Yang-Mills theory on the lattice*, JHEP **1803** (2018) 113, [arXiv: `1801.08062` [`hep-lat`]].

5. S. Ali, G. Bergner, H. Gerber, I. Montvay, G. Münster, S. Piemonte and P. Scior, *Analysis of Ward identities in supersymmetric Yang–Mills theory*, Eur. Phys. J. **C 78** (2018) 404, [arXiv: `1802.07067` [`hep-lat`]].

6. S. Ali, G. Bergner, H. Gerber, P. Giudice, I. Montvay, G. Münster, S. Piemonte, P. Scior, *Investigation of Theories beyond the Standard*

Model. Proceedings of the NIC Symposium 2018, Series Volume 49, Jülich, 2018, p. 195.

7. S. Ali, G. Bergner, H. Gerber, P. Giudice, I. Montvay, G. Münster, S. Piemonte and P. Scior, *Ward identities in $\mathcal{N} = 1$ supersymmetric SU(3) Yang-Mills theory on the lattice*, [arXiv: `1711.05504` [`hep-lat`]].

8. S. Ali, G. Bergner, H. Gerber, P. Giudice, S. Kuberski, I. Montvay, G. Münster, S. Piemonte and P. Scior, *Supermultiplets in $\mathcal{N} = 1$ SU(2) SUSY Yang-Mills Theory*, [arXiv: `1710.07464` [`hep-lat`]].

9. S. Ali, G. Bergner, H. Gerber, P. Giudice, S. Kuberski, I. Montvay, G. Münster, S. Piemonte and P. Scior, *Improved results for the mass spectrum of $\mathcal{N} = 1$ SU(3) supersymmetric Yang-Mills theory*, [arXiv: `1710.07105` [`hep-lat`]].

10. S. Ali, G. Bergner, H. Gerber, P. Giudice, I. Montvay, G. Münster and S. Piemonte, *Simulations of $\mathcal{N} = 1$ supersymmetric Yang-Mills theory with three colours*, [arXiv: `1610.10097` [`hep-lat`]].

Conferences and Talks

1. Interface of effective field theories and lattice gauge theories,MIAPP, Garching, Munich {29.10.–09.11.2018}

2. 1st Workshop on High Energy Theory and Gender, CERN, Geneve {26.–29.09.2018}

3. Annual Retreat 2018 of the DFG Research Training Group (RTG) 2149 at Hotel Haus Griese, Körbecke, Germany {10.–13.09.2018}

4. "Symposium on Quantum and Statistical Field Theory", Münster {29.–30.06.2018}

5. Lattice Winter School, University of Southern Denmark, Odense {27.11–01.12.2017}

154

6. GRK 2149 Annual Retreat 2017, Franz Dohrmann Haus, Marienheide, Germany (talk) {25.–29.09.2017}

7. Workshop on Standard Model and Beyond, Corfu, Greece {02.–10.09.2017}

8. Lattice2017, Granada, Spain.(contributed talk) {18.–24.06.2017}

9. Deutsche Physikalische Gesellschaft (DPG) Jahrestagung 2017, Münster, Germany (contributed talk) {27.–31.03.2017}

10. International Scientific School(ISS) 2017, NCP, Islamabad, Pakistan (poster presentation) {13.–17.03.2017}

11. GRK 2149 Annual Retreat 2016, Hotel Griese, Körbecke (Möhnesee), Germany (poster presentation) {19.–22.09.2016}

12. Saalburg Summer School on "Foundations and New Methods in Theoretical Physics", Trockenborn-Wolfersdorf, Germany {05.–16.09.2016}

13. GRK 2149 Annual Retreat 2015, Heidehotel Waldhütte, Telgte, Germany {05.–16.09.2016}

14. International Conference on "Physics and Contemporary Needs", GC University, Lahore, Pakistan {19.–21.11.2014}

15. 1st International Conference on Modern Communication and Computing Technologies (MCCT'14), QUEST Nawabshah, Pakistan {19.–21.11.2014}

16. 5th International meeting on Particles and Fields 2013, University of the Punjab, Lahore, Pakistan {25.27.03.2013}

17. International Scientific Spring(ISS) 2013, NCP, Islamabad, Pakistan {11.–15.03.2013}

Awards

- DAAD Research Grants-Doctoral Programmes in Germany (2015)

- University Gold Medal (2011), University of the Punjab Lahore, Pakistan

- Inter Departmental Merit Scholarship (2009), University of the Punjab Lahore, Pakistan

- Inter Departmental Merit Scholarship (2008), University of the Punjab Lahore, Pakistan

Professional Occupation

- Lecturer: Department of Physics GC University, Lahore Pakistan (01.10.2010–date, now on study leave)

- Research Assistant: Institute for Theoretical Physics, University of Münster (01.02.2017–30.09.2019)